NLRP1 drives inflammasome responses in the human respiratory epithelium

Thesis submitted to the University of Dublin for the degree of Doctor of Philosophy

by

Nathaniel Laurence Lam

Supervisors: Dr John Wright, Dr Edith Hessel, Professor Luke O'Neill, Dr Soren Beinke, and Professor Clare Bryant

Trinity College Dublin, the University of Dublin

January 2023

Declaration

This thesis is submitted by the undersigned to Trinity College Dublin, the University of Dublin for the examination of Doctor of Philosophy. I declare that this thesis has not been submitted as an exercise for a degree at this or any other university and is entirely my own work, except for the following figures:

Figure 3.3, Figure 3.4, Figure 3.5, and Figure 5.11

Interpreted with assistance from Sylvia Fung and Dr David Lewis.

Figure 3.4

Pooled NLRP3 KO THP-1 clones were provided by Dr Anna Gram.

Figure 4.7

Optimised with assistance from Dr Robert Pickering.

Figure 6.1

SARS-CoV-2 infection, cell fixation and western blot analysis were performed by Dr Charlotte Passemar.

Figure 6.2

In silico analysis was performed by Dr Nikolai Belyaev.

I agree to deposit this thesis in the University's open access institutional repository or allow the library to do so on my behalf, subject to the Irish Copyright Legislation and Trinity College Library conditions of use and acknowledgement. I consent to the examiner retaining a copy of the thesis beyond the examining period, should they so wish (EU GDPR May 2018).

Nathaniel Lam

Acknowledgements

Without the help and support of the following people this thesis would not have been possible. I would like to thank:

Professor Clare Bryant and Dr Soren Beinke (primary supervisors) for their continual support and guidance, as well as their encouragement to pursue a career in science.

Dr John Wright and Dr Edith Hessel (secondary supervisors) for their mentorship, particularly at the early and unpredictable stages of this project.

Professor Luke O'Neill (nominal supervisor) for initiating this collaboration and his invaluable advice while hosting me at Trinity.

My current/past colleagues at GSK, in particular Antonella, Natalie, Hannah, Tracey, Monika, Aliza, Max, Caitlin, Gisela, and Oliver for scientific assistance and ensuring I stayed motivated.

And finally, my family (Mum, Dad, and Thomas) and godparents (Linda and Wilson) for always believing in me.

In loving memory of Agnes Jean Bingham and Pak Ying Lam who missed the end of this adventure.

Table of Contents

Declaration 1

Acknowledgements 2

List of Figures 6

List of Tables 9

Abbreviations 10

Abstract 13

Chapter 1. Introduction 14

1.1 Airway epithelial cells 14

1.2 Airway epithelial cell ontogeny 14

1.3 Notch signalling in the airways 17

1.4 The apical junctional complex and TEER 18

1.5 Pattern recognition receptors of the airway epithelium 19

1.6 Inflammasomes 22

1.7 NLRP1 and CARD8 24

1.8 Inflammasomes in AECs 27

1.9 IL-1 biology 29

1.10 IL-18 biology 30

1.11 IL-33 biology 30

1.12 Additional functions of inflammasome components 31

1.13 COPD pathophysiology 32

1.14 Human rhinovirus in COPD 33

1.15 Bacterial infection in COPD 34

1.16 Inflammasomes in COPD 35

1.17 Modelling the airway epithelium 36

1.18 Project aims 40

Chapter 2. Materials and methods 42

2.1 Human tissue and HBECs 42
2.2 Cell culture and HBEC differentiation 43
2.3 Immunohistochemistry and immunocytochemistry 44
2.4 TLR stimulations 45
2.5 Bacterial cell culture and infection 45
2.6 *M. catarrhalis* adhesion and invasion assays 47
2.7 Flow cytometry 48
2.8 Quantitative reverse transcription PCR (RT-qPCR) analysis 51
2.9 Western blotting 53
2.10 Inflammasome stimulations 54
2.11 Inflammasome inhibition 54
2.12 Immunofluorescence of ASC specks 55
2.13 Immunofluorescence of ALI-differentiated HBECs 58
2.14 LDH cytotoxicity assays 58
2.15 ELISA assays 58
2.16 Luminex assays 59
2.17 CRISPR-Cas9 KO 59
2.18 Statistical analysis 60
Chapter 3. Pattern recognition receptors of the respiratory epithelium 61
3.1 Rationale 61
3.2 Epithelial cells have a restricted repertoire of inflammasome sensor molecules 62
3.3 ASC expression is polarised in epithelial cells 65
3.4 TLR3 stimulation primes the epithelial inflammasome 66
3.5 Nigericin-induced epithelial death is NLRP3-independent 68
3.6 Common respiratory bacteria drive minimal epithelial inflammasome responses 69

3.7 NLRC4 and non-canonical inflammasome stimuli are unable to drive IL-1β secretion from BEAS-2B cells 75
3.8 Discussion 77
Chapter 4. NLRP1 in health and disease 80
4.1 Rationale 80
4.2 IL-1β levels may be enhanced in COPD frequent exacerbators 80
4.3 VBP-induces inflammasome activation in HBEC3-KT and THP-1 cells 83
4.4 VBP alone drives inflammasome responses in primary basal cells 85
4.5 VBP-induced inflammasome activation is NLRP1-dependent 87
4.6 NLRP1 activation is enhanced in basal cells from COPD patients 92
4.7 NLRP1 activation is enhanced in ALI-differentiated HBECs from COPD patients 95
4.8 Discussion 96
Chapter 5. The role of NLRP1 in epithelial differentiation 100
5.1 Rationale 100
5.2 Chronic NLRP1 activation arrests epithelial differentiation and leads to sustained cytokine release 101
5.3 Deletion of NLRP1 protects cells from VBP 104
5.4 Deletion of NLRP1 has minimal impact on barrier formation 107
5.5 NLRP1 and CARD8 protein levels are reduced following ALI culture 108
5.6 KO of NLRP1 may reduce the progenitor cell pool 109
5.7 Discussion 117
Chapter 6. General discussion and future perspectives 120
6.1 NLRP1 in airway defence 120
6.2 NLRP1 in airway disease 123
6.3 NLRP1 in airway differentiation 126
Chapter 7. References 129

List of Figures

Figure 1.1. Gross and microanatomy of the airways. 15

Figure 1.2. Notch-independent self-renewal and Notch-dependent differentiation of airway basal cells. 18

Figure 1.3. TLR expression in human AECs is polarised. 21

Figure 1.4. The current model of inflammasome activation. 23

Figure 1.5. Domain architecture of human/rodent NLRP1 and CARD8. 25

Figure 1.6. 'Functional degradation' model of NLRP1 and CARD8 activation. .. 26

Figure 1.7. NLRP1 activation drives mucin upregulation or secretory cell differentiation. 32

Figure 1.8. Submerged, primary basal cells with the phenotypic "cobblestone-like" morphology. 38

Figure 1.9. *In vitro* generation of a pseudostratified columnar epithelium using the ALI system. 39

Figure 2.1. Growth curves for (A) *M. catarrhalis*, (B) NTHi and (C) *P. aeruginosa* in supplemented BHI (sBHI)/LB broth and PneumaCult. 47

Figure 2.2. Gating strategy and stained populations are indicated. 50

Figure 2.3. Quantification of ASC specks in 2D cultures. 57

Figure 3.1. ALI-differentiated HBECs have a high basal expression of TLR3 and NLRP1. 62

Figure 3.2. Titration of HBEC and THP-1 whole cell lysates reveals differential expression of NLRP1 and CARD8. 63

Figure 3.3. NLRP1 and NLRP3 are expressed in the human bronchial epithelium. 64

Figure 3.4. Characterisation of rabbit anti-human NLRP3 in KO THP-1 cells. 65

Figure 3.5. ASC and caspase-1 are expressed in the human bronchial epithelium. 66

Figure 3.6. Poly (I:C) efficiently primes the inflammasome in HBECs. 67

Figure 3.7. Nigericin induces epithelial cell death and cytokine secretion at later timepoints. 68

Figure 3.8. Nigericin-induced cell death is NLRP3-independent in HBECs. 69

Figure 3.9. *M. catarrhalis* adheres to BEAS-2B cells. 70

Figure 3.10. *M. catarrhalis* does not drive epithelial inflammasome responses. 72

Figure 3.11. NTHi drives minimal epithelial inflammasome responses. 73

Figure 3.12. *P. aeruginosa* drives modest epithelial inflammasome responses. 74

Figure 3.13. NLRC4 and the non-canonical inflammasome stimuli drive minimal inflammasome responses in BEAS-2B cells. 76

Figure 4.1. Cytokine profiles in the BALF from healthy smokers and COPD patients. 82

Figure 4.2. HBEC3-KT cells respond to VBP treatment at later timepoints. 83

Figure 4.3. VBP and nigericin drive inflammasome responses in THP-1 cells but not in BEAS-2B cells. 84

Figure 4.4. NLRP1 is activated in basal epithelial cells. 86

Figure 4.5. Basal epithelial cells are unable to activate NLRC4 or the non-canonical inflammasome. 87

Figure 4.6. VBP-induced inflammasome activation is caspase or proteasome-dependent in basal epithelial cells. 88

Figure 4.7. siRNA-mediated KD of GAPDH in HBEC3-KT cells. 89

Figure 4.8. VBP-induced inflammasome activation is NLRP1-dependent in basal epithelial cells. 91

Figure 4.9. NLRP1 activation in basal cells from COPD donors leads to enhanced ASC speck formation, cell death and IL-1β secretion. 93

Figure 4.10. *NLRP1* levels are enhanced in COPD basal cells. 94

Figure 4.11. Poly (I:C) induces modest inflammasome responses in primary HBECs. 95

Figure 4.12. NLRP1 is activated in ALI-differentiated airway epithelial cells. 96

Figure 5.1. Progenitor/secretory cell populations are enhanced upon chronic VBP exposure. 103

Figure 5.2. Chronic dosing of ALI-differentiating HBECs with VBP induces sustained cytokine secretion. 104

Figure 5.3. NLRP1 protein levels are abolished in KO basal cells. 105

Figure 5.4. NLRP1 KO abrogates ASC speck formation and cytokine secretion. 106

Figure 5.5. Deletion of NLRP1 may enhance poly (I:C)-induced IL-6 secretion in cells from COPD patients. 107

Figure 5.6. Deletion of NLRP1 has no impact on barrier formation. 108

Figure 5.7. NLRP1 and CARD8 protein levels are reduced following ALI culture of KO cells. 109

Figure 5.8. HBEC cell populations were unaltered following NLRP1 KO at later timepoints. 111

Figure 5.9. KO of NLRP1 induces a modest reduction of progenitor cells and a modest enhancement of double-negative cells. 115

Figure 5.10. Deletion of NLRP1 reduces KRT4 but not KRT13 expression. 116

Figure 5.11. Deletion of NLRP1 reduces KRT4 expression in the pseudostratified columnar cell layer 117

Figure 6.1. SARS-CoV-2 variant B.1.1.7 is unable to induce ASC speck formation in basal cells due to the absence of ACE2. 122

Figure 6.2. Interactome of proteins downstream of DPP8 and DPP9. 125

Figure 6.3. Proposed role of NLRP1 in the differentiation of HBECs. 128

List of Tables

Table 1.1. TLRs and their cognate ligands. 20

Table 1.2. Summary of AEC inflammasomes. 28

Table 1.3. Comparison of primary HBECs and commonly utilised human AEC lines. 37

Table 2.1. Summary of human bronchial epithelial cell (HBEC) donors. 43

Table 2.2. Bacterial culture media. 46

Table 2.3. Flow cytometry staining cocktail. 48

Table 2.4. RT-qPCR primers. 52

Table 2.5. Silencer Select siRNA. 55

Table 2.6. crRNA utilised for gRNA generation. 59

Table 6.1. Summary of published DPP8/9 substrates. 126

Abbreviations

ACE2	Angiotensin-converting enzyme 2
ACTB	β-actin
AEC	Airway epithelial cell
AIM2	Absent in melanoma 2
AJC	Apical junctional complex
ALI	Air-liquid interface
ALR	Absent in melanoma 2-like receptors
ANOVA	Analysis of variance
ASC	Apoptosis-associated speck-like protein containing a caspase activation and recruitment domain
BALF	Bronchoalveolar lavage fluid
BEGM	Bronchial epithelial cell growth medium
BHI	Brain heart infusion
CARD	Caspase activation and recruitment domain
CCL	C-C motif chemokine ligand
CFU	Colony-forming unit
CLR	C-type lectin receptor
COPD	Chronic obstructive pulmonary disease
CRISPR-Cas9	Clustered regularly interspaced short palindromic repeat-CRISPR-associated protein 9
crRNA	CRISPR RNA
CXCL	C-X-C motif chemokine ligand
DAMP	Danger-associated molecular pattern
DKO	Double knockout
DPP	Dipeptidyl peptidase
dsDNA	Double-stranded DNA
dsRNA	Double-stranded RNA
ELISA	Enzyme-linked immunosorbent assay
FACS	Fluorescence-activated cell sorting
FEV_1	Forced expiratory volume in one second
FFPE	Formalin-fixed, paraffin-embedded
FIIND	Function to find domain
gRNA	Guide RNA
HBEC	Human bronchial epithelial cell
FCS	Foetal calf serum

HRV	Human rhinovirus
HRV-3Cpro	Human rhinovirus 3C protease
H&E	Haematoxylin and eosin
ICAM-1	Intercellular adhesion molecule 1
ICC	Immunocytochemistry
IF	Immunofluorescence
IFN	Interferon
IHC	Immunohistochemistry
Il	Interleukin
IL-1R1	IL-1 receptor, type 1
KD	Knockdown
KO	Knockout
KRT	Cytokeratin
LDH	Lactate dehydrogenase
LPS	Lipopolysaccharide
LRR	Leucine-rich repeat
MDA5	Melanoma differentiation-associated protein 5
MUC5AC	Mucin 5 subtypes A and C
MOI	Multiplicity of infection
MyD88	Myeloid differentiation primary response 88
NBD	Nucleotide-binding domain
NF-κB	Nuclear factor-kappa B
NLR	NOD-like receptor
NTHi	Non-typeable *H. influenzae*
PAMP	Pathogen-associated molecular pattern
PBS	Phosphate-buffered saline
PMA	Phorbol-12-myristate 13-acetate
PRR	Pattern recognition receptor
PYD	Pyrin domain
qPCR	Quantitative real-time PCR
RIG-I	Retinoic acid-inducible gene I
RLR	Retinoic acid-inducible gene I-like receptor
RNP	Ribonucleoprotein
SARS-CoV-2	Severe acute respiratory syndrome coronavirus 2
SCGB1A1	Secretoglobin family 1A member 1
scRNA-seq	Single-cell RNA sequencing
SD	Standard deviation

SEM	Standard error of the mean
siRNA	Small interfering RNA
SNP	Single nucleotide polymorphism
T3SS	Type III secretion system
TEER	Transepithelial electrical resistance
TBS	Tris-buffered saline
TGF	Transforming growth factor
T_H	T helper
TLR	Toll-like receptor
TNF	Tumour necrosis factor
VBP	Valinyl-L-boroproline
WT	Wildtype
ZO-1	Zonula occludens-1

Abstract

The airway epithelium is now considered crucial to the orchestration of respiratory inflammatory responses and tissue remodelling. It functions as the first line of defence against inhaled concomitants and coordinates the resulting innate and adaptive immune pathways. Little information is available, however, on epithelial inflammasomes, particularly their functions and contributions to chronic respiratory diseases. Here it was observed that although most inflammasome components were present in human bronchial epithelium, minimal inflammasome responses were detected following infections with common respiratory bacteria. Optimal inflammasome priming occurs following TLR3 stimulation which suggests that these cells may instead mediate antiviral responses. In parallel with a recent publication, shown here is that NLRP1 is the dominant inflammasome in primary bronchial epithelial cells (Robinson et al., 2020). These cells fail to respond to NLRP3, NLRC4 and AIM2 inflammasome stimuli. In contrast, basal and air-liquid interface-differentiated cells activate NLRP1 to undergo cell death and cytokine secretion upon Valinyl-L-boroproline treatment. In COPD patients, IL-1β levels in the airways may be enhanced compared with healthy smokers, correlating with exacerbation frequency. Bronchial epithelial cells may contribute to the disease since the expression of NLRP1 and its negative regulators, dipeptidyl peptidase 8 and 9 (DPP8/9), are elevated in basal cells from patients with COPD. Valinyl-L-boroproline inhibition of DPP8/9 in these cells leads to marked inflammasome activation, which is dependent on caspase or proteasome activity and is reduced by knockdown or knockout of NLRP1. In addition to basal cells, NLRP1 activation is also enhanced in air-liquid interface-differentiated cells from COPD patients in response to Valinyl-L-boroproline or human rhinovirus 16. Preliminary evidence suggests that chronic Valinyl-L-boroproline treatment during differentiation leads to sustained NLRP1 inflammasome activation and arrested epithelial development. Following CRISPR/Cas9-mediated NLRP1 knockout, progenitor cell numbers (the intermediate stage between basal cells and terminally differentiated cells) are reduced, implicating NLRP1 in initial cell fate decisions. Targeting the NLRP1 inflammasome pathway may, therefore, be a novel therapeutic approach for the treatment of conditions such as COPD viral exacerbations, as well as other disorders involving dysregulated epithelial differentiation.

Chapter 1. Introduction

1.1 Airway epithelial cells

Airway epithelial cells (AECs) lining the bronchial tree represent a key interface between the external environment and the internal milieu, where they are exposed to a diverse array of inhaled concomitants. Hitherto AECs were assumed to have a primarily structural function; selectively permissive to water and ions, yet curtailing the entry of airborne particles and facilitating their clearance via the mucociliary 'escalator' (Hiemstra et al., 2015). It is now acknowledged that AECs are indispensable for the initiation of immune responses, inflammation, and tissue remodelling. They are equipped with a diverse repertoire of pattern recognition receptors (PRRs) including Toll-like receptors (TLRs), C-type lectin receptors (CLRs), absent in melanoma 2 (AIM2)-like receptors (ALRs), retinoic acid-inducible gene I (RIG-I)-like receptors (RLRs) and NOD-like receptors (NLRs) (Gavino et al., 2005; Kummer et al., 2007; Liu et al., 2007; Mayer et al., 2007; Slevogt et al., 2007; Hirota et al., 2012; Heyl et al., 2014). Ligation of these PRRs allows AECs to participate in various innate immune responses via the production of antimicrobial peptides (including defensins and cathelicidins), reactive species, cytokines (particularly type I and III interferons [IFNs]), chemokines and growth factors (Bals and Hiemstra, 2004; Parker and Prince, 2011). Moreover, epithelial-derived soluble mediators and cell surface molecules expedite the interactions with intraepithelial dendritic cells, T cells and B cells, to bridge innate with adaptive immunity (Schleimer et al., 2007). Importantly, AEC (dys)function contributes to and is modified during the pathogenesis of chronic respiratory disorders, such as chronic obstructive pulmonary disease (COPD) and asthma. Although there have been significant advances in the understanding of AEC-expressed PRRs (not least due to representative air-liquid interface [ALI] models), there remains a dearth of information on inflammasome function in these cells, the focus of this project. As the first line of defence at this key barrier site, AECs with functional inflammasomes may be integral to respiratory physiology and pathology.

1.2 Airway epithelial cell ontogeny

The epithelial lining of the large airways is characterised histologically as a pseudostratified columnar epithelium, erroneously appearing stratified due to the

asymmetrical distribution of cell nuclei. It is principally composed of basal, progenitor, secretory (club, goblet, and serous cells) and ciliated cells (Rock et al., 2010) (**Figure 1.1**).

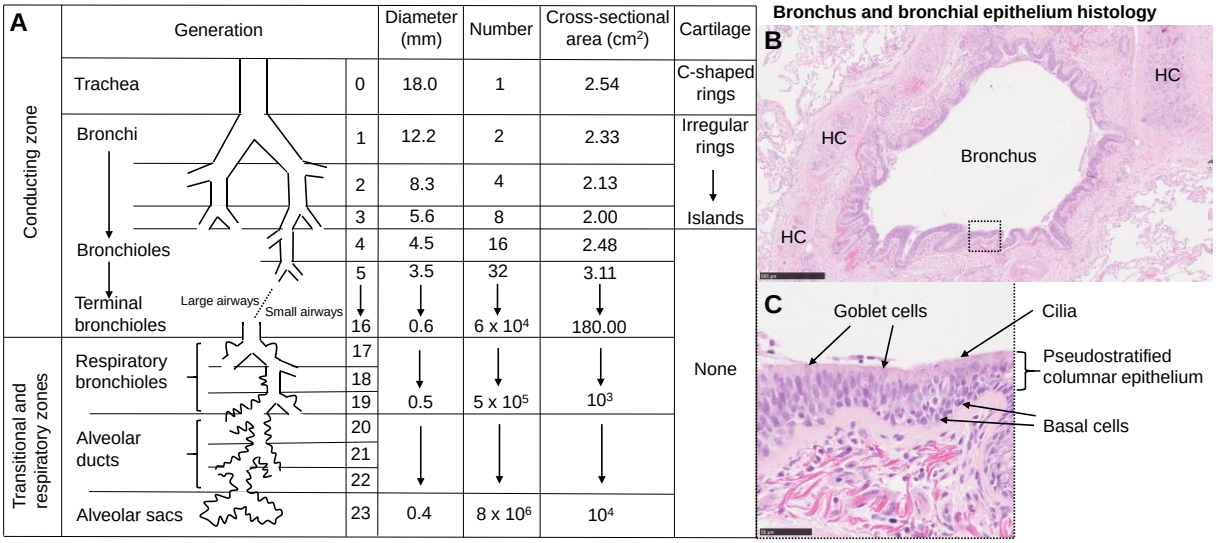

Figure 1.1. Gross and microanatomy of the airways.

(**A**) The first 16 generations of vessels represent the conducting airways and are disconnected from gas exchange (the anatomical dead space). Budding alveoli begin to egress from the respiratory bronchioles of the transitional zone, and these are further elaborated in the alveolar ducts and sacs of the respiratory zone. Human lung section stained with haematoxylin and eosin (H&E) enables the visualisation of a (**B**) bronchus and (**C**) human bronchial epithelial cells (HBECs). Note the folded mucosa indicative of incomplete distension of the airway, and thus the low diameter measurement. HC, hyaline cartilage. Adapted from multiple sources (Ali et al., 2010; West, 2012).

Cell populations deviate along the proximal-distal axis, with less abundant basal and goblet cells, but relatively more ciliated and club cells in the columnar/cuboidal small airways (from generation eight onwards). From generation 17, these cells are gradually substituted for gas-exchanging type I pneumocytes and surfactant-producing type II pneumocytes (Whitsett and Alenghat, 2014). Human bronchial epithelial cells (HBECs) decorating the large airways have been the emphasis of this project so subtypes will be discussed in further detail.

Basal cells reside in juxtaposition with the basement membrane and comprise ~30 % of the total HBEC population (Boers et al., 1998). They are the dominant

multipotent stem cell capable of self-renewal and differentiation into all specialised cell types. Previously they have been profiled by the expression of transformation-related protein 63 (TRP63), cytokeratin 5 (KRT5), KRT14 (subset restricted), nerve growth factor receptor (NGFR/CD271) and integrin α6 (ITGA6/CD49f) (Nakajima et al., 1998; Araya et al., 2007; Rock et al., 2009). The initial stage of differentiation generates an intermediate early progenitor which retains KRT5 but induces the expression of luminal cell markers such as KRT8 (Rock et al., 2011; Ruiz García et al., 2019). There has been much interest in basal cells since their altered proliferation or cell fate decisions instigate pathological airway remodelling, such as squamous metaplasia and goblet cell hyperplasia in COPD (Rock et al., 2010). They may also influence the inflammatory microenvironment through the secretion of various polypeptides such as interleukin (IL)-8, and by expressing a plethora of receptors such as the tumour necrosis factor (TNF) receptors (Crystal, 2014).

Club cells have more recently emerged as the next stage of the differentiation pathway, due to lineage tracing and single-cell RNA-sequencing (scRNA-seq) approaches (Watson et al., 2015; Montoro et al., 2018; Ruiz García et al., 2019). In addition to generating terminally differentiated goblet and ciliated cells, there is evidence for club cell dedifferentiation into basal cells upon airway damage (Tata et al., 2013). Club cells are the primary producers of secretoglobin family 1A member 1 (SCGB1A1, also known as uteroglobin), which is believed to have immunomodulatory functions. For example, SCGB1A1 inhibits lipopolysaccharide (LPS)-induced mucin 5 subtypes A and C (MUC5AC) secretion from goblet cells (Tokita et al., 2014).

Goblet cells are classically associated with the production of high-molecular-weight glycoproteins termed mucins. These can be partitioned into two subfamilies, with the secreted mucins (MUC5AC and MUC5B) constituting a gel-like mucus layer, overlaying a periciliary liquid layer formed by the epithelial-tethered mucins (MUC1, MUC4 and MUC16) (Lillehoj et al., 2013). Canonically, the highly viscous mucus layer binds to foreign particles, while the low viscosity periciliary liquid layer remains conducive to periciliary brush function. The epithelial-tethered mucins may fulfil more dynamic functions, however, by signalling via their cytoplasmic domains and operating as mucin decoys for pathogen binding upon sheddase cleavage (Singh and Hollingsworth, 2006; Lillehoj et al., 2019).

Ciliated cells may project 200 – 300 cilia comprised of an axonemal cytoskeleton (doublet microtubules associated with dynein ATPase arms) (Fliegauf et al., 2007; Whitsett and Alenghat, 2014). Ciliary beating is both coordinated and directional, due to the intricate intracellular communication conveyed by connexins, facilitating mucus transport proximally toward the pharynx (Bou Saab et al., 2014). Emerging evidence suggests that certain COPD endotypes, i.e. ciliopathy-associated COPD, may fall within the ciliopathy spectrum which includes diseases such as bronchiectasis (caused by primary ciliary dyskinesia) (Perotin et al., 2021). Genes associated with both ciliogenesis and cilia length appear to be dysregulated in COPD which, concomitant with goblet cell hyperplasia, may impair the mucociliary 'escalator'.

Rare cell populations including hillock cells, tuft cells, ionocytes and pulmonary neuroendocrine cells have been identified primarily by scRNA-seq (Hewitt and Lloyd, 2021). Despite representing only ~2 % of the epithelium, they have distinct and critical functions, such as chemoreception by tuft cells. They are not universally identifiable, however, due to their infrequency and so were not investigated in this project.

1.3 Notch signalling in the airways

The Notch signalling axis governs lung development during embryogenesis, as well as repair and cell differentiation in the mature lung (Kiyokawa and Morimoto, 2020). The Notch pathway is an evolutionarily conserved cell-cell signalling cascade, composed of transmembrane ligands (Jagged [JAG] 1 and 2, and Delta-like ligands [DLL] 1, 3 and 4) and receptors (Notch 1-4) (Kopan and Ilagan, 2009). Ligand/receptor binding promotes Notch intracellular domain shedding via gamma-secretase and a disintegrin and metalloproteinase (ADAM)-family metalloprotease activity. Following nuclear translocation, Notch intracellular domain engages Notch target genes, such as hairy and enhancer-of-split (HES) and HES related with YRPW motif (HEY), to dictate cell fate decisions.

Although basal cells express *JAG1*, *JAG2*, *DLL1* and *NOTCH1*, the pathway is inactive possibly due to negative regulation of JAG1 signalling by *LFNG* and appears to be dispensable for basal cell maintenance (Rock et al., 2011; Ruiz García et al., 2019). Active Notch 1/3 and Notch 2 signalling (with elevated

expression of Notch target genes HEY1 and HES4) are characteristic of differentiating early progenitor cells and club/goblet cells, respectively. Conversely, Notch repression via *CIR1*, *SAP30* and *DYRK1A* enables the *MCIDAS* – *FOXJ1* transcriptional cascade leading to ciliated cell differentiation (Stubbs et al., 2012; Boon et al., 2014) (**Figure 1.2**).

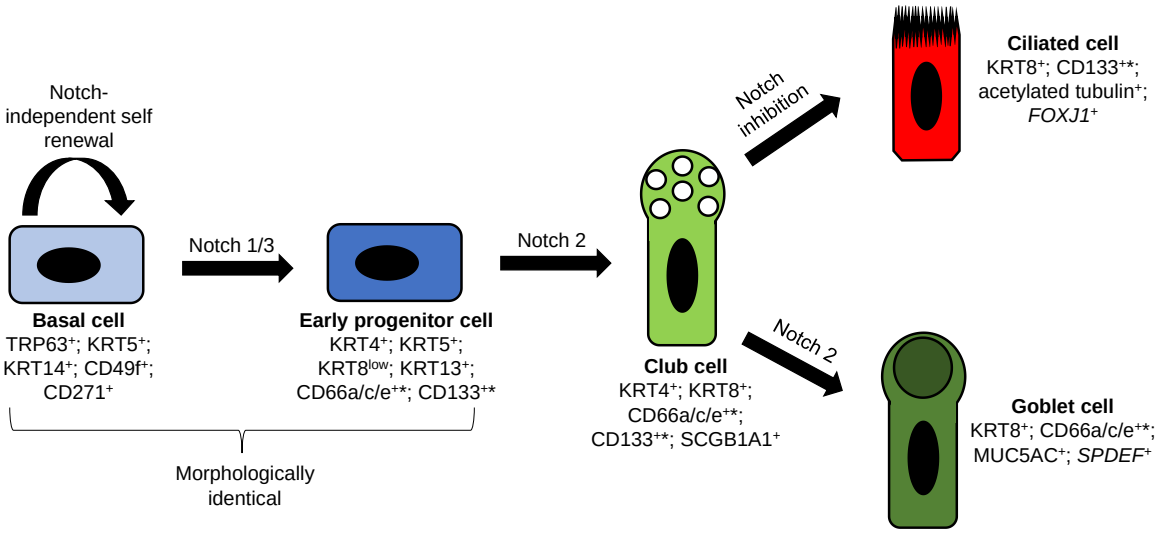

Figure 1.2. Notch-independent self-renewal and Notch-dependent differentiation of airway basal cells.

Maintained Notch signalling is required for the differentiation of basal cells into secretory lineages. Notch inhibitors, e.g. *DYRK1A*, are highly expressed in ciliated cells (and their deuterosomal cell intermediates) and facilitate their formation. Markers utilised during characterisation are indicated and those denoted with an * represent those identified during in-house transcriptomics (GlaxoSmithKline, unpublished data). Adapted from multiple sources (Rock et al., 2011; Watson et al., 2015; Ruiz García et al., 2019).

1.4 The apical junctional complex and TEER

The apical junctional complex (AJC) is integral for barrier formation between adjacent epithelial cells and for tissue compartmentalisation, while still permitting selective diffusion across paracellular connections. In chordates, the AJC is organised apically to basolaterally and comprises tight junctions (claudin, occludin and zonula occludens-1 [ZO-1]), adherens junctions (cadherins and catenins) and desmosomes. The AJC contributes to the property of transepithelial electrical

resistance (TEER) in cell cultures which may be used as a real-time proxy for barrier impedance (Powell, 1981; Lo et al., 1999). Following the application of a current to the epithelial layer, the resistance conferred by both the paracellular and cell/substrate contacts can be measured by using apical and basolateral electrodes. Values recorded in ohms (Ω) can then be used to calculate the TEER relative to the culture surface area.

1.5 Pattern recognition receptors of the airway epithelium

Reminiscent of other airway cells (alveolar macrophages, antigen-presenting cells, and neutrophils), AECs express germline-encoded PRRs which detect pathogen-associated molecular patterns (PAMPs), such as LPS, or danger-associated molecular patterns (DAMPs), such as heat-shock proteins.

The human TLR family comprises 10 membrane-bound receptors containing a N-terminal leucine-rich repeat (LRR)-containing domain, a transmembrane helix, and a cytoplasmic Toll/interleukin-1 receptor (TIR) homology domain (O'Neill, 2008). Although the TIR domain is conserved across all members of the IL-1R/TLR superfamily, the TLRs respond to exogenous or endogenous PAMPs or DAMPs, rather than cytokines, via their LRR ectodomain. Detection of microbial surface structures is primarily mediated by the plasma membrane-localised TLRs (TLR1, TLR2, TLR4, TLR5, TLR6 and TLR10), while the endosomal membrane-localised TLRs (TLR3, TLR7, TLR8 and TLR9) recognise microbial and host nucleic acids (**Table 1.1**):

Table 1.1. TLRs and their cognate ligands.

Pam3CSK4 and FSL-1 are detected by the TLR2-TLR1 and TLR-2-TLR6 heterodimers, respectively. Adapted from multiple sources (Akira and Takeda, 2004; Regan et al., 2013; Lee et al., 2014; Oosenbrug et al., 2017).

Receptor	Biological ligands	Synthetic ligands used
TLR1	Triacyl lipopeptides	Pam3CSK4
TLR2	Glycolipids, heat-shock protein 70, lipoteichoic acid, lipopeptides, peptidoglycan, zymosan	Pam3CSK4, FSL-1 (*Mycoplasma salivarium*)
TLR3	dsRNA	Poly (I:C)
TLR4	Fibrinogen, heat-shock protein 60, heat-shock protein 70, LPS	LPS (*Escherichia coli*)
TLR5	Flagellin	Flagellin (*Pseudomonas aeruginosa*)
TLR6	Diacyl lipopeptides, lipoteichoic acid, zymosan	FSL-1 (*M. salivarium*)
TLR7	ssRNA	-
TLR8	ssRNA	-
TLR9	CpG motifs	-
TLR10	*Listeria monocytogenes* and Influenza A components	-

Signalling via myeloid differentiation primary response 88 (MyD88) or TIR domain-containing adaptor protein inducing IFN-β (TRIF) culminates in nuclear factor-kappa B (NF-κB) and mitogen-activated protein kinase (MAPK) activation. Although AECs express all TLRs except TLR8, several of these (TLR2 and TLR4) are hypo-responsive under homeostatic conditions due to restricted coreceptor expression (CD36 for TLR2, MD2 and CD14 for TLR4) and polarised TLR distribution (TLR2 basolaterally and TLR4 apically) (Becker et al., 2000; Jia et al., 2004; Sha et al., 2004; Mayer et al., 2007; Ioannidis et al., 2013) (**Figure 1.3**).

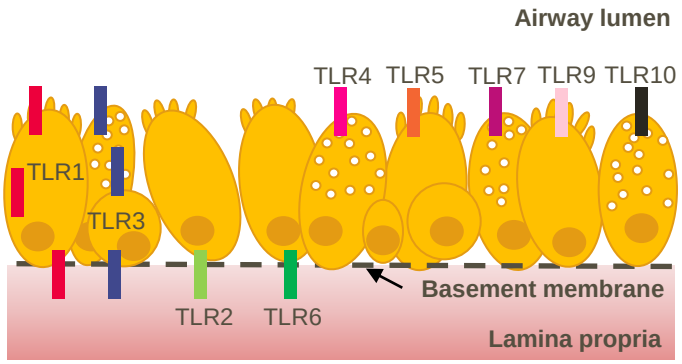

Figure 1.3. TLR expression in human AECs is polarised.

TLR1 and TLR3 are distributed throughout the epithelial layer; TLR2 and TLR6 are primarily expressed basolaterally; TLR4, TLR5, TLR7, TLR9 and TLR10 are located apically. In the differentiated epithelium, the endosomal TLRs (TLR3, TLR7 and TLR9) are expressed both intracellularly and on the plasma membrane (Ioannidis et al., 2013).

Nevertheless, should this sensor threshold be overcome during pathology, TLR engagement leads to the expulsion of anti-microbial substances (β-defensins, lysozyme, reactive nitrogen species, and cathelicidins), cytokines (type I and type III IFNs), chemokines (TNF-α, IL-5, IL-6, IL-8, C-C motif chemokine ligand [CCL]3, CCL4, CCL5, C-X-C motif chemokine ligand [CXCL]1, CXCL2, CXCL3 and transforming growth factor-beta [TGF-β]), mucins (directly or indirectly via TNF-α and IL-8) and survival factors (B cell activation factor of the TNF family [BAFF] and a proliferation-inducing ligand [APRIL]) (Bals et al., 1998; Bautista et al., 2009; Wu et al., 2010; Levy et al., 2011; Ohkuni et al., 2011; Ioannidis et al., 2013; Ryu et al., 2013).

The CLRs consist of one or more C-type lectin domains, and they primarily detect microbial and/or allergenic saccharides within the extracellular milieu. Despite representing the largest PRR family, CLRs have mostly been overlooked in AECs, however, epithelial Dectin-1 has been shown to recognise mycobacteria and Aspergillus (Lee et al., 2009; Sun et al., 2012). Unlike most TLR responses, CLRs also mediate inhibitory responses, for example, IL-33 secretion is abrogated by the binding of arthropod tropomyosin to AEC Dectin-1 (Gour et al., 2018).

The ALRs are located intracellularly and comprise of a N-terminal pyrin domain (PYD) and one/two haematopoietic interferon-inducible nuclear antigens with 200-

amino-acid repeat (HIN200) domains (Hornung et al., 2009; Kerur et al., 2011). Detection sites and responses differ between the ALRs, with AIM2 sensing microbial or host DNA in the cytosol and inciting IFN-independent responses, whereas interferon-γ inducible protein 16 (IFI16) recognises nuclear DNA and induces type I IFN production. In the small airways, both AIM2 and IFI16 are critical for influenza pathogenesis (Zhang et al., 2017; Mishra et al., 2022).

The RLR family of RNA helicases, including melanoma differentiation-associated protein 5 (MDA5) and RIG-I, are expressed in AECs and respond to RNA viruses by inciting type I IFN production. Due to the propensity of both MDA5 and RIG-I to sense cytosolic double-stranded RNA (dsRNA), there is considerable overlap in viral detection (Rehwinkel and Gack, 2020). Nevertheless, MDA5 does appear particularly important in picornavirus responses, while RIG-I specifically recognises the 5′-triphosphate RNA of viral genomes, such as those from Influenza A and Flaviviridae family members (Kato et al., 2006; Pichlmair et al., 2006; Chazal et al., 2018; Hertzog et al., 2018).

The NLRs are also cytosolic receptors but contain a LRR domain, a nucleotide-binding domain (NBD/NATCH/NOD) and an interaction region (PYD, caspase-recruitment domain [CARD], or baculovirus inhibitor repeats [BIR]), and they primarily detect bacterial or viral components. Although prior work has focused on NOD1 and NOD2-mediated peptidoglycan sensing, current interest has centred around NLR protein (NLRP)1, NLRP3 and NLR family CARD-containing (NLRC4), which assemble multimeric protein complexes termed inflammasomes (Parker and Prince, 2011).

1.6 Inflammasomes

In addition to NLRP1, NLRP3 and NLRC4, the AIM2 and RIG-I inflammasomes have been best characterised (Geddes et al., 2001; Martinon et al., 2002; O'Connor Jr et al., 2003; Hornung et al., 2009; Poeck et al., 2010). Typically, these PRRs engage with caspase-1 via the bipartite adaptor protein, apoptosis-associated speck-like protein containing a CARD (ASC), consisting of a PYD and CARD domain (this process also involves NAIP receptors in the case of NLRC4) (Rathinam and Fitzgerald, 2016). Canonical inflammasome activation is a two-signal process

with Signal one (priming step), conferred by TLR agonists, upregulating the inflammasome sensor molecule, caspase-1 and IL-1β via NF-κB (**Figure 1.4**).

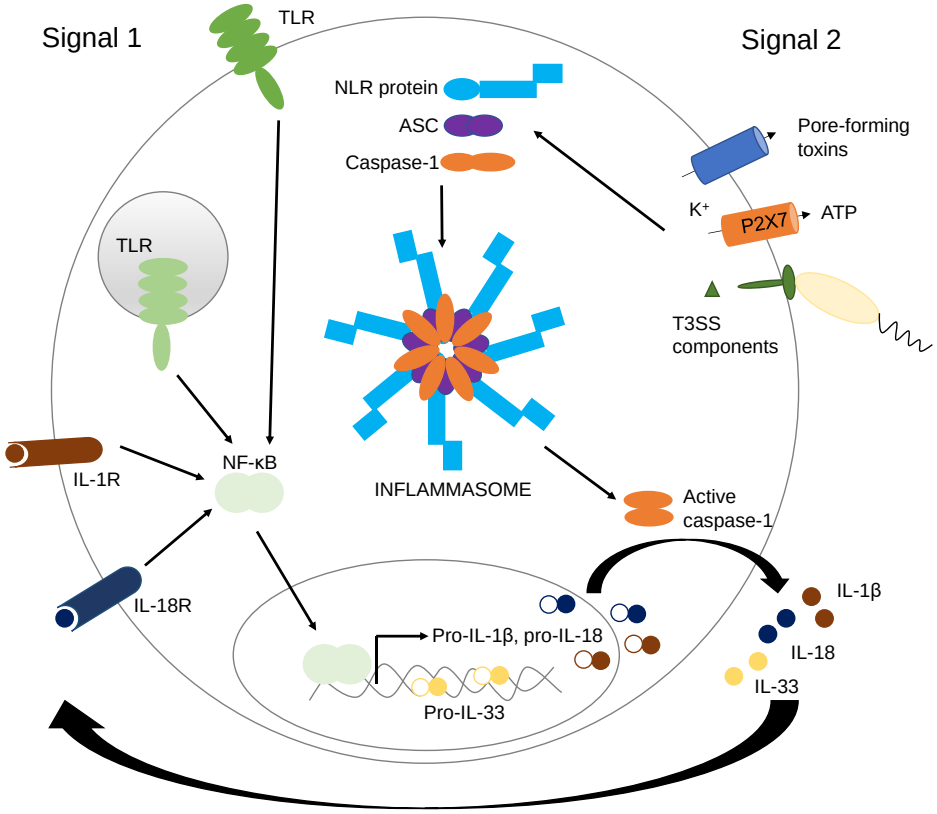

Figure 1.4. The current model of inflammasome activation.

A bona fide TLR ligand binds to its cognate receptor and initiates signalling cascades which culminate in NF-κB activation. NF-κB induces the transcription of inflammasome components, including the inflammasome sensor. The inflammasome sensor functions as a cytosolic PRR and detects a second signal (PAMPs or DAMPs), oligomerises and recruits ASC which assembles into large filaments (termed an ASC 'speck'). ASC then binds and activates caspase-1 which cleaves and activates IL-1β and IL-18, initiating pyroptotic cell death. In addition, epithelial cells express IL-33 which is cleaved and inactivated by caspase-1. They also express IL-1R1 and IL-18R which may facilitate autocrine signalling.

PRR recognition of Signal two (activation step) including ATP, pore-forming toxins (nigericin), viral RNA, particulate matter, or other intracellular bacterial components, induces PRR binding to ASC, inducing ASC oligomerisation into a large (~2 μm diameter) protein aggregate, termed a 'speck,' via homotypic PYD-PYD interactions. Monomeric pro-caspase 1 precursors are co-localised by ASC via

CARD-CARD interactions, which promotes self-cleavage and the production of an active caspase-1 (Bryant and Fitzgerald, 2009). Active caspase-1 proteolytically cleaves pro-IL-1β, pro-IL-18 and pro-IL-33 into biologically active IL-1β and IL-18, but inactive IL-33 (Cayrol and Girard, 2009). Caspase-1 also proteolytically processes the pyroptotic factor gasdermin D (Kayagaki et al., 2015; Shi et al., 2015). The cleaved N terminal of gasdermin D binds to inner leaflet lipids, oligomerises, and forms pores in the plasma membrane which culminates in lytic cell death. Since this cell death pathway is highly inflammatory and associated with the release of cleaved IL-1β and IL-18 it is termed pyroptosis. Different inflammasomes are activated depending upon different stimuli with NAIP/NLRC4 sensing bacterial flagellin and type III secretion system (T3SS) components, AIM2 sensing double-stranded DNA (dsDNA), and NLRP3 sensing a range of molecules many of which cause cellular perturbations such as ATP and crystalline structures (Bauernfeind and Hornung, 2013; Guo et al., 2015; Gram et al., 2021). Cytosolic LPS is recognised by murine caspase-11 or human caspase-4/5 directly leading to the formation of a non-canonical NLRP3 inflammasome (Kayagaki et al., 2015; Shi et al., 2015).

1.7 NLRP1 and CARD8

Despite being the first PRR shown to generate an inflammasome, the mechanisms by which human NLRP1 is activated are only recently becoming elucidated (Martinon et al., 2002). Since initial observations that the murine ortholog, NLRP1B, recognises *Bacillus anthracis* lethal toxin, additional activators have been identified such as *Shigella flexneri* IpaH7.8 and *Toxoplasma gondii* (Gorfu et al.; Boyden and Dietrich, 2006; Ewald Sarah et al., 2014; Sandstrom et al., 2019). These findings, however, have not translated to human NLRP1 and specific pathogenic ligands have remained elusive until recently, potentially due to the differences in protein structure (**Figure 1.5**)**.**

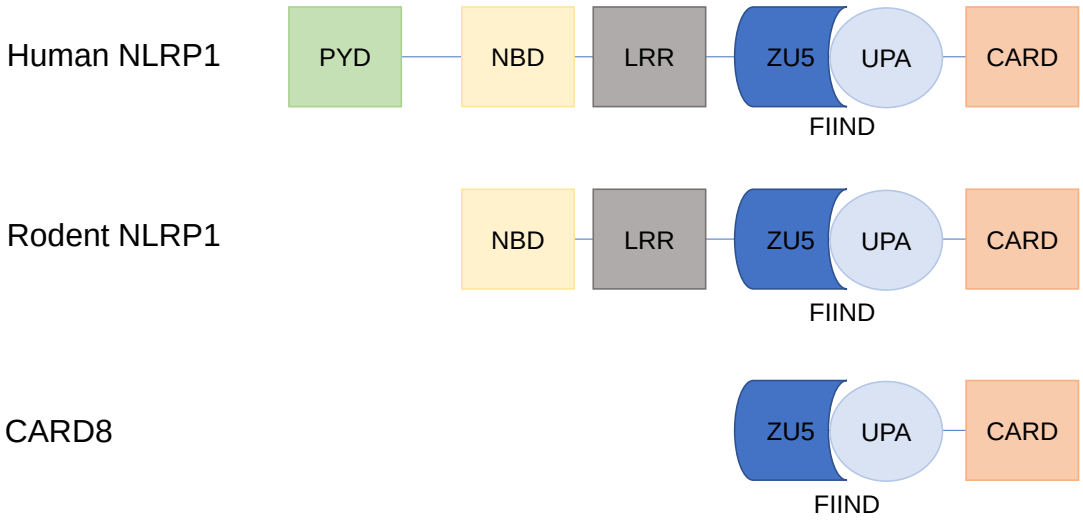

Figure 1.5. Domain architecture of human/rodent NLRP1 and CARD8.

The function to find domain (FIIND) (comprised of the found in ZO-1 and UNC5 [ZU5] and the conserved in UNC5, PIDD, and Ankyrin [UPA] subdomains) and caspase-recruitment domain (CARD) are conserved across human/rodent NLRP1 and CARD8. The pyrin domain (PYD) exclusively or the PYD, nucleotide-binding domain (NBD) and leucine-rich repeat (LRR)-containing domain are absent in rodent NLRP1 and CARD8, respectively, and are dispensable for inflammasome formation. Adapted from multiple sources (Mitchell et al., 2019; Huang et al., 2021).

Human NLRP1 is a 1473 amino acid protein and contains a N-terminal PYD, a NBD, a LRR domain, a function to find domain (FIIND), and a C-terminal CARD (Chu et al., 2001). Unique to this NLR and structurally similar proteins is the requirement for 'functional degradation' as a prerequisite for inflammasome assembly (Sandstrom et al., 2019). Under resting conditions, the dipeptidyl peptidase (DPP) family members, DPP8/9, interact with the NLRP1 or CARD8 FIIND and repress their activity (Zhong et al., 2018; Griswold et al., 2019) (**Figure 1.6**).

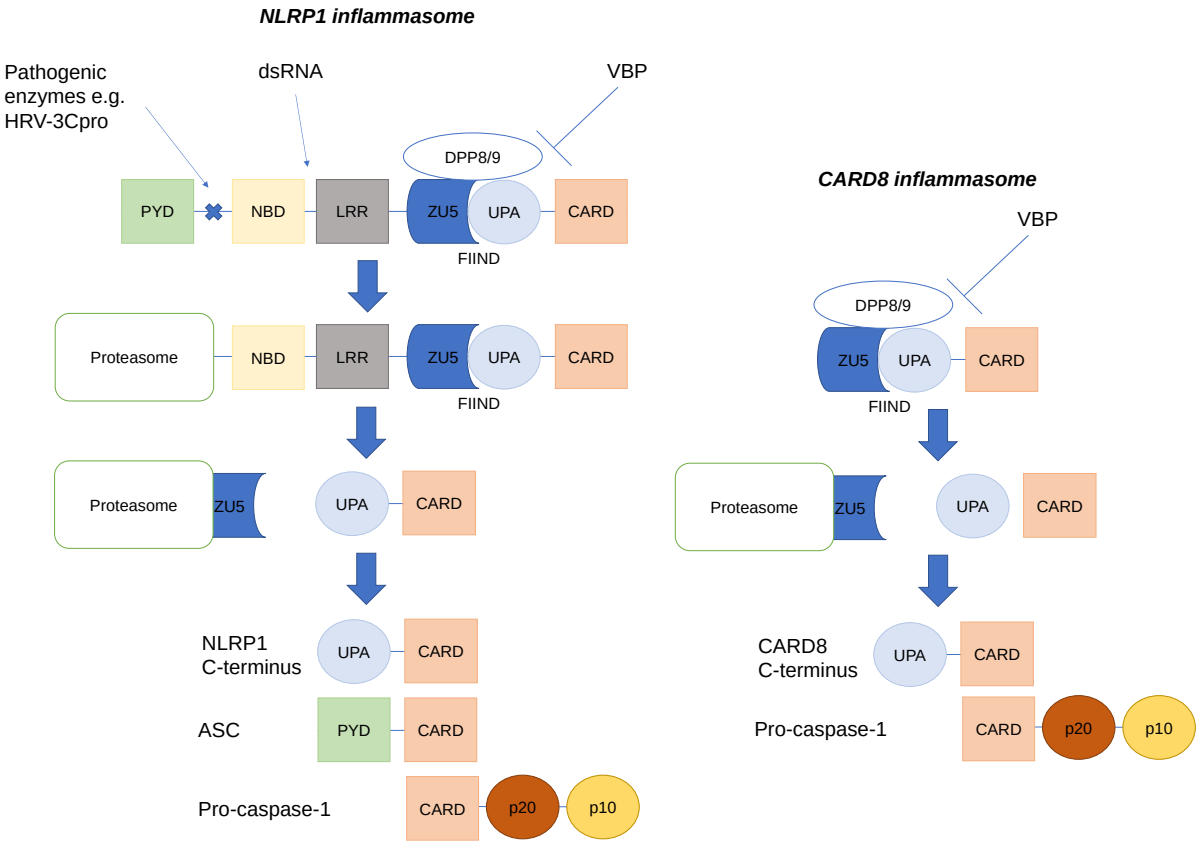

Figure 1.6. 'Functional degradation' model of NLRP1 and CARD8 activation.

Destabilised N-termini generated by the direct proteolytic cleavage of NLRP1 by pathogenic enzymes are detected and ubiquitinylated, by the cullin$^{ZER1/ZYG11B}$ complex in the case of human rhinovirus 3C protease (HRV-3Cpro), leading to proteasomal targeting. Alternatively, NLRP1:dsRNA binding or DPP8/9 inhibition also target NLRP1 or CARD8 for proteasomal degradation by yet undefined mechanisms that are independent of the N-degron pathway. Irrespective of the activation signal, obliteration of the autoinhibitory N-termini leads to FIIND auto-proteolysis and liberation of the UPA-CARD fragments to initiate the NLRP1 or CARD8 inflammasomes. Adapted from multiple sources (Mitchell et al., 2019; Robinson et al., 2020; Bauernfried et al., 2021).

Diverse pathogen-encoded effectors or DPP8/9 inhibition, however, can overcome this repression and activate NLRP1 or CARD8. Since the found in ZO-1 and UNC5 subdomain (ZU5) is autoinhibitory, processive processing of the N-terminal via the proteasome facilitates FIIND auto-processing and the release of the bioactive C-terminal region to activate the NLRP1 or CARD8 inflammasomes (Sandstrom et al., 2019). The species and/or cell type appear to determine whether the inflammasome

response is driven by NLRP1 or the closely related CARD8. CARD8 was formerly shown to bind to and inhibit the NLRP3 inflammasome, but under certain conditions, can itself form an inflammasome (Ito et al., 2014; Johnson et al., 2018). Since CARD8 is absent from the murine genome, both pathogenic enzymes and DPP8/9 inhibition by Valinyl-L-boroproline (VBP) activate NLRP1 isoforms (Chavarría-Smith and Vance, 2013; Okondo et al., 2018; Sandstrom et al., 2019). In human cells, however, inhibition of DPP8/9 activates NLRP1 in keratinocytes but CARD8 in myeloid and T cells (Johnson et al., 2018; Zhong et al., 2018; Linder et al., 2020). NLRP1 forms a classical ASC-containing inflammasome, surprisingly via CARD-CARD interactions, whilst CARD8 recruits caspase-1 directly and thus activation leads to minimal IL-1β secretion (Okondo et al., 2017; Zhong et al., 2018; Ball et al., 2020)

1.8 Inflammasomes in AECs

Although research has predominantly focused on myeloid cell inflammasomes, emerging evidence suggests that non-haematopoietic cells can also activate inflammasome-dependent programs (Jha et al., 2017; Chen et al., 2018b; Sellin et al., 2018; Bai et al., 2020).

Previous reports have suggested that an array of inflammasome-forming complexes may be important in the respiratory epithelium (**Table 1.2**):

Table 1.2. Summary of AEC inflammasomes.

Note that AECs denoted with * were not derived from commercial sources and [#] indicates that a specific inflammasome sensor was not confirmed.

Cell type	Species	Inflammasome	Activator	Reference
Primary HBEC	Human	NLRP1	VBP or HRV16	(Robinson et al., 2020)
HBEC3-KT	Human	NLRP1	dsRNA	(Bauernfried et al., 2021)
16HBE14o-	Human	NLRP3[#]	Cigarette smoke extract	(Mortaz et al., 2011)
Primary AEC*	Human	NLRP3	Urban particulate matter	(Hirota et al., 2012)
BEAS-2B	Human	NLRP3	Silica particles	(Peeters et al., 2013)
Primary HBEC	Human	NLRP3	HRV14	(Piper et al., 2013)
Primary HBEC	Human	NLRP3	RSV	(Triantafilou et al., 2013)
Primary HBEC and 16HBE14o-	Human	NLRP3	LL-37 and *P. aeruginosa*	(McHugh et al., 2019)
Primary AEC* Primary HBEC	Mouse Human	NLRP3 NLRP3 and RIG-I MxA	Influenza A	(Allen et al., 2009) (Pothlichet et al., 2013) (Lee et al., 2019)
TC-1	Mouse	Non-canonical caspase-11	*B. thailandensis*	(Wang et al., 2018b)

Pseudomonas aeruginosa (in the presence of the cathelicidin LL-37), Influenza A, respiratory syncytial virus, and human rhinovirus 14 (HRV14) infection have all been associated with caspase-1 activation and IL-1β secretion (Allen et al., 2009; Piper et al., 2013; Pothlichet et al., 2013; Triantafilou et al., 2013; McHugh et al., 2019). NLRP3 was suggested to be the specific inflammasome sensor, however, little direct evidence implicates this NLR. Indeed, there is controversy regarding the levels of epithelial NLRP3, particularly when compared with luminal immune cells (Kummer et al., 2007; Hirota et al., 2012; Rossios et al., 2018). This, alongside more recent findings that the non-canonical inflammasome mediates *Burkholderia thailandensis* infection via caspase-11, and the discovery that the novel human myxoma resistance protein 1 (MxA) inflammasome orchestrates responses to Influenza A infection, suggest that multiple epithelial inflammasomes may be functional (Wang et al., 2018b; Lee et al., 2019).

While this project was ongoing, the first biological ligand for human NLRP1, human rhinovirus 3C protease (HRV-3Cpro), was identified using primary HBECs (Robinson et al., 2020). Analogous to rodent NLRP1B activation by *B. anthracis* lethal toxin, HRV-3Cpro directly cleaves human NLRP1 between Glu^{130} and Gly^{131} to generate destabilised N-termini for proteasomal degradation (**Figure 1.5**). This may also apply to other *Picornaviridae* family members encoding 3Cpro since 3Cpro-mediated inflammasome activation has been corroborated using other cell types (Tsu et al., 2021). Even more recently, it was revealed that dsRNA (generated by positive-strand RNA viruses during replication) activates the NLRP1 inflammasome in the HBEC3-KT cells line, likely via direct interactions with the LRR domain and NBD (Bauernfried et al., 2021). Activation was proteasome-dependent but N-end rule pathway-independent, thus the exact mechanism of action remains to be elucidated. Together this suggests that HBECs mount an NLRP1-driven response following viral challenge.

1.9 IL-1 biology

IL-1α and IL-1β constitute the IL-1 subfamily of pro-inflammatory cytokines and both orchestrate acute inflammatory responses but differ in terms of expression patterns and processing. Full-length IL-1α is constitutively expressed in non-hematopoietic cells and can be released as an 'alarmin' upon necrosis (Kim et al., 2013). Secretion may be mediated by inflammasome activation; however, processing is reliant on calpains rather than caspase-1 (Fettelschoss et al., 2011; Groß et al., 2012). Conversely, pro-IL-1β accumulation in macrophages, neutrophils, lymphocytes, epithelial cells, and fibroblasts is driven by local cytokines or TLR engagement (Dinarello, 1994). Intracellularly, active caspase-1 drives N-terminal cleavage at residue A117 to produce mature, bioactive IL-1β (Netea et al., 2015). The mechanism underlying mature IL-1β secretion remains unclear, but proposals include lysosome exocytosis, microvesicle shedding, exosome shedding, cell death, and 'sublethal' gasdermin pores (Andrei et al., 2004; Bianco et al., 2005; Qu et al., 2007; Bergsbaken et al., 2009; Evavold et al., 2018). Pro-IL-1β may also be released into the extracellular milieu following cell lysis or tissue injury (Lopez-Castejon and Brough, 2011). Here it is cleaved into bioactive IL-1β by serine proteases and metalloproteinases including cathepsin-G, elastase, chymase, chymotrypsin (Y113), proteinase 3 (V114) and the meprins (D116) (Netea et al.,

2015). Both full-length and cleaved IL-1α, but only cleaved IL-1β, bind to the ubiquitously expressed IL-1 receptor, type 1 (IL-1R1) (Mosley et al., 1987). This induces the recruitment of the IL-1R accessory protein (IL-1RAcP) and the formation of a multimeric protein complex (Sims et al., 1988). In turn, this complex recruits MyD88, IL-1R-associated kinase 1 (IRAK) and TNF receptor-associated factor (TRAF)6 adaptor proteins (Greenfeder et al., 1995). This culminates in NF-κB activation which further enhances pro-IL-1β expression, driving the secretion of TNF-α and IL-6, to recruit and activate neutrophils and macrophages. Negative regulation of IL-1 signalling is conferred by the IL-1R antagonist (IL-1Ra) and IL-1R2 which function as competitive inhibitors of IL-1R1 or IL-1 cytokines, respectively (Dripps et al., 1991; Symons et al., 1995).

1.10 IL-18 biology

The IL-1 superfamily also encompasses IL-18 or IFN-γ-inducing factor. Like IL-1β, inactive pro-IL-18 requires inflammasome-dependent or -independent processing for biological activity. Pro-IL-18 can be processed by caspase-1 (N36), proteinase 3 (I47), meprin β (D52) and chymase (L56) (Netea et al., 2015). Pro-IL-18 is constitutively expressed and is predominantly found in macrophages and dendritic cells upon activation (Dinarello et al., 2013). IL-18 can induce the differentiation of $CD83^+$ $CCR7^+$ NK helper cells with the capacity to produce IFN-γ (Mailliard et al., 2005). It also has a pleiotropic role in either T helper type 1 (T_H1) or T_H2 responses depending on the prevailing cytokine environment (Nakanishi et al., 2001). Synergism with IL-12 or IL-15 upregulates IL-18Rβ co-receptor expression, which stabilises the IL-18/IL-18Rα interaction and induces IFN-γ. A T_H2 response, however, is induced in the absence of IL-12 or IL-15, and responses in the context of sterile inflammation may contribute to inflammatory diseases including COPD (Imaoka et al., 2008). To mitigate this, IL-18 signalling is under tight regulation by the restricted expression of IL-18Rβ (T cells and dendritic cells) and by IL-18 binding protein (IL-18BP) which has a high affinity for cleaved IL-18 (Dinarello et al., 2013).

1.11 IL-33 biology

IL-33 (or nuclear factor from high endothelial venule [NF-HEV]) is the most recent addition to the IL-1 superfamily. Full-length IL-33 is chromatin-associated within endothelial and epithelial cells and, like full-length IL-1α, is released as an ‘alarmin’

(Lefrançais et al., 2012). Although pro-IL-33 can be cleaved by caspase-1 (at residue D178), caspase-1 processing results in biological inactivity and it is dispensable for extracellular release upon LPS stimulation (Cayrol and Girard, 2009; Ohno et al., 2009). Full-length IL-33, or extracellularly processed IL-33, can bind to ST2 (IL1RL1) on type 2 innate lymphoid cells (ILC2s), T_H2 cells, mast cells, basophils, eosinophils, invariant NK cells and NK cells. The aa95-270, aa99-270 and aa109-270 forms matured by neutrophil elastase, cathepsin G and proteinase 3 have a 10-fold greater activity than full-length IL-33 in cellular assays (Lefrançais et al., 2012). Like other IL-1 superfamily members, the IL-33-ST2 dimer forms a complex with IL-1RAcP, which activates signalling via MyD88, and drives a predominantly T_H2 cytokine response (but also T_H1 and T_H17 responses in pro-inflammatory diseases) (Borthwick, 2016). Two additional splice variants of the ST2 gene exist; soluble ST2 (sST2) which functions as a decoy receptor, and ST2V which may modify IL33-ST2 signalling in the gastrointestinal tract (Tago et al., 2001; Hayakawa et al., 2007).

1.12 Additional functions of inflammasome components

While considerable attention has focused on the role of inflammasome-forming PRRs in assembling caspase-activating platforms, it is becoming increasingly evident that several components also fulfil inflammasome-independent functions. For example, while NLRP3 and ASC protect mice from pneumococcal pneumonia during *Streptococcus pneumoniae* infection, caspase-1/11, IL-1β and IL-18 appear dispensable. Upon infection, NLRP3 maintains barrier integrity by enhancing pneumocyte adhesion to the extracellular matrix (Kostadinova et al., 2016). Moreover, NLRP3 and ASC facilitate STAT6 phosphorylation and downstream sterile alpha motif pointed domain-containing ets transcription factor (*Spdef*) expression, culminating in the induction of mucosal defence factors such as MUC5AC (Fang et al., 2019). NLRP3 also engages in inflammasome-independent programmes in response to other pathogens including *Francisella tularensis* and *Nippostrongylus brasiliensis* nematodes (Periasamy et al., 2016; Chenery et al., 2019).

In non-respiratory tissues, AIM2 represses colon tumorigenesis in the absence of ASC and IL-1β (Wilson et al., 2015). This is due to the suppression of Akt activation via AIM2:DNA-dependent protein kinase binding and inhibition, a finding which was

further elaborated by a recent microglial publication (Ma et al., 2021). Currently, there has been little investigation into the inflammasome-independent functions of NLRC4, however, it may also be implicated in malignancy progression. Indeed, mice deficient in NLRC4 but not ASC or caspase-1 have increased tumour growth compared with wildtype (WT) controls (Janowski et al., 2016).

Finally, there are several examples of additional roles which are currently inseparable from inflammasome function. For example, the more recently characterised NLRP6 sensor appears to mediate both pyroptosis and necroptosis in mice infected with *Staphylococcus aureus* (Ghimire et al., 2018). It may also drive mucin secretion from intestinal goblet cells through exocytosis regulation (Wlodarska et al., 2014; Birchenough et al., 2016). It is therefore perhaps not surprising, due to the shared embryonic origin and cell types, that other NLRs may be implicated in airway secretory cell functions. As such, HRV16- or VBP-mediated NLRP1 activation causes increased mucin expression in HBECs (Robinson et al., 2020) (**Figure 1.7**).

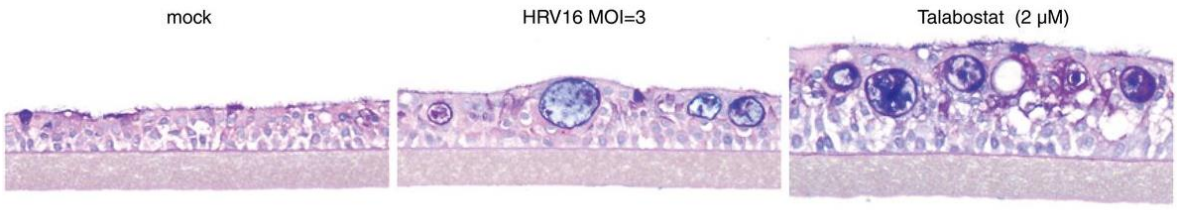

Figure 1.7. NLRP1 activation drives mucin upregulation or secretory cell differentiation.

HBECs treated with HRV16 or VBP (Talabostat) for 48 hours were FFPE and sectioned, before Alcian blue and periodic acid–Schiff (AB-PAS) staining. AB stains acidic mucins blue whereas PAS stains neutral mucins magenta (Robinson et al., 2020).

It is unclear if activating the NLRP1 inflammasome impacts secretory cell differentiation or merely induces their production of mucins, which may be indirectly attributed to downstream cytokine responses.

1.13 COPD pathophysiology

COPD is defined as the presence of irreversible airflow obstruction with a forced expiratory volume in one second (FEV_1) and forced vital capacity (FVC) ratio of <

70 %, and an overall reduction in FEV_1 (Meijer et al., 2013). It is frequently progressive and is associated with an abnormal inflammatory response to noxious particles, which is amplified during viral (primarily HRV, coronavirus, and influenza A and B) or bacterial exacerbations (primarily *Haemophilus influenzae*, *Moraxella catarrhalis* and *S. pneumoniae*) (Seemungal et al., 2001; Rosell et al., 2005). Histopathological alterations in the lungs of COPD patients show alveolar destruction (emphysema) and/or inflammation and mucus hyperplasia (chronic bronchitis). Risk factors include tobacco smoking, environmental exposures (including wood smoke and cadmium) and occasionally genetic abnormalities such as α_1-antitrypsin deficiency which accounts for ~1 % of cases (DeMeo and Silverman, 2004). In the UK, an estimated 1.2 million patients have COPD, resulting in 30,000 deaths/year and healthcare costs of £500 million/year (Snell et al., 2016).

1.14 Human rhinovirus in COPD

Up to 67 % of COPD exacerbations are associated with viruses, and of these, HRVs (family: Picornaviridae; genus: Enterovirus) are the most frequently detected in patient sputum samples (Seemungal et al., 2001; Calderazzo et al., 2019). HRVs are positive-sense, single-stranded RNA (ssRNA) viruses with three serotypes: HRV-A, HRV-B and HRV-C. Intercellular adhesion molecule 1 (ICAM-1) on AECs is the primary entry receptor for most HRV-A and HRV-B genotypes, however, the low-density lipoprotein receptor (LDLR) and cadherin-related family member 3 (CDHR3) mediate the entry of several HRV-A serotypes and all HRV-C serotypes, respectively (Hofer et al., 1994; Bochkov et al., 2015). Once intracellular, HRV induces endosomal rupture or the formation of ion channel pores, enabling the release of viral ssRNA into the cytosol (Jacobs et al., 2013). Here, it is translated by the host cell machinery into a polyprotein which is processed by virally encoded proteases, 2A protease and 3Cpro, into capsid (VP1-4) and replication-dependent proteins.

Receptor expression may be the rate-limiting stage of productive HRV infection. Only < 9 % of differentiated cells express ICAM-1 compared with ~33 % of basal cells and this may explain the low rates of ciliated cell infection and cytotoxicity (Lopez-Souza et al., 2004; Jakiela et al., 2008; Warner et al., 2019). In AECs from COPD versus control patients, however, ICAM-1 mRNA is increased, and the disrupted barrier function may facilitate access to the more sensitive basal cells

(Schneider et al., 2010; Aghapour et al., 2018). HRV infections in susceptible COPD patients may also precipitate secondary bacterial infections by augmenting bacterial adhesion to the respiratory epithelium and by impairing the functions of alveolar macrophages and antimicrobial peptides (Oliver et al., 2008; Wang et al., 2009; Mallia et al., 2012).

1.15 Bacterial infection in COPD

Bacteria are present in the airways of stable COPD patients and during exacerbations, where the bacterial load increases and new strains may be acquired (Sethi et al., 2002; Rosell et al., 2005). Antibiotics are considered a mainstay of exacerbation treatment where the sputa is purulent (yellow/green mucus containing polymorphonuclear neutrophils), and early bacterial clearance ameliorates inflammatory markers including neutrophil myeloperoxidase (Anthonisen et al., 1987; White et al., 2003). This reliance on antibiotics, however, may have increased the airway prevalence of less sensitive Gram-negative species, now commonly attributed to bacterial exacerbations.

H. influenzae is a facultative anaerobe and a commensal resident of the nasopharynx (Osman et al., 2018). It is the main aetiological agent of bacterial exacerbations and is categorised into the typable serotypes (a-f) or non-typeable *H. influenzae* (NTHi) based on the presence or absence of the polysaccharide capsule, respectively.

M. catarrhalis is an obligate aerobe and a frequent commensal of the upper respiratory tract flora (Sethi and Murphy, 2001). An inciting incident, however, such as viral infection may instigate COPD exacerbations and facilitate the detection of pure *M. catarrhalis* diplococci in sputum samples or transtracheal aspirates.

P. aeruginosa is a common facultative anaerobe in cystic fibrosis and bronchiectasis, and can be identified in COPD patients requiring hospitalisation (Garcia-Vidal et al., 2009). *P. aeruginosa* isolates are heterogenous and include highly motile organisms, as well as more sessile isolates which secrete extracellular polysaccharides to form biofilms, enhancing bacterial aggregation and antibiotic resistance (Faure et al., 2018; Zhao et al., 2020).

For these commensals and opportunistic pathogens, the existence or mechanisms indicating a circuitous intracellular life cycle within AECs have yet to be fully elucidated, however, host cell adhesion has been well documented (de Vries et al., 2009; Duell et al., 2016; Badaoui et al., 2020). This involves type IV pilus and outer membrane protein binding to host cell receptors including ICAM1, carcinoembryonic antigen-related cell adhesion molecule 1 (CEACAM1) or integrin β1. Inflammasome activation may be a key consequence of bacterial infection since sputum IL-1β manifests as the only specific biomarker reflecting bacterial exacerbations of COPD, however, the cellular source remains to be determined (Bafadhel et al., 2011).

1.16 Inflammasomes in COPD

Although not well defined in COPD, molecules involved in inflammasome activation are elevated in patient bronchoalveolar lavage fluid (BALF), including high mobility group protein B1 (HMGB1), extracellular ATP, ASC, and reactive oxygen species, whereas NLRP3 and caspase-1 mRNA are increased in peripheral blood mononuclear cells (PBMCs) and bronchial tissue (Hou et al., 2011; Muller et al., 2011; Franklin et al., 2014; De Falco et al., 2017; Wang et al., 2018a). Recent evidence has also suggested that AIM2 is enhanced in alveolar macrophages and HBECs from COPD patients compared with healthy controls and that it redistributes from the nucleus to the cytoplasm upon cigarette smoke exposure (Tran et al., 2021). Additionally, dysregulated inflammasome-regulated cytokines (IL-1β, IL-18 and IL-33) likely contribute to the pathogenesis of the disease.

IL-1β in the sputum and cells is elevated in stable COPD patients compared with non-COPD controls (Keatings et al., 1996; Botelho et al., 2011; Pauwels et al., 2011). Serum IL-1β and IL-17 are further enhanced during COPD exacerbations, and these cytokines positively correlate with serum C-reactive protein levels, neutrophil levels, and smoking pack-years, but inversely correlate with FEV_1 (Zou et al., 2017). Furthermore, IL-1R1 knockout (KO) mice are protected from cigarette smoke-induced accumulation of inflammatory cells in the BALF and tissue sections, and neutrophil accumulation in the WT BALF is attenuated following anti-IL-1β treatment (Pauwels et al., 2011).

IL-18 over-expression causes emphysematous lesions, the accumulation of inflammatory cells ($CD8^+$ T cells, macrophages, neutrophils, and eosinophils) and

associated cytokines in mice (IFN-γ, IL-5 and IL-13) (Hoshino et al., 2007). Moreover, IL-18Rα KO mice are protected against cigarette smoke-induced inflammation and emphysema (Kang et al., 2007). In COPD patients, IL-18 is elevated in alveolar macrophages (IL-18R expression is also increased), $CD8^+$ T cells and epithelial cells, and serum IL-18 negatively correlates with predicted FEV_1 (Imaoka et al., 2008; Singh et al., 2011).

IL-33 and ST2 expression are increased in COPD sufferers and murine models, as is the infiltration of neutrophils and macrophages, and the expression of associated pro-inflammatory genes (TNF-α, IL-1β, IL-17, CCL2 and MUC5AC), which can be abrogated in mice using anti-IL-33 therapy (Qiu et al., 2013; Xia et al., 2015). IL-33 is highly expressed in human and murine bronchial cells and PBMCs, and the latter's stimulation with cigarette smoke plus IL-33 has a synergistic effect on IL-6 and IL-8 synthesis (Wu et al., 2014; Zhao et al., 2015). Cigarette smoke also downregulates ST2 on ILC2s, but upregulates ST2 on NK cells and macrophages, exacerbating T_H1-like inflammation at the expense of T_H2 cytokine responses.

Human genetic evidence also supports the concept that inflammasomes are involved in COPD. Coding single nucleotide polymorphisms (SNPs) in *NLRP1* are associated with decreased lung function and elevated serum IL-1β levels in patients (Ozretić et al., 2019).

1.17 Modelling the airway epithelium

Classically, human AEC lines have been used to maximise utility and cost-effectiveness, while minimising the intra- and inter-donor variability associated with primary cells. Patently, many of these immortalised cells fail to sufficiently recapitulate *in vivo* physiology (**Table 1.3**):

Table 1.3. Comparison of primary HBECs and commonly utilised human AEC lines.

The capacity of AEC models to form tight junctions, cilia and mucus upon ALI culture is indicated. SV40, Simian Virus 40. hTERT, human telomerase. CDK4, cyclin-dependent kinase four.

Cell type	Origin	Morphology	Tight junctions	Cilia formation	Mucus production	References
Primary HBECs	HBECs from non-cancerous patients	"Cobblestone-like"	Yes	Yes	Yes	(Stewart et al., 2012; Rayner et al., 2019; Luengen et al., 2020)
A549	Alveolar epithelial cells from adenocarcinoma	"Cobblestone-like"	Non-functional	N/A	N/A (surfactants)	(Lieber et al., 1976; Winton et al., 1998)
BEAS-2B	HBECs transformed with SV40 plasmid	"Cobblestone-like"	No	No	No	(Reddel et al., 1988; You et al., 2004; Stewart et al., 2012)
Calu-3	HBECs from adenocarcinoma	"Cobblestone-like" islands	Yes	Pseudo-cilia	Yes	(Winton et al., 1998; Grainger et al., 2006; Stewart et al., 2012)
HBEC3-KT	HBECs transformed with CDK4 and hTERT	"Cobblestone-like"	Yes	Yes	Yes	(Ramirez et al., 2004; Vaughan et al., 2006; Delgado et al., 2011)
16HBE14o-	HBECs transformed with SV40 plasmid	"Cobblestone-like"	Yes	Yes	No	(Cozens et al., 1994; Winton et al., 1998; Tong et al., 2014)

Mechanistic studies of the respiratory epithelium have benefitted extensively from the conception and refinement of primary culture models. Primary epithelial cells from brushed or digested nasal turbinates, trachea or bronchi can be assayed under submerged conditions, facilitating the expansion of $CD49f^+$ $CD271^+$ basal epithelial cells to represent the dominant population (Fulcher and Randell, 2013). Such monocultures may be useful for investigating basal cell-specific phenotypes using high-throughput approaches, but additional models are required to represent the multicellular complexity of the *in vivo* epithelium (**Figure 1.8**).

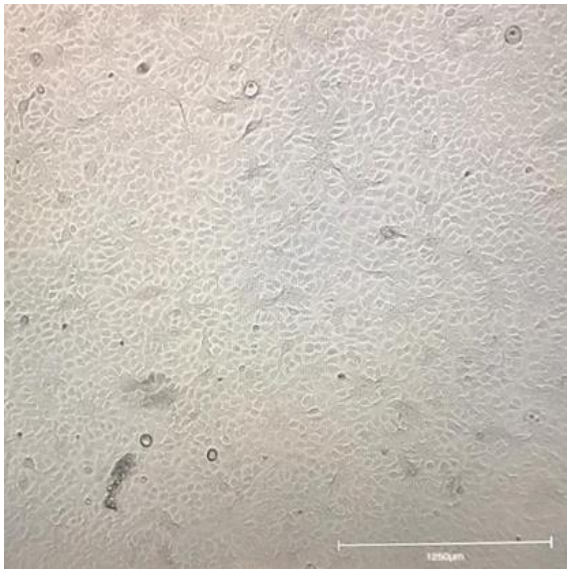

Figure 1.8. Submerged, primary basal cells with the phenotypic "cobblestone-like" morphology.

HBECs were revived from liquid nitrogen and cultured for seven days in T75 flasks until confluence. Brightfield image was acquired on an EVOSM500 at 4x objective. Scale bar: 1250 μm.

The most universal of these is the ALI system which facilitates the *in vitro* reconstruction of a pseudostratified columnar epithelium, consisting of basal, progenitor, secretory and ciliated cells (**Figure 1.9**).

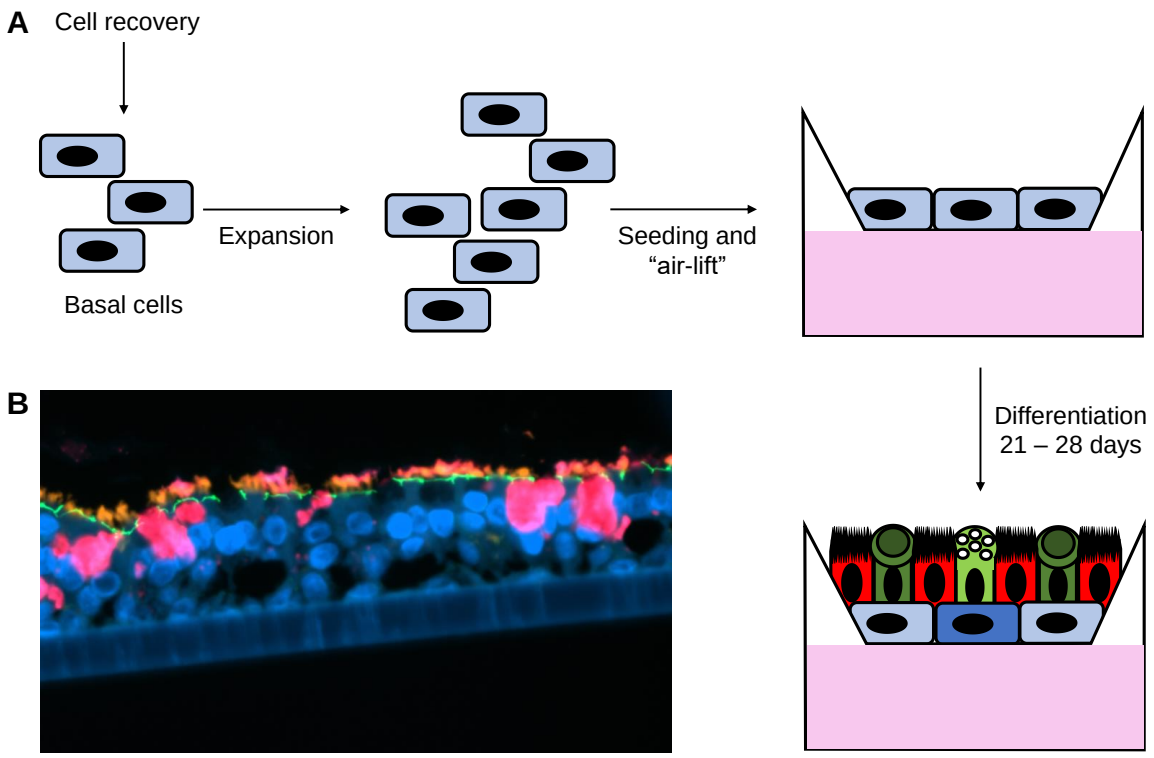

Figure 1.9. *In vitro* generation of a pseudostratified columnar epithelium using the ALI system.

(**A**) Following an expansion phase, basal cells are seeded onto porous cell culture inserts. The apical medium is removed (“air-lifting”) and basal cells differentiate over a 21-28-day period. (**B**) Immunofluorescence was performed on FFPE ALI-differentiated HBECs. Nuclei were stained with Hoechst (blue), goblet cells with MUC5AC (red), ciliated cells with acetylated-tubulin (orange) and tight junctions with ZO-1 (green). Cells were visualised using an Axio Scan Z1 (Zeiss).

To mimic native conditions, primary basal cells are seeded onto permeable culture plate inserts, then exposed to air apically and a differentiation-supporting medium basolaterally. Commercial differentiation media compositions are generally proprietary; however, several components are known/can be speculated due to compensatory details from vendors and laboratory-specific preparations. For example, supplementing with retinoic acid inhibits squamous metaplasia and enhances mucin expression, while incorporating hydrocortisone facilitates mucociliary clearance by engaging ion transport pathways (Yoon et al., 1997; Yoon et al., 1999; Zaidman et al., 2016). The resulting differentiated cultures are morphologically and transcriptionally analogous to the *in vivo* epithelium; producing mucins, inflammatory mediators, and functional cilia (Karp et al., 2002; Dvorak et

al., 2011; Pezzulo et al., 2011). HBECs from healthy donors also establish TEER values of 0.5 – 1.2 kΩ/cm^2 between days eight and 28, and there is some evidence that TEER is reduced in cells from COPD donors (Lin et al., 2007; Pezzulo et al., 2011; Gindele et al., 2020). In addition to recapitulating epithelial biology, ALI-cultured epithelium is amenable to clustered regularly interspaced short palindromic repeat-CRISPR-associated protein 9 (CRISPR-Cas9) genome editing (Rapiteanu et al., 2020). Delivery of a ribonucleoprotein (RNP) complex, composed of a guide RNA (gRNA; itself composed of the targeting crispr RNA [crRNA] and tracr RNA scaffold) and the Cas9 nuclease, generates a double-strand break at the target DNA locus. Endogenous repair processes, namely non-homologous end joining, or homology-directed repair (in the presence of a template) may then lead to gene KOs or knockins (KIs), respectively. CRISPR-Cas9 can therefore facilitate the determination of individual gene contributions to physiology and pathology.

1.18 Project aims

The objective of this project was to ascertain the role of HBEC inflammasomes in respiratory physiology and pathology. Based upon the literature summarised above, it was hypothesised that inflammasomes other than NLRP3 may be important in the respiratory epithelium and that the inflammasome repertoire may be limited to mitigate spontaneous activation. It was also hypothesised that inflammasome responses may be disproportionate in COPD and that NLRs could be involved in epithelial differentiation. The following aims were developed to test these hypotheses:

- Determine the expression profiles of inflammasome components in human lung tissue and cultured HBECs.
- Quantify inflammasome responses to PRR agonists and common respiratory pathogens.
- Compare inflammasome responses in HBECs derived from healthy and COPD patients.
- Generate CRISPR-Cas9 KO HBECs to validate findings and investigate NLR contributions to differentiation.

Overall, it was identified that inflammasome activity in HBECs is specifically driven by NLRP1 and this has recently been confirmed by an external publication

(Robinson et al., 2020). DPP8/9 inhibition with VBP drives a canonical inflammasome response, characterised by ASC speck formation, cell death and cytokine secretion. In addition, it was demonstrated that NLRP1, DPP8 and DPP9, are upregulated in basal epithelial cells derived from COPD patients in comparison to healthy controls, leading to exaggerated responses. Also revealed here is that NLRP1 contributes to HBEC differentiation, particularly at the progenitor cell stage. These data, therefore, support the concept that NLRP1 is the dominant inflammasome in HBECs and, due to the susceptibility of COPD patients to viral exacerbations and differentiation defects, suggest that NLRP1 may be a novel therapeutic target for individuals with this respiratory disease.

Chapter 2. Materials and methods

2.1 Human tissue and HBECs

Human biological samples were collected with informed consent under the IRB/EC approved protocol IRAS ID 212537. Cancer-adjacent lung tissues were supplied within 24 hours post tumour resection surgery from Birmingham Heartlands Hospital, United Kingdom. Sections containing large airways (> 6 mm diameter) were dissected out and transferred to 4 % Parafix (PEC/R/38, Pioneer). BALF samples were obtained during bronchoscopy and collected in 50 mL normal saline (0.9 % NaCl) by the Medicines Evaluation Unit (MEU) Manchester, United Kingdom. BALF from healthy smokers (no history of chronic respiratory disorders), COPD infrequent exacerbators (0 exacerbations in the previous year) and COPD frequent exacerbators (≥3 exacerbations in the previous year or ≥2 exacerbations in each of the last two years) were snap-frozen and stored at -80°C until Luminex assay. Primary HBECs were purchased from Epithelix or Lonza and used at passage 1-2 (**Table 2.1**):

Table 2.1. Summary of human bronchial epithelial cell (HBEC) donors.

The smoking status was not disclosed for Asthma 0000344668 and 0000470633.

Product number	Source	Batch number	Health status	Sex	Age	Smoker?
EP40	Epithelix	AB037201	Healthy	Male	78	No
EP40	Epithelix	AB039401	Healthy	Male	55	No
EP42	Epithelix	02AB061001	Healthy	Female	47	Yes
EP42	Epithelix	AB053201	Healthy	Male	55	Yes
EP42	Epithelix	02AB066902	Healthy	Female	46	Yes
TAN 25424	Lonza	000333288	Healthy	Female	54	No
TAN 28318	Lonza	0000446317	Healthy	Male	67	Yes
TAN 28910	Lonza	0000482214	Healthy	Male	62	No
TAN 35773	Lonza	18TL127524	Healthy	Male	69	No
EP41	Epithelix	AB049502	Asthma	Male	52	No
EP53	Epithelix	02AB066501	Asthma	Female	55	No
TAN 25786	Lonza	0000344668	Asthma	Female	54	?
TAN 28695	Lonza	0000470633	Asthma	Male	69	?
TAN 29734	Lonza	0000534647	Asthma	Female	55	No
EP18	Epithelix	AB006302	COPD	Female	73	Yes
EP44	Epithelix	02AB066702	COPD	Male	65	Yes
EP44	Epithelix	AB005801	COPD	Male	52	Yes
TAN 26680	Lonza	0000370751	COPD	Female	65	No
TAN 27571	Lonza	0000415058	COPD	Male	53	Yes

2.2 Cell culture and HBEC differentiation

Primary HBECs, BEAS-2B cells (CRL-9609, ATCC) or HBEC3-KT cells (CRL-4051, ATCC) were expanded in bronchial epithelial cell growth medium (BEGM; Lonza). Upon confluency, cells were dissociated by trypsinization and seeded in BEGM at 1.0×10^4 cells/well in 96-well Imaging Microplates (Corning) or seeded at 1.0×10^5 cells/well in 6-well plates for small interfering RNA (siRNA)-mediated knockdown

(KD) and cultured overnight. For ALI culture, cells were seeded at 1.5 x 10^5 cells/collagen-coated Transwell (6.5 mm with 0.4 µm pore, Corning). 1 mL BEGM was added to the basolateral chamber. After 48 hours, apical BEGM was removed to initiate ALI culture and the basolateral media was replaced with PneumaCult ALI Medium (Stem Cell). Basolateral PneumaCult was replenished every two days and a pseudostratified columnar cell layer developed over a 21-28-day period. WT and pooled NLRP3 KO THP-1 cells were provided by Anna Gram and have been characterised previously (Gram et al., 2021). These cells were cultured in RPMI, supplemented with 10 % heat-inactivated foetal bovine serum, 1 % GlutaMAX and 1 % sodium pyruvate (Gibco). THP-1 cell density was maintained between 0.2 x 10^6 and 1 x 10^6 cells/mL. Where indicated, macrophage-like differentiation was induced using 200 ng/mL phorbol-12-myristate 13-acetate (PMA) for 24 hours.

2.3 Immunohistochemistry and immunocytochemistry

Airway tissues were fixed overnight then processed using a Tissue-Tek VIP 6 and embedded using a Tissue-Tek TEC 5 (Sakura). For undifferentiated THP-1 cells, 10 million cells were fixed for 20 minutes and resuspended in HistoGel (Thermo Fisher) before processing and embedding. Alternatively, Transwells were bisected and embedded vertically before sectioning. Serial paraffin sections (4 µM) were prepared using a RM2135 Rotary Microtome (Leica) and deparaffinised with xylene before staining for NLRP1, NLRP3, NLRC4, ASC or caspase-1. Sections were heated for 15 minutes at 98˚C in a citrate acid-based antigen unmasking solution (Vector Laboratories), then endogenous peroxidase activity was blocked with 3 % hydrogen peroxide for 15 minutes. Individual slides were stained in goat serum (1:5; G9023, Sigma) containing rabbit polyclonal anti-NLRP1 (1:200; ab3683 Abcam), rabbit polyclonal anti-NLRP3 (1:200; HPA012878, Sigma-Aldrich), rabbit monoclonal anti-NLRC4 (1:50; 12421S, Cell Signalling), rabbit polyclonal anti-ASC (1:300; AG-25B-0006, AdipoGen), or rabbit polyclonal anti-caspase-1 (1:150; PA5-29342, Thermo Fisher) for 90 minutes at 37°C. Isotype control sections were incubated with matched concentrations of polyclonal (ab27478, Abcam) or monoclonal rabbit IgG (ab172730, Abcam). With intermediate Tris-buffered saline (TBS) washing steps, sections were incubated with goat anti-rabbit immunoglobulins/biotin (1:500; E0432, Dako) followed by streptavidin/HRP (1:500; P0397, Dako), both for 30 minutes at room temperature. Staining was visualised

by application of diaminobenzidine for five minutes. Slides were counterstained with haematoxylin to stain the nuclei and mounted in DPX Mountant (Sigma-Aldrich) using a CV5030 Fully Automated Glass Coverslipper (Leica), then digitally scanned using a Nanozoomer 2.0HT at 40x objective (Hamamatsu).

2.4 TLR stimulations

ALI-differentiated HBECs were stimulated with a panel of TLR agonists (InvivoGen) to determine the optimal conditions required for inflammasome priming. Since AECs may be hyporesponsive to TLR stimulation compared with myeloid cells, concentrations at the upper range of the manufacturer's recommendations were selected (Guillot et al., 2004; Platz et al., 2004). They were also based on a previous publication which demonstrated TLR-mediated IFN, IL-6 and IL-8 secretion from primary AECs (Ioannidis et al., 2013). TLR ligands were resuspended in endotoxin-free physiological water to 100 µg/mL. Stimuli were applied to Transwells both apically and basolateral (removing the apical stimuli after one hour) in PneumaCult without hydrocortisone and without antibiotics at the following concentrations: Pam3CSK4 (1 µg/mL; TLR1/2), poly I:C high molecular weight (10 µg/mL; TLR3), ultrapure LPS from *Escherichia coli* (10 µg/mL; TLR4), ultrapure flagellin from *P. aeruginosa* (1 µg/mL; TLR5), and FSL-1 (100 ng/mL; TLR2/6). After three or 24 hours, MagNa Pure LC RNA Isolation Tissue lysis buffer (Roche) was added, and the cell lysates stored at -80°C until qPCR.

2.5 Bacterial cell culture and infection

The bacteria used in this study were *M. catarrhalis* Bc-30 (ATCC 43627), non-typeable *H. influenzae* (NTHi) 1479 (ATCC 53600) and *P. aeruginosa* PA01 (provided by GlaxoSmithKline ID CEDD). Media compositions are outlined below (**Table 2.2**):

Table 2.2. Bacterial culture media.

Base media and supplements for the culture of *M. catarrhalis*, NTHi and *P. aeruginosa* are indicated. BHI broth, brain heart infusion broth.

Bacteria	Plate culture	Liquid culture	Liquid culture supplements
M. catarrhalis	Columbia blood agar (Oxoid)	BHI broth (Oxoid)	5 mM $MgCl_2$, 1.5 mM CaCl, 10 mM NaCl, 10 µg/mL hemin, and 0.15 % gelatin solution
NTHi	Columbia chocolate agar (Oxoid)	BHI (Oxoid)	10 µg/mL NAD, 10 µg/mL hemin, and 44 µL/mL glycerol
P. aeruginosa	LB agar (Invitrogen)	LB broth (Invitrogen)	None

Bacteria were streaked from frozen glycerol stocks onto the appropriate agar plates and then cultured overnight at 37°C. LB broth was inoculated with a single colony of *P. aeruginosa* and incubated with aeration and shaking at 200 RPM for 16 – 24 hours. *M. catarrhalis*/NTHi directly from the plate cultures, or *P. aeruginosa* from the intermediate liquid culture, were then resuspended in supplemented BHI (sBHI)/LB broth to OD_{600} = 0.1 (measured using an BioPhotometer [Eppendorf]) and incubated with aeration and shaking at 200 RPM. Every hour, OD_{600} was measured, and Miles Misra was used to enumerate the colony-forming unit (CFU) (Miles et al., 1938). To assess growth and survival, growth curves were generated for broth and static infection medium cultures (PneumaCult without hydrocortisone and without antibiotics) (**Figure 2.1**).

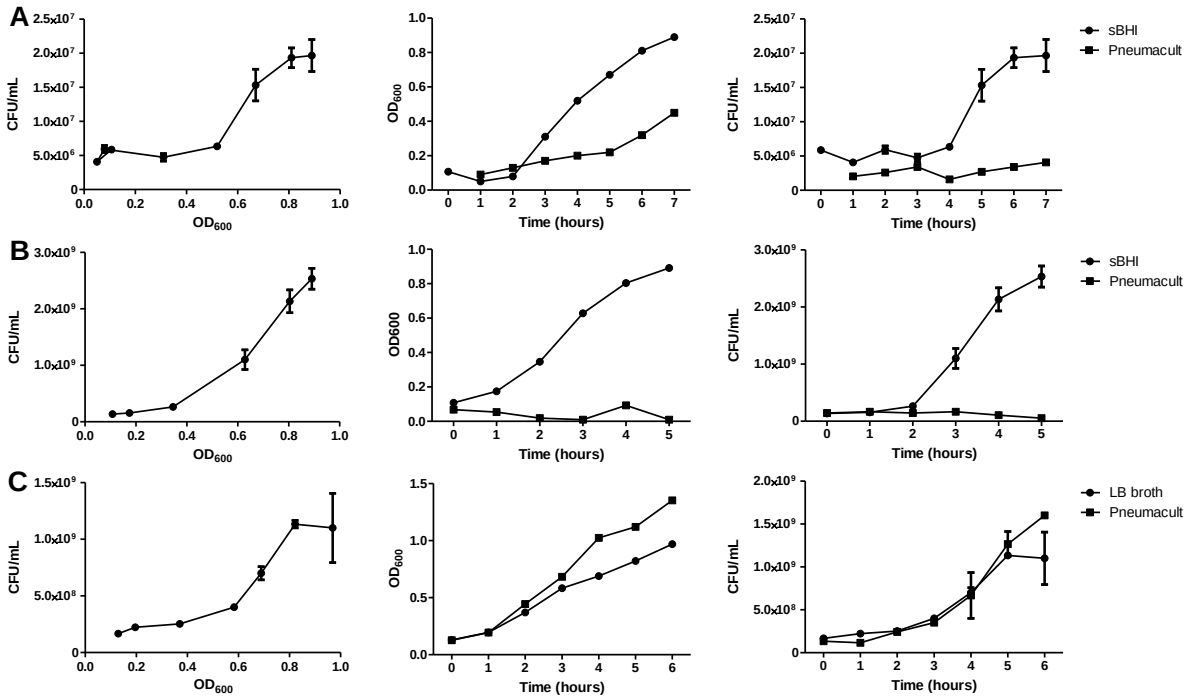

Figure 2.1. Growth curves for (A) *M. catarrhalis*, (B) NTHi and (C) *P. aeruginosa* in supplemented BHI (sBHI)/LB broth and PneumaCult.

Bacterial species were cultured in the indicated media at 37°C with 5 % CO_2. OD_{600} and CFU/mL measurements were recorded every hour. Except for *P. aeruginosa*, little to no growth was observed in PneumaCult potentially due to the lack of nutrient availability or clumping. Bacterial exposure to the apical surface of HBECs was therefore limited to one hour. Where indicated, data shown are the mean of three technical replicates ± SEM.

One day prior to the infection assay, ALI-differentiation medium was replaced with the infection medium. Once bacterial growth reached mid-logarithmic phase, OD_{600} = ~0.65, growth curves were used to calculate the CFU/mL required for the desired multiplicity of infection (MOI). ALI-differentiated HBECs were washed apically with phosphate-buffered saline (PBS) twice and then bacteria were applied in 50 µL infection medium. After one-hour, the apical medium was removed, and the cells were returned to the incubator for the desired timepoint until supernatant collection for Luminex assay.

2.6 *M. catarrhalis* adhesion and invasion assays

CFU-based adhesion and invasion assays have been described elsewhere (Slevogt et al., 2005; Zeng et al., 2020). In brief, confluent BEAS-2B monolayers were

inoculated with mid-log phase cultures corresponding to MOI 10, 50 and 100. After 30 minutes, non-adherent bacteria and aggregates were removed by washing with PBS three times and cells were returned to the incubator. At 30, 60, 120 and 240 minutes, cells were incubated in 1 % saponin for seven minutes at 37°C. Cell lysates were then plated by Miles Misra to enumerate CFU/mL and percentage adhesion relative to the initial inoculum. At six hours, culture medium containing 50 µg/mL gentamicin was added for one hour, and then replaced with 10 µg/mL gentamicin for 24 hours. Cells were then lysed and plated to calculate the percentage invasion relative to the initial inoculum.

2.7 Flow cytometry

To assess the contributions of basal and differentiated populations, cells were subjected to flow cytometry following antigen staining: CD49f and CD271 for basal cells, CD66a/c/e and CD133 for progenitor cells, CD66a/c/e for goblet cells, and CD133 for ciliated cells (Rock et al., 2009) (GlaxoSmithKline, unpublished data). After washing with PBS, submerged and ALI-differentiated HBECs were detached by applying StemPro Accutase (both apically and basolaterally in the case of ALI-differentiated HBECs; Gibco) for 15 minutes at 37˚C. Dissociated cells were transferred into tubes containing IMDM supplemented with L-glutamine, 25 mM HEPES and 10 % foetal calf serum (FCS) to quench the reaction. Following counting, HBECs were blocked in Human TruStain FcX (Biolegend) for 10 minutes at 4˚C. Cells were washed and resuspended in PBS with 2 % bovine serum albumin (BSA) and 0.5 M ethylenediaminetetraacetic acid (EDTA) containing the following staining cocktail (**Table 2.3**):

Table 2.3. Flow cytometry staining cocktail.

Antigen	Conjugate	Clone	Supplier	Catalogue no.	Dilution
Mouse anti-human CD66a/c/e	FITC	ASL-32	BioLegend	342306	1:25
Mouse anti-human CD133	APC	AC133	Miltenyi Biotec	130 090 826	1:50
Mouse anti-human CD271	Brilliant Violet 421	C40-1457	BD Biosciences	562562	1:12.5
Rat anti-human CD49f	PE	GoH3	BD Pharmingen	555736	1:10

After incubating for 20 minutes at 4˚C, cells were stained with 7-AAD (1:100; A1310, Thermo Fisher) according to the manufacturer's instructions. Following a final wash in PBS with 2 % BSA and 0.5 M EDTA, stained HBECs were acquired on an Attune NxT Flow Cytometer (Thermo Fisher), alongside single stained controls to determine the levels of compensation and fluorescence minus one (FMO) controls to inform the gating. Data were analysed in FlowJo 10 (Tree Star): viable cells were gated by FSC-A x SSC-A; single cells were gated by FSC-A x FSC-H; 7-AAD negative live cells were selected; basal cells ($CD49f^+$ $CD271^+$) and differentiated cells ($CD49f^-$ $CD271^-$) were gated by the indicated markers; differentiated cells were further separated into double-negative cells ($CD66a/c/e^-$ $CD133^-$), progenitor cells ($CD66a/c/e^+$ $CD133^+$), goblet cells ($CD66a/c/e^+$ $CD133^-$) and ciliated cells ($CD66a/c/e^-$ $CD133^+$) (**Figure 2.2**).

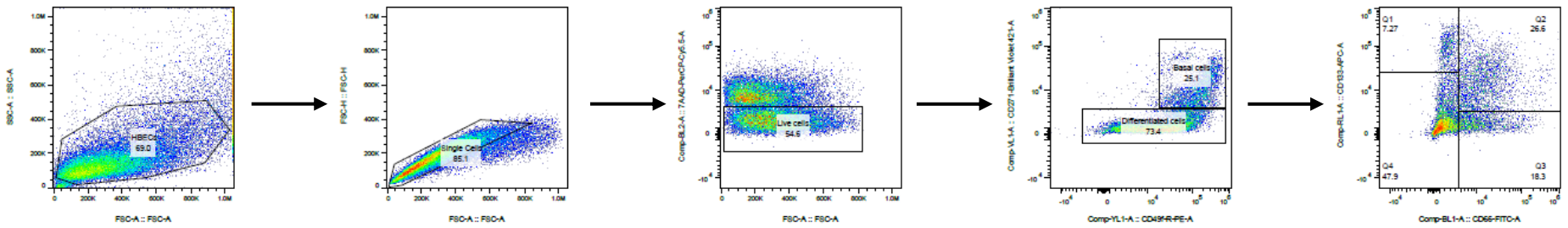

Figure 2.2. Gating strategy and stained populations are indicated.

To determine the presence of basal cells (CD49f^{+} CD271^{+}), progenitor cells (CD66a/c/e^{+} CD133^{+}), goblet cells (CD66a/c/e^{+} CD133^{-}) and ciliated cells (CD66a/c/e^{-} CD133^{+}), dissociated cells were stained with anti-CD49f, anti-CD271, anti-CD66a/c/e and anti-CD133 for flow-cytometric analysis. Live, single cells were gated based on FSC, SSC and 7AAD-negativity.

2.8 Quantitative reverse transcription PCR (RT-qPCR) analysis

RNA from basal or ALI-differentiated cells was isolated using a MagNA Pure 96 Cellular RNA Large Volume Kit in combination with a MagNA Pure 96 System (Roche) and converted to cDNA using the High-Capacity cDNA Reverse Transcription Kit (Thermo Fisher). RT-qPCR was performed using LightCycler 480 Probes Master (Roche) on a LightCycler 480 Instrument II, using the following TaqMan probes (Thermo Fisher) (**Table 2.4**):

Table 2.4. RT-qPCR primers.

Gene	Assay	Lot	RefSeq	Exon	Location	Amplicon	gDNA?
TLR2	Hs02621280_s1	1623784	NM_001318787.1	4-4	3601	112	Y
			NM_001318789.1	3-3	3391		
			NM_001318790.1	3-3	3368		
			NM_001318791.1	3-3	3357		
			NM_001318793.1	3-3	3353		
			NM_001318795.1	3-3	3332		
			NM_001318796.1	3-3	3317		
			NM_003264.4	3-3	3376		
TLR3	Hs01551078_m1	1559391	NM_003265.2	3-4	738	132	N
TLR4	Hs00152939_m1	1626615	NM_003266.3	3-4	679	89	N
			NM_138554.4	2-3	559		
TLR5	Hs01920773_s1	1588876	NM_003268.5	6-6	3227	89	Y
NLRP1	Hs00248187_m1	1405644	NM_001033053.2	6-7	3256	93	N
			NM_014922.4				
			NM_033004.3				
			NM_033006.3				
			NM_033007.3				
NLRP3	Hs00918082_m1	1591318	NM_001079821.2	3-4	421	84	N
			NM_001127461.2	2-3	1063		
			NM_001127462.2	1-2	1029		
			NM_001243133.1	1-2	1029		
			NM_004895.4	1-2	1029		
			NM_183395.2	1-2	1029		
NLRC4	Hs00892666_m1	1498665	NM_001199138.1	4-5	2519	98	N
			NM_001199139.1		2402		
			NM_021209.4		2533		
AIM2	Hs00915710_m1	1515486	NM_004833.1	4-5	1062	106	N
CARD8	Hs01088227_m1	1885254	NM_001184900.1	5-6	588	127	N
			NM_001184901.1	5-6	535		
			NM_001184902.1	8-9	951		
			NM_001184903.1	6-7	685		
			NM_014959.3	6-7	646		
PYCARD	Hs01547324_gH	1585894	NM_013258.2	1-2	361	103	Y
CASP1	Hs00354836_m1	1573803	NM_001223.4	7-8	1099	76	N
			NM_001257118.2	8-9	1162		
			NM_001257119.2	7-8	1099		
			NM_033292.3	8-9	1162		
			NM_033293.3	7-8	883		
			NM_033294.3	6-7	739		
			NM_033295.3	3-4	214		
IL1B	Hs01555410_m1	1594147	NM_000576.2	3-4	190	91	N
IL18	Hs01038788_m1	1569273	NM_001243211.1	3-4	431	115	N
			NM_001562.3	4-5	443		
DPP8	Hs00214745_m1	1535281	NM_001320875.1	12-13	1830	106	N
			NM_001320876.1	11-12	1799		
			NM_017743.5	11-12	1694		
			NM_130434.4	11-12	1694		
			NM_197960.3	12-13	1735		
			NM_197961.3	12-13	1830		
DPP9	Hs00373589_m1	1499385	NM_139159.4	4-5	574	83	N
ACTB	Hs99999903_m1	1570236	NM_001101.3	1-1	53	171	?

Ct values were determined on the instrument using the 'Mono colour hydrolysis probe' programme. Data were presented as relative expression ($1/\Delta Ct$) with normalisation to *β-actin* (*ACTB*; **Figure 3.1**). Alternatively, fold change ($2^{-\Delta\Delta Ct}$) relative to cells derived from untreated controls or healthy patients was calculated

as previously described with normalisation to *ACTB* (Taylor et al., 2019) (**Figure 3.6, Figure 4.10**).

2.9 Western blotting

To determine the endogenous, post siRNA-mediated KD, or post CRISPR/Cas9-mediated KO levels of NLRP1, CARD8, KRT4, KRT13 or GAPDH, cells were harvested in RIPA Lysis and Extraction Buffer (Pierce) supplemented with Halt Protease and Phosphatase Inhibitor Cocktail (Thermo Fisher). Protein quantification was performed using a BCA Protein Assay Kit, according to the manufacturer's instructions (Pierce). Equivalent amounts of individual or pooled samples were loaded onto NuPAGE 4-12 % Bis-Tris Protein Gels (Invitrogen) and separated by SDS-PAGE using NuPAGE MOPS SDS Running Buffer (Invitrogen). Proteins were transferred to Immobilon-FL PVDF Membranes (0.45 µm pore size; Millipore) by wet transfer at 30 V for two hours using NuPAGE Transfer Buffer (Invitrogen). Membranes were blocked in Intercept (TBS) Blocking Buffer (Li-Cor) for 30 minutes at room temperature. Membranes were incubated with Intercept (TBS) Blocking Buffer containing sheep polyclonal anti-NLRP1 (1:400; AF6788, R&D Systems), rabbit polyclonal anti-CARD8 (1:250; ab24186, Abcam), rabbit monoclonal anti-KRT4 (1:1000; ab51599, Abcam), rabbit monoclonal anti-KRT13 (1:100000; ab92551, Abcam) or mouse monoclonal anti-GAPDH (1:1000; ab8245, Abcam) overnight at 4 °C. Membranes were washed in TBS containing 0.5 % Tween 20 three times and incubated in Intercept (TBS) Blocking Buffer containing Donkey anti-sheep AF680 (1:10000; A21102, Invitrogen), IRDye 680RD Donkey anti-Mouse IgG (1:10000; 926-68072, Li-Cor), IRDye 680RD Donkey anti-Rabbit IgG (1:10000; 926-68023, Li-Cor) or IRDye 800CW Donkey anti-Rabbit IgG (1:10000; 926-32213, Li-Cor) for one hour at room temperature. Blots were washed again and visualised on an Odyssey CLx Imager (Li-Cor). To control for gel loading, membranes were re-probed with mouse monoclonal anti-ACTB (1:10000; Sigma, A2228) or rabbit monoclonal anti-ACTB (1:1000; Cell Signalling Technology, 4970S). Where indicated, densitometric analysis was performed on the device and the intensity ratios of control bands compared to treatment bands were calculated following normalisation to ACTB.

2.10 Inflammasome stimulations

To screen for inflammasome activation, HBECs or PMA-differentiated THP-1 cells were directly stimulated with VBP (NLRP1), ATP and nigericin (NLRP3) or poly (dA:dT) (AIM2). Where applicable, the dimethyl sulfoxide (DMSO) content was consistent in all samples (0.04 %). Cells were treated with the indicated concentrations of VBP (Tocris), 200 ng/mL LPS, 10 µg/mL poly (I:C) (Invivogen) or HRV16 MOI 1 (Virapur) (apically only in the case of ALI-differentiated HBECs, removing the apical stimuli after one hour). After 23 hours, primed cells were stimulated with 5 mM ATP, 10 µM nigericin or 5 µg/mL poly (dA:dT) (Invivogen) for an additional one hour. After a total of 24 or 48 hours, supernatants were harvested (using apical washes to collect supernatants in the case of ALI-differentiated HBECs) and cells lysed for determining residual lactate dehydrogenase (LDH) or fixed for ASC speck immunofluorescence (IF) as described below.

To trigger the NLRC4 inflammasome or the non-canonical inflammasome, submerged HBECs were transfected with the *Salmonella enterica* serovar Typhimurium T3SS protein, PrgI (GenScript), or LPS (InvivoGen), respectively. Following priming with 10 µg/mL poly (I:C) for three hours, 70 ng PrgI or 1000 ng LPS were transfected into cells using Lipofectamine 2000 (Thermo Fisher). Alternatively, 200 ng/mL poly (I:C) was transfected into cells to activate the NLRP1 inflammasome. After 24 hours, endpoints were collected as described.

For chronic NLRP1 activation assays, Transwell media was replaced with DMSO or 2 µM VBP in PneumaCult containing 0.1 % trifluoroacetic acid (TFA) from the day of ALI, then replenished every other day. On days seven, 14 and 21, basal supernatants and cells were harvested for enzyme-linked immunosorbent assays (ELISAs) and flow cytometry, respectively.

2.11 Inflammasome inhibition

For inhibition assays, submerged cells were pre-treated with inhibitors for one-hour prior VBP stimulation. 1 µM MCC950 (InvivoGen) was used to inhibit the NLRP3 inflammasome. 20 µM Z-VAD-FMK or Z-WEHD-FMK (R&D Systems) were used to inhibit pan-caspase or caspase-1, respectively. 100 nM MG-132 (Calbiochem) or bortezomib (Alfa Aesar) were used to inhibit the proteasome.

All KD reagents were purchased from Thermo Fisher. Submerged HBECs were transfected with Silencer Select GAPDH positive control or a combination of two Silencer Select siRNAs (20 nM total) targeting NLRP1, CARD8 or Negative Controls #1 and #2 (**Table 2.5**):

Table 2.5. Silencer Select siRNA.

Gene	Assay ID	RefSeq	Targeted exon(s)	siRNA location
NLRP1	s22520	NM_001033053.2 NM_014922.4 NM_033004.3 NM_033006.3 NM_033007.3	4	2729
NLRP1	s22522	NM_001033053.2 NM_014922.4 NM_033004.3 NM_033006.3 NM_033007.3	13 13 13 12 12	4172 4160 4160 4070 4070
CARD8	s22622	NM_001184900.1 NM_001184901.1 NM_001184902.1 NM_001184903.1 NM_014959.3	8 8 11 9 9	1186 1133 1549 1283 1244
CARD8	s22623	NM_001184900.1 NM_001184901.1 NM_001184902.1 NM_001184903.1 NM_014959.3	5 5 8 6 6	492 439 855 589 550

Lipofectamine RNAiMAX was used as the transfection vehicle and applied to the cells for 48 hours. Transfection media was then removed, and the cells were treated with VBP for 24 hours. Supernatants were harvested for ELISAs, and cells lysed for western blot as described above. Densitometric analysis of the bands was used to assess the efficacy of siRNA-mediated KD as described above.

2.12 Immunofluorescence of ASC specks

Submerged HBECs were immunostained for ASC specks using a modified protocol (Beilharz et al., 2016). In brief, cells were fixed in 4 % Parafix and then permeabilised/blocked in PBS containing 3 % FCS, 0.5 % BSA and 0.5 % saponin, for 15 minutes each. Rabbit anti-human ASC (AL177, AdipoGen) was added to the wells already containing permeabilisation/blocking buffer for a final concentration of 1 µg/mL and cells were incubated overnight at 4˚C. After washing in PBS twice, cells were stained with 1 µg/ml goat anti-rabbit-AF488 (A11034, Invitrogen) and 400 ng/mL Hoechst 33342 (H3570, Thermo Fisher) for one hour at room temperature.

After a final PBS wash, cells were imaged in PBS using an IN Cell Analyzer 2200 (GE Healthcare) using the Hoechst and 488 channels. Quantification of ASC specks was performed in Columbus 2.8.3 (Perkin Elmer) using a script designed to identify nuclei, exclude artefacts, and identify specks based on size, high fluorescence intensity, and high fluorescence intensity/area. Since extracellular specks may have been visible due to cell pyroptosis, total cell counts were calculated by combining the nuclei number with the number of extracellular specks. The percentages of cells with specks were calculated by dividing the ASC specks number by the total cell count and multiplying by 100 (**Figure 2.3**).

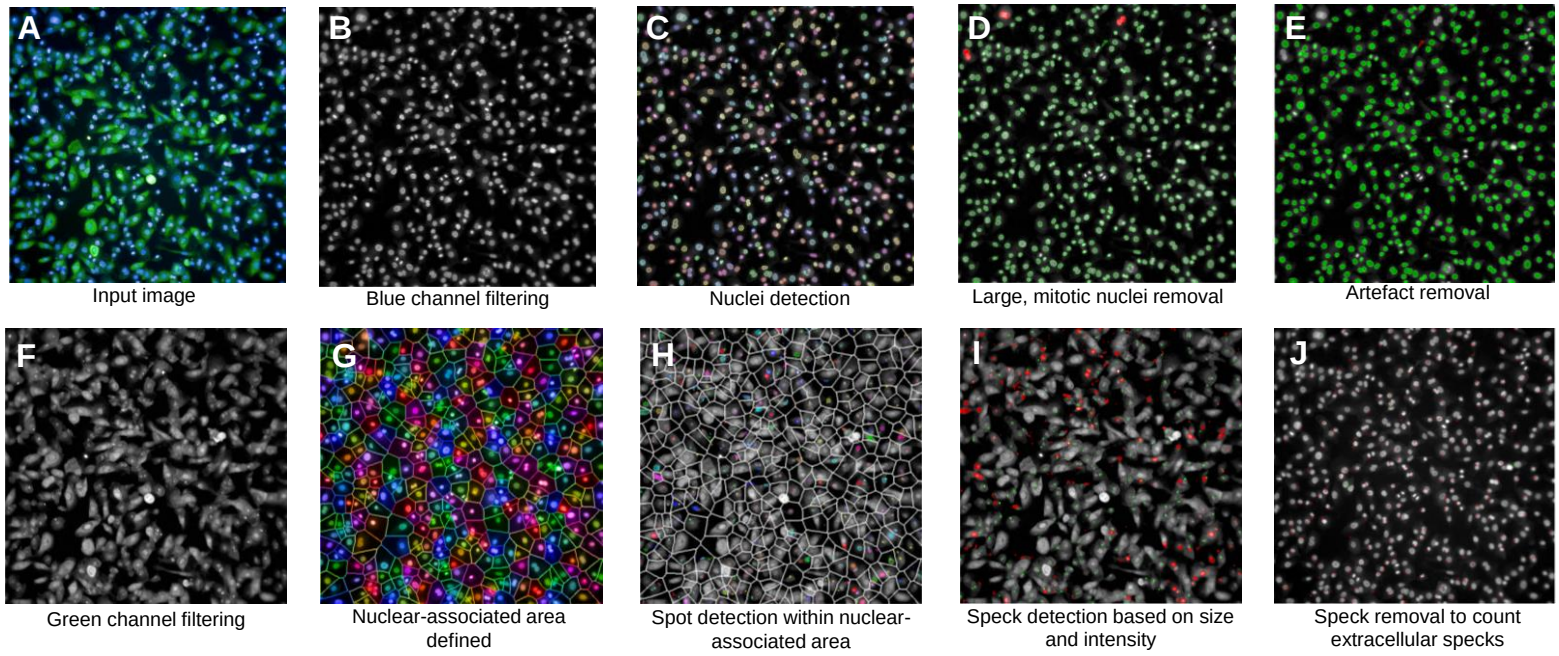

Figure 2.3. Quantification of ASC specks in 2D cultures.

(**A**) Images were imported into Columbus 2.8.3 (Perkin Elmer). (**B**) Filtering was applied to the blue channel using the sliding parabola function and a curvature of 0.2. (**C**) Nuclei were detected by selecting for areas > 30 μm^2, setting the common threshold to 0.5 and a split factor of 3. (**D**) Nuclear area was set to < 250 μm^2 to exclude large, mitotic nuclei. (**E**) Artefacts were removed by setting the nuclear intensity mean to > 2000. (**F**) Filtering was applied to the green channel using the sliding parabola function and a curvature of 0.1. (**G**) Nuclear outer borders were set to -300 pixels. (**H**) Spots were detected within the nuclear regions using a relative spot intensity > 0.15 and a splitting coefficient of 0.505. (**I**) Spots with an area < 9 μm^2, an intensity/area > 550 and a mean spot intensity > 450 were designated as specks. (**J**) Nuclei-associated specks removed to include extracellular specks in total cell counts.

2.13 Immunofluorescence of ALI-differentiated HBECs

IF was performed with formalin-fixed, paraffin-embedded (FFPE) Transwells using a Ventana Discovery Ultra (Ventana Inc.). Samples were deparaffinised and an antigen retrieval step was performed using the Ultra Cell Conditioning solution CC1 (950-224, Roche). Mouse IgG1 anti-MUC5AC was applied (1:1000; MA5-12175, Thermo Fisher) and detected using Ventana OmniMap anti-Ms HRP (760-4310, Roche). CY5 TSA (1:250; FP1171, Perkin Elmer) was applied to produce a fluorescent signal. Bound antibodies were denatured with Ultra CC2 reagent (950-223, Roche; CY5 signal was unaffected). Mouse IgG2b anti-acetylated tubulin (1:4000; T6793, clone 6-11B-1, Sigma) and rabbit monoclonal anti-KRT4 (1:100; ab51599, Abcam) were applied and detected using goat anti-mouse IgG Alexa Fluor Plus 555 (1:200; A32727, Thermo Fisher) and goat anti-rabbit IgG Alexa Fluor 488 (1:200; A11034) to produce a fluorescent signal. Nuclei were stained using Hoechst 33342 (1:5000 in PBS; H3570, Invitrogen). Slides were washed in soapy water, followed by distilled water, and then mounted using Prolong Gold Antifade reagent (P10144, Thermo Fisher). Fluorescence microscopy was performed using a Zeiss, Axioscan Z1 microscope (Carl Zeiss Ltd.).

2.14 LDH cytotoxicity assays

Cell survival was determined using a LDH Cytotoxicity Assay Kit (Pierce). Residual cell viability was assessed by adding 50 µL Lysis Buffer for 30 minutes, followed by 50 µL LDH Substrate Mixture, and incubating until a colourimetric change was visible. The reaction was quenched by adding LDH Stop Solution and values were measured at 490 nm with wavelength correction at 680 nm, as described above. Untreated samples were assigned 100 % cell survival and the residual cell proportion following treatment was calculated.

2.15 ELISA assays

IL-1α, IL-1β, IL-6, IL-18 and IL-33 levels in supernatants were determined by DuoSet ELISAs, according to the manufacturer's instructions (R&D Systems). Supernatants were used neat or diluted as required. Samples were measured at 450 nm with wavelength correction at 570 nm on a SpectraMax MiniMax 300 Imaging Cytometer (Molecular Devices). Values were determined using four-parameter logistic regression of the standard curve. Basolateral measurements

from ALI-differentiated HBECs were adjusted to account for the apical/basolateral volume differences.

2.16 Luminex assays

For multiplex analysis of BALF and infected HBEC supernatants, a Human Custom ProcartaPlex 10-plex (PPX-10-MXAAAM4) was run according to the manufacturer's instructions (Thermo Fisher). Levels of IL-1α, IL-1β, IL-1RA, IL-18, IL-33, IL-6, IL-8, CXCL10, CCL20 and TNF- α were assayed in neat samples. Data was recorded using a FLEXMAP 3D and xPONENT® software (Luminex) and analysed using Bio-Plex Manager, version 6.1 (Bio-Rad). Values were determined using a five-parameter logistic equation of the standard curve.

2.17 CRISPR-Cas9 KO

Unless specified otherwise, all KO reagents were purchased from Integrated DNA Technologies. NLRP1 and/or CARD8 KO HBECs were generated using a modified protocol (Rapiteanu et al., 2020). In brief, gRNA was generated by heating 100 µM ALT-R CRISPR tracr RNA with 100 µM crRNA (Alt-R Cas9 Negative Control crRNA #1 or three pooled target crRNAs) at 95°C for five minutes then slowly cooled to room temperature (**Table 2.6**):

Table 2.6. crRNA utilised for gRNA generation.

Each crRNA was resuspended to 100 µM in Nuclease-Free Duplex Buffer (Integrated DNA Technologies) before combination to generate pooled NLRP1 or CARD8 crRNA stocks.

crRNA	Position	Strand	Sequence	PAM
Hs.Cas9.NLRP1.1.AA NLRP1	5559968	-	GGTGGTAGGAACGCCCCCAC	AGG
Hs.Cas9.NLRP1.1.AB	5582741	-	CTGGATCCATGAATTGCCGG	CGG
Hs.Cas9.NLRP1.1.AC	5583774	+	ATACTGAGCCACCAGGTACG	AGG
Hs.Cas9.CARD8.1.AA	48230916	-	GTCACAGTGACGATTGCGTT	TGG
Hs.Cas9.CARD8.1.AB	48238446	-	GTTGGTTGACAATAGCATAC	GGG
Hs.Cas9.CARD8.1.AC	48234420	-	GTTCCTGAGTGTCAACTATC	TGG

RNP complex was assembled by incubating 9 µL gRNA with 1.5 µL Alt-R Cas9 Nuclease V3 (10 mg/mL) for five minutes. RNP was then incubated with 0.9 µL Alt-R Cas9 Electroporation Enhancer (100 µM) for 10 minutes. The total mixture was combined with 2 x 10^5 HBECs resuspended in 8.6 µL P3 Primary Cell Nucleofector

Solution and transferred to a 16-well Nucleocuvette® Strip (Lonza). Electroporation was performed using an Amaxa 4D Nucleofector (Lonza) and the CM-113 pulse code. Cells were immediately transferred to a 6-well plate containing pre-warmed BEGM and incubated at 37°C. Upon confluency, successful KO was validated by WB and VBP treatment, as described above. Alternatively, cells were seeded in Transwells, and differentiation was assessed post-ALI initiation. Flow cytometry and IF were performed on 21-day differentiated cultures, as described above. TEER was recorded on days 2-, 6-, 12- and 18-post ALI using an EVOM2 Epithelial Voltohmmeter and EndOhm chamber for 6 mm culture cups (World Precision Instruments). Following measurement of the electrical resistance (Ω) across Transwells containing collagen alone (R_{BLANK}) and the resistance of Transwells containing cells (R_{TOTAL}), normalised resistance across a known Transwell area (R_{TISSUE}) was then calculated using the following formulae:

$$\text{Transwell growth area} = \pi r^2$$

$$R_{TISSUE}\ (k\Omega/cm^2) = ((R_{TOTAL} - R_{BLANK}) \times \text{Transwell growth area})$$

Due to a Transwell diameter of 6.5 mm, therefore a radius of 3.25 mm, the Transwell growth area was calculated to be 0.3318 cm^2.

2.18 Statistical analysis

Data are presented as individual donors with the mean, mean values ± standard deviation (SD) for biological replicates where N = 2, or mean values ± standard error of the mean (SEM) for cell line data. Levels of significance between parameters denoted in the figure legends were determined by one-way or two-way analysis of variance (ANOVA) with a Bonferroni or Dunnett's post hoc test using GraphPad Prism 5.0.4. Significance was represented with *p <0.05, **p <0.01, ***p <0.001, or ****p <0.0001.

Chapter 3. Pattern recognition receptors of the respiratory epithelium

3.1 Rationale

In **Chapter 3**, the expression of various inflammasome components in HBECs was determined, and inflammasome responses to PRR agonists and common respiratory bacteria were characterised.

Although it has been reported that HBECs express NLRP1 and caspase-1, there is controversy regarding the levels of epithelial NLRP3 (Kummer et al., 2007; Hirota et al., 2012). Furthermore, compared with sputum samples, NLRP3 expression may be low in bronchial biopsies and brushings (Rossios et al., 2018). An absence of NLRP3 may explain the reported negligible responses to NLRP3-relevant stimuli, but this may also have been due to ineffective LPS priming (Tang et al., 2012; Peeters et al., 2013). Here, RNA and protein approaches were employed to investigate the levels of inflammasome components and the ability of diverse TLR agonists to prime inflammasome activation.

Both *H. influenza* and *M. catarrhalis* are present in the airways of stable COPD patients and undergo outgrowth during exacerbations (Rosell et al., 2005). Although discerned less frequently, *P. aeruginosa* is isolated from patients with severe disease, characterised by increased dyspnoea, previous hospital admissions and systemic steroid therapy (Garcia-Vidal et al., 2009). Since AECs represent the primary site of colonisation/infection, it was speculated that these bacteria may activate epithelial inflammasomes to drive the increased IL-1β, IL-18 and IL-33 signatures in COPD. Indeed, previous evidence suggests that *M. catarrhalis* induces IL1B expression in pharyngeal epithelial cells and that NTHi drives IL-1β and IL-18 secretion from lung tissue explants (de Vries et al., 2013; Rotta detto Loria et al., 2013). Moreover, modest IL-1β and caspase-1 activation were reported following *P. aeruginosa* infection of primary HBECs (McHugh et al., 2019). Since these observations were reported in healthy cells or tissues (where immune cells may contribute to cytokine responses), isolated cells derived from COPD patients were used, where these bacteria may have greater clinical relevance.

3.2 Epithelial cells have a restricted repertoire of inflammasome sensor molecules

Although previous studies have reported that NLRP1 and NLRP3 are expressed in the bronchial epithelium, limited data is available for other inflammasome sensors as well as their relative levels (Kummer et al., 2007; Hirota et al., 2012; Robinson et al., 2020). Firstly, the expression profiles of selected TLRs (TLR2, TLR3, TLR4 and TLR5) and inflammasome sensors (NLRP1, NLRP3, NLRC4, AIM2 and CARD8) were assessed in primary HBECs differentiated at the ALI. All PRRs measured were detected but *NLRP3* and *NLRC4* returned high Ct values (~35) indicating low gene expression. *TLR3* and *NLRP1* were the most abundantly expressed TLR and inflammasome sensor, respectively (**Figure 3.1**).

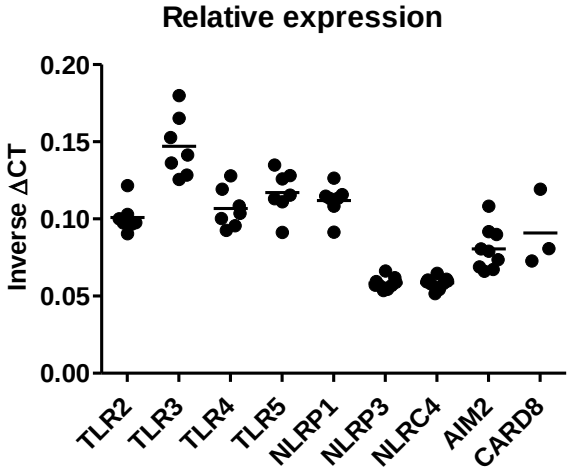

Figure 3.1. ALI-differentiated HBECs have a high basal expression of TLR3 and NLRP1.

RNA was isolated from HBECs differentiated at the ALI for 28 days and reverse transcribed to cDNA. RT-qPCR was used to determine the baseline expression (1/ΔCt) of *TLR2, TLR3*, *TLR4*, *TLR5*, *NLRP1*, *NLRP3*, *NLRC4*, *AIM2* and *CARD8* following normalisation to the *ACTB* housekeeping gene. Data points represent three – seven individual donors with the mean (Healthy AB037201, AB039401, 02AB061001, AB053201, 02AB066902, 000333288 and 0000482214).

Since NLRP1 and CARD8 have overlapping activation pathways and there was evidence for co-expression, it was next determined whether these RNA findings translated to protein levels (D'Osualdo et al., 2011). CARD8 expression and activation have been demonstrated in THP-1 cells, therefore WT cells were used as

the positive control, and compared with titrated pooled HBECs (Linder et al., 2020). High levels of NLRP1 but low levels of CARD8 were detected in HBECs, and vice versa for THP-1 cells (**Figure 3.2**).

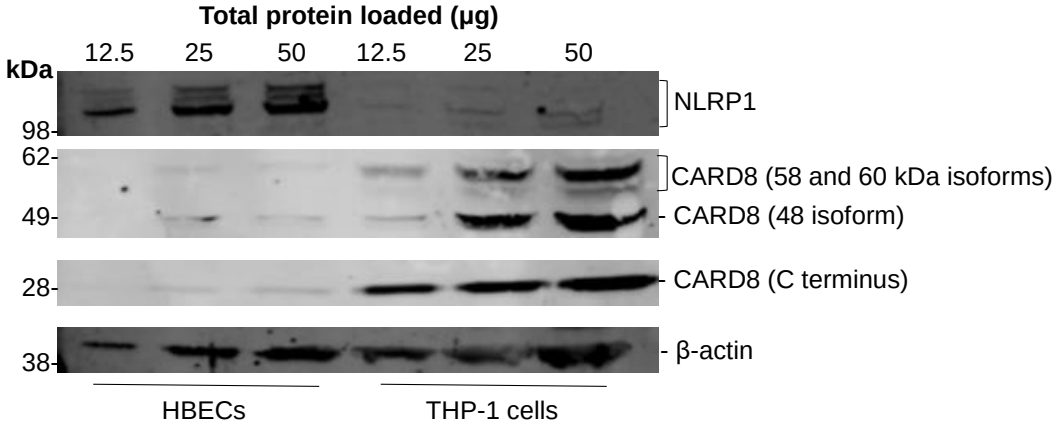

Figure 3.2. Titration of HBEC and THP-1 whole cell lysates reveals differential expression of NLRP1 and CARD8.

Basal cells from healthy donors and THP-1 cells were lysed in RIPA buffer, proteins separated by SDS gel electrophoresis followed by transfer to a PVDF membrane. Levels of NLRP1 (~150 kDa), CARD8 isoforms (48, 58 and 60 kDa) and CARD8 C-terminus (~28 kDa) were detected using the relevant primary antibodies. Representative blot shown from two independent experiments consists of lysates from three pooled HBEC donors (Healthy 02AB061001, 02AB066902 and 000333288) or WT THP-1 cells.

To identify the subcellular localisation of inflammasome sensors in the human bronchial epithelium, immunohistochemistry (IHC) on tumour-adjacent lung tissue samples containing large airways was performed. As a positive control, macrophages within these tissue samples were immunolabelled for NLRP1, NLRP3 and NLRC4, and all these NLRs were expressed in these cells (**Figure 3.3**).

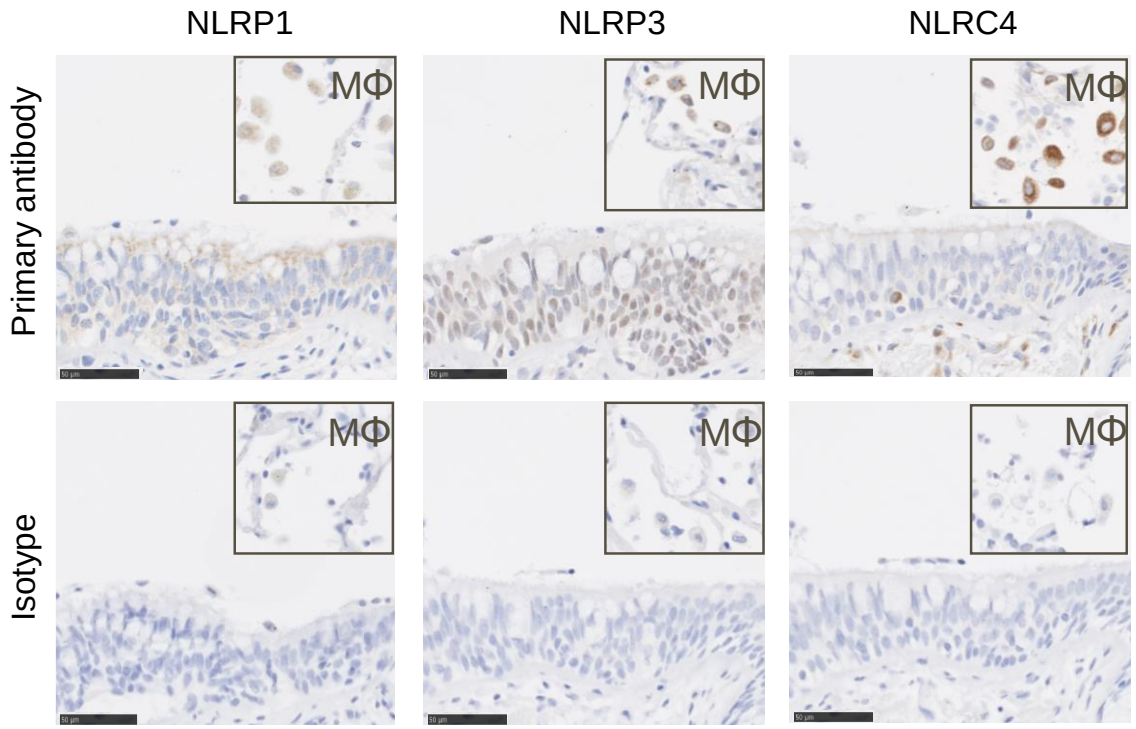

Figure 3.3. NLRP1 and NLRP3 are expressed in the human bronchial epithelium.

Tissues containing large airways from three donors were fixed before embedding in paraffin. Sections of 4 µm were prepared using a microtome and then stained (brown) for NLRP1, NLRP3, NLRC4 or isotype controls. Nuclei were counterstained with haematoxylin. Tissue sections were visualised using a Nanozoomer 2.0HT at 40x objective. Representative images from FFPE sections generated and stained in three independent experiments are shown for one donor; a 66-year female, ex-smoker with COPD and lung cancer. Scale bar: 50 µm. MΦ, macrophages.

In tissue sections from three donors, NLRP1 was found to be abundantly expressed in the respiratory epithelium and was predominantly cytoplasmic. There was little evidence of generalised NLRC4 staining, but some was apparent in several apical patches. NLRP3 levels appeared to be variable and surprisingly showed a nuclear localisation.

To confirm the specificity of the NLRP3 antibody used, previously generated WT and pooled NLRP3 KO THP-1 cells were employed (Gram et al., 2021). Minimal immunocytochemistry (ICC) staining was observed with anti-NLRP3 in NLRP3 KO cells, suggesting that this antibody is specific in FFPE samples (**Figure 3.4**).

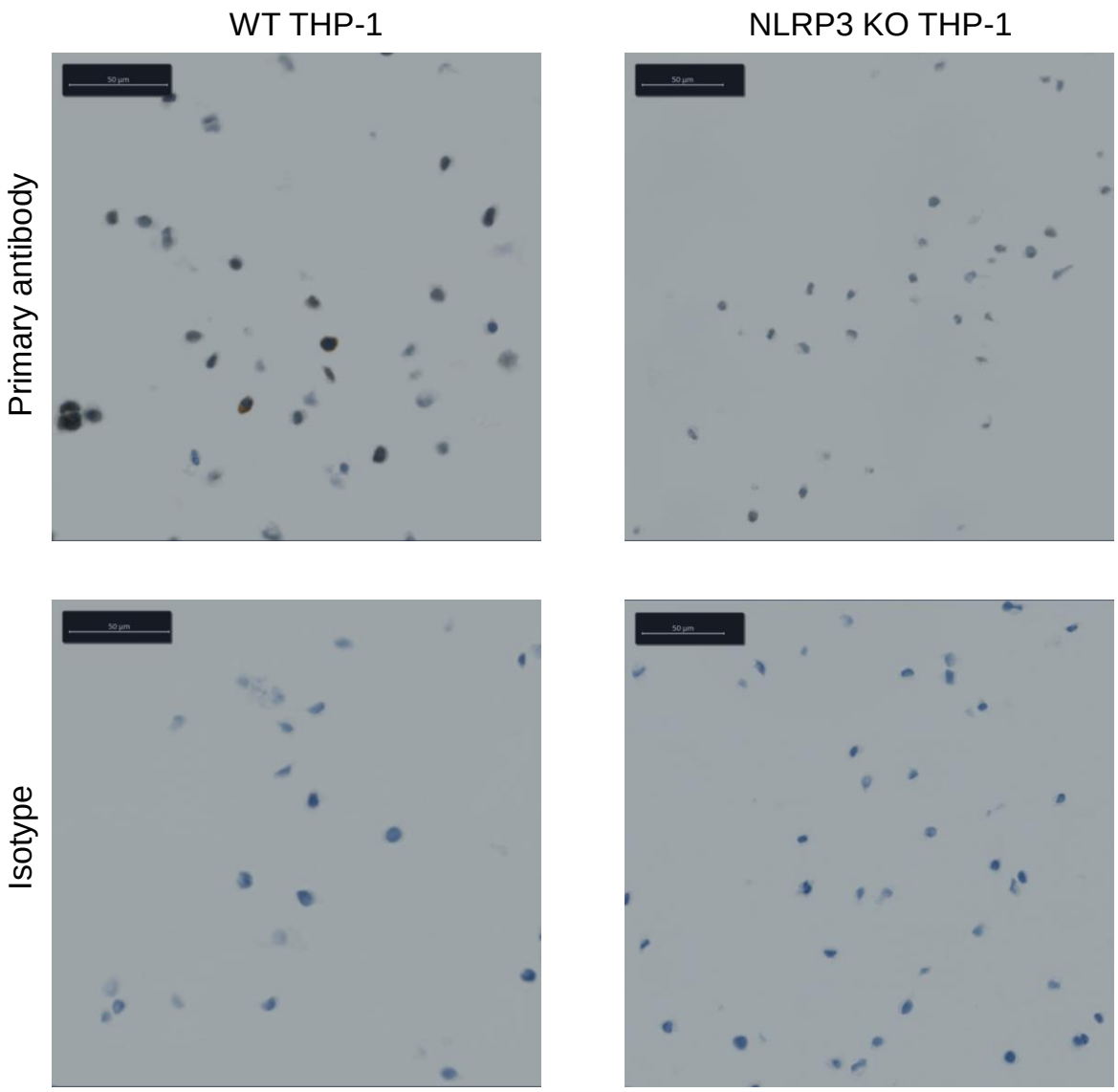

Figure 3.4. Characterisation of rabbit anti-human NLRP3 in KO THP-1 cells.

10 million WT and pooled NLRP3 KO cells were fixed and resuspended in HistoGel before embedding in paraffin. Sections of 4 µm were prepared using a microtome and then stained (brown) for NLRP3 or isotype control. Nuclei were counterstained with haematoxylin. Sections were visualised using a Nanozoomer 2.0HT at 40x objective. Representative images are shown from FFPE sections generated and stained in two independent experiments. Scale bar: 50 µm.

3.3 ASC expression is polarised in epithelial cells

Next, the subcellular localisation of the inflammasome components, ASC and caspase-1, downstream of the inflammasome sensor molecules was determined. In tissue samples from three donors, positive cytosolic staining for ASC was

observed within macrophages, lymphocytes, and basal cells of the columnar epithelium (**Figure 3.5**).

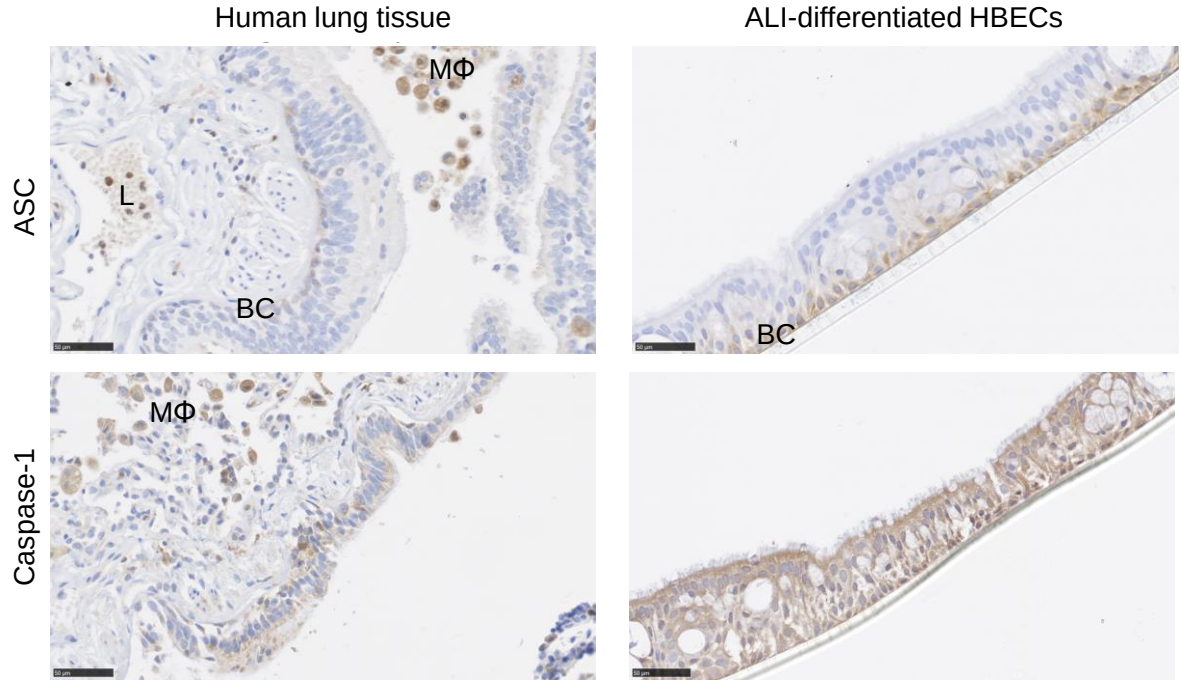

Figure 3.5. ASC and caspase-1 are expressed in the human bronchial epithelium.

Tissues containing large airways from three donors or ALI-differentiated HBECs from three donors were fixed before embedding in paraffin. Sections of 4 μm were prepared using a microtome and then stained (brown) for ASC or caspase-1. Nuclei were counterstained with haematoxylin. Tissue and cell sections were visualised using a Nanozoomer 2.0HT at 40x objective. Representative images from FFPE sections generated and stained in three independent experiments are shown for two donors; a 38-year female, ex-smoker with lung cancer and cell culture sections (Healthy 000333288). Scale bar: 50 μm. MΦ, macrophages. L, lymphocytes. BC, basal cells.

Caspase-1 was also detected within tissue macrophages and, in disconnect with ASC, it was ubiquitously expressed throughout the epithelium. The same pattern of staining was observed in ALI-differentiated HBECs.

3.4 TLR3 stimulation primes the epithelial inflammasome

Compared with myeloid cells, AECs show low levels of caspase-1 activity and/or secrete minimal IL-1β when exposed to inflammasome-relevant stimuli (Tang et al.,

2012; Peeters et al., 2013). Since LPS was previously used as the priming signal and AEC TLR4 may be hypo-responsive, it was hypothesised that minimal inflammasome responses may have been due to insufficient priming (Becker et al., 2000; Jia et al., 2004). Consequently, the ability of diverse TLR agonists to prime inflammasome activation in ALI-differentiated HBECs was investigated. Since epithelial TLRs have a polarised distribution, cells were stimulated both apically and basolaterally to maximise responses (Ioannidis et al., 2013). Poly (I:C) was by far the most effective agonist, upregulating the *AIM2*, *CASP1* and *IL1B* transcripts after 24 hours (**Figure 3.6**).

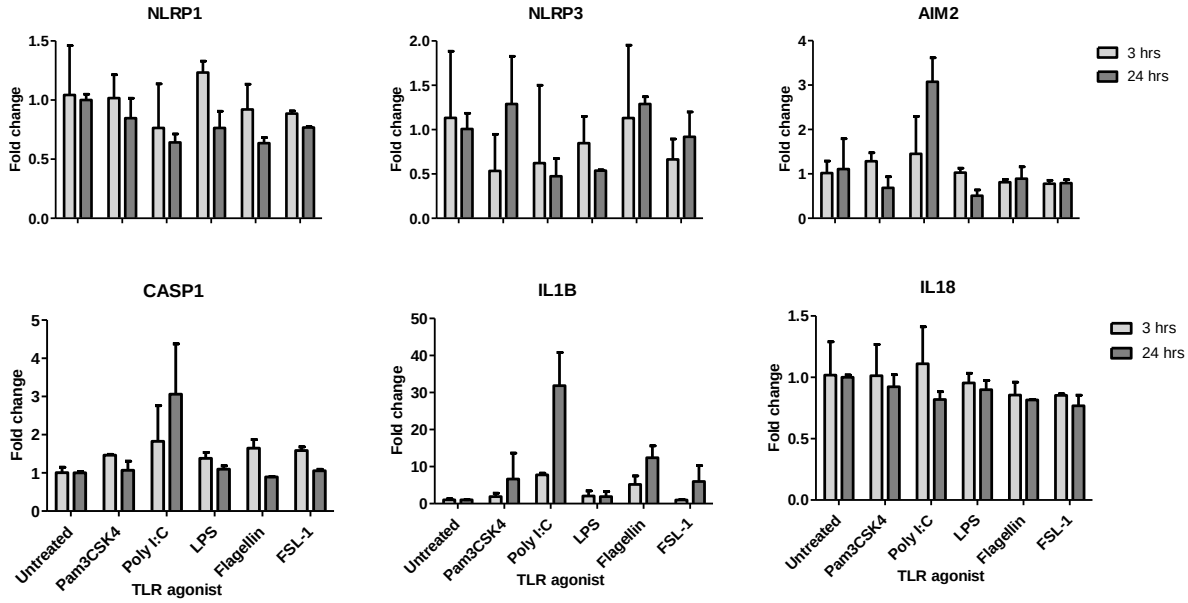

Figure 3.6. Poly (I:C) efficiently primes the inflammasome in HBECs.

All treatments occurred both apically and basolaterally. ALI-differentiated HBECs from healthy donors were treated with 1 µg/mL Pam3CSK4, 10 µg/mL poly I:C, 10 µg/mL LPS 1 µg/mL flagellin or 100 ng/mL FSL-1 for three or 24 hours, removing the apical stimulus after one hour. RNA was isolated from cells and reverse transcribed to cDNA. RT-qPCR was used to determine the fold change ($2^{-\Delta\Delta Ct}$) between untreated and TLR-treated cells, following normalisation to the *ACTB* housekeeping gene. Data shown represent the mean of two biological replicates ± SD (Healthy AB039401 and 0000446317).

A modest induction of *IL1B* was also observed following stimulation with flagellin or FSL-1. As expected, cells were not sensitive to Pam3CSK4 or LPS treatment, and *IL18* transcript levels were maintained across all stimuli. After 24-hour stimulation

with several TLR agonists, *NLRP1* and possibly *NLRP3* expression were downregulated. *NLRP3* quantification, however, may have been inaccurate due to low transcript amplification.

3.5 Nigericin-induced epithelial death is NLRP3-independent

Provided that HBECs express the components required to form a functional inflammasome, NLRP3 inflammasome activation was attempted following poly (I:C) priming. At 12 hours, only IL-1β and IL-18 secretion were measured but this was below the lower limit of detection. At 48 hours post poly (I:C) and nigericin treatment, however, higher levels of cell death and modest IL-1β and IL-18 secretion were observed (**Figure 3.7**).

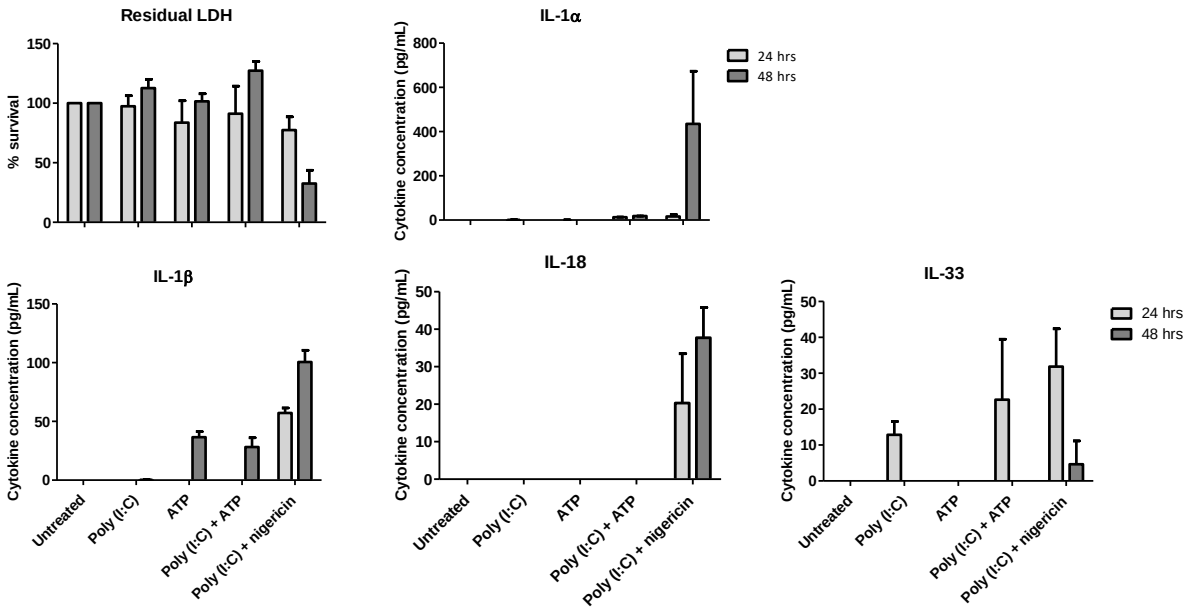

Figure 3.7. Nigericin induces epithelial cell death and cytokine secretion at later timepoints.

All treatments occurred both apically and basolaterally. ALI-differentiated HBECs from healthy donors were treated with 10 µg/mL poly (I:C), removing the apical stimulus after one hour. After 23 hours, poly (I:C)-primed cells were stimulated with 5 mM ATP or 10 µM nigericin, removing the apical stimulus after one hour. After 24 or 48 hours, supernatants were harvested for ELISAs (via apical washes), and the remaining cells lysed for LDH. Data shown represent the mean of two biological replicates ± SD (Healthy 000333288 and 0000446317).

Since cell death was also accompanied by the release of IL-1α and IL-33 alarmins, it was postulated that stimulating with the high nigericin concentration for an extended timeframe may have induced non-pyroptotic cell death. Indeed, cells pre-treated with the NLRP3 inhibitor MCC950 were not impaired in their ability to undergo cell death, although a slight rescue of cell death was observed following pan-caspase inhibition with Z-VAD-FMK (**Figure 3.8**).

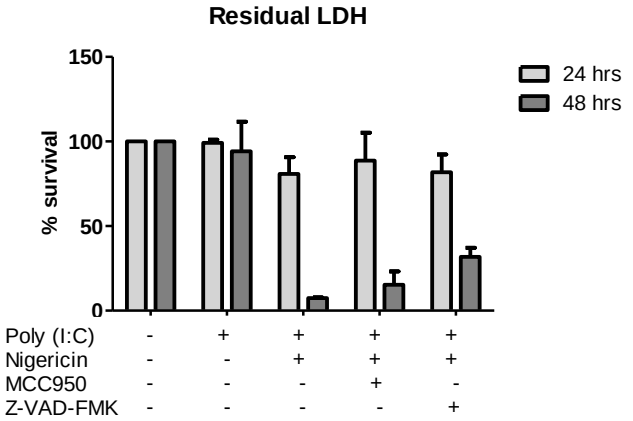

Figure 3.8. Nigericin-induced cell death is NLRP3-independent in HBECs.

All treatments occurred both apically and basolaterally. HBECs from healthy donors were differentiated at the ALI for 28 days and then pre-treated with 1 μM MCC950 or 20 μM Z-VAD-FMK for one hour. HBECs were stimulated with poly (I:C) for 24 hours, then treated with 10 μM nigericin for a further 24 or 48 hours. The remaining cells were lysed for LDH. Data shown represent the mean of two biological replicates ± SD (Healthy 000333288 and 0000446317).

3.6 Common respiratory bacteria drive minimal epithelial inflammasome responses

Since PRR agonists were unable to initiate robust inflammasome responses, live *M. catarrhalis*, NTHi and *P. aeruginosa* were then screened for their ability to induce inflammasome-regulated cytokine secretion. The multiplex panel designed also incorporated markers of productive infection, such as IL-6, IL-8 and CCL20 (Su et al., 2012; Su et al., 2018; Nakamoto et al., 2019). Minimal IL-1β, IL-18 and IL-33 production were observed following infection with all bacterial species, and concentrations were typically outside the linear range of the standard.

In a pilot experiment, *M. catarrhalis* was confirmed to adhere to BEAS-2B cells within 30 minutes of incubation and adhesion increased to ~60 % at four hours, however, no invasion was detected up to 24 hours as demonstrated by an absence of colonies following gentamicin protection assay (**Figure 3.9**).

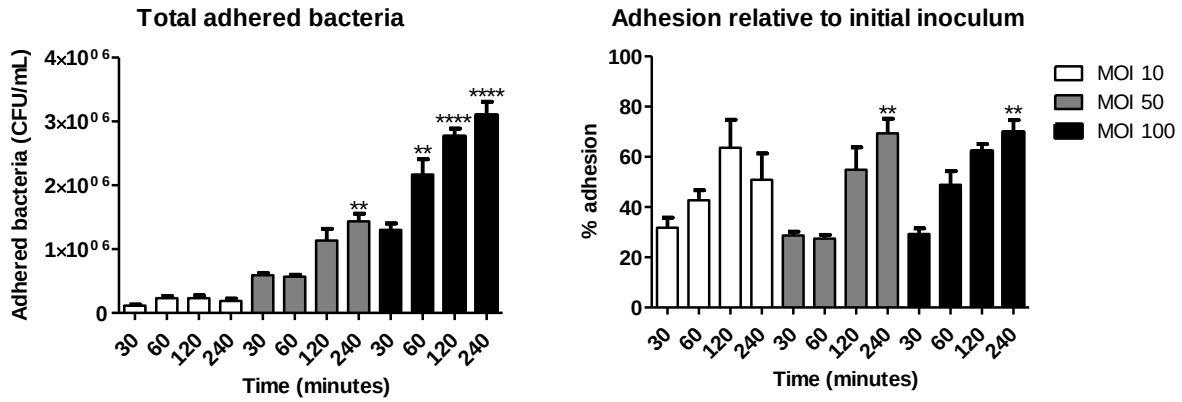

Figure 3.9. *M. catarrhalis* adheres to BEAS-2B cells.

BEAS-2B cells were incubated with *M. catarrhalis* (MOI 10, 50 and 100) for 30 minutes before washing with PBS. At the indicate timepoints, cells were lysed with saponin, and viable adhered bacteria or percentage adhesion were determined by CFU-based measurements. Alternatively, at six hours, cells were incubated with gentamicin for 24 hours prior to cell lysis to calculate percentage invasion. Only adhesion data was plotted since no colonies were observed following gentamicin protection assay. Data shown represent the mean of three technical replicates ± SEM from one experiment. One-way ANOVA with a Bonferroni post hoc test, 30 minutes adherence vs 60 – 240-minute adherence, **p <0.01, or ****p <0.0001.

At eight and 24 hours, *M. catarrhalis* induced the secretion of IL1RA, IL-1α, IL-6, IL-8 and CCL20 from primary HBECs, however, minimal differences were observed between MOI 1, 5 and 10 (**Figure 3.10**). IL-1β, IL-18, IL-33, CXCL10 and TNF- α were all below the lower limit of detection, suggesting an inability to activate epithelial inflammasomes. Infection with NTHi was less successful since the infection medium alone induced high levels of cytokine secretion, particularly IL-6 and IL-8 (**Figure 3.11**). At MOI 50, there was evidence that IL1RA, CXCL10, and low levels of IL-1β, were secreted into the apical supernatants. Despite the four-hour incubation time, *P. aeruginosa* induced a robust inflammatory response with the greatest signal-to-background ratio. High levels of IL-1RA, IL-6, CCL20 and

TNF-a were secreted apically, while IL-1α and IL-8 were secreted basolaterally (**Figure 3.12**). There was also some evidence for inflammasome activation since modest levels of IL-1β and IL-33 were detected, although this was not accompanied by IL-18 production.

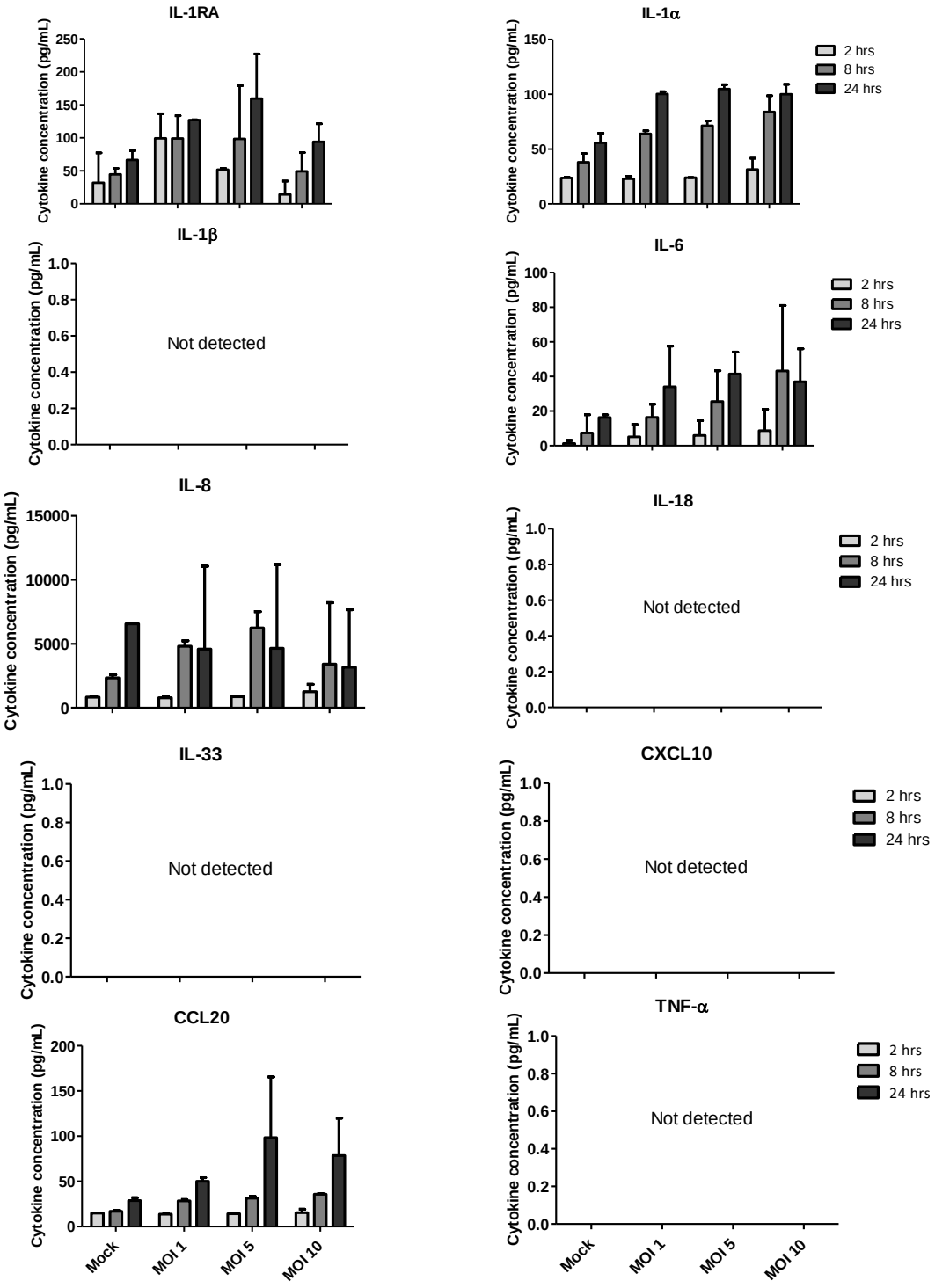

Figure 3.10. *M. catarrhalis* does not drive epithelial inflammasome responses. ALI-differentiated HBECs from COPD donors were infected apically with the indicated MOIs of exponential phase-grown bacteria, removing the apical stimulus after one hour. After two, eight or 24 hours, basolateral supernatants were harvested for Luminex assay. Data represent the mean of two biological replicates ± SD from two independent experiments (COPD AB006302 and 02AB066702).

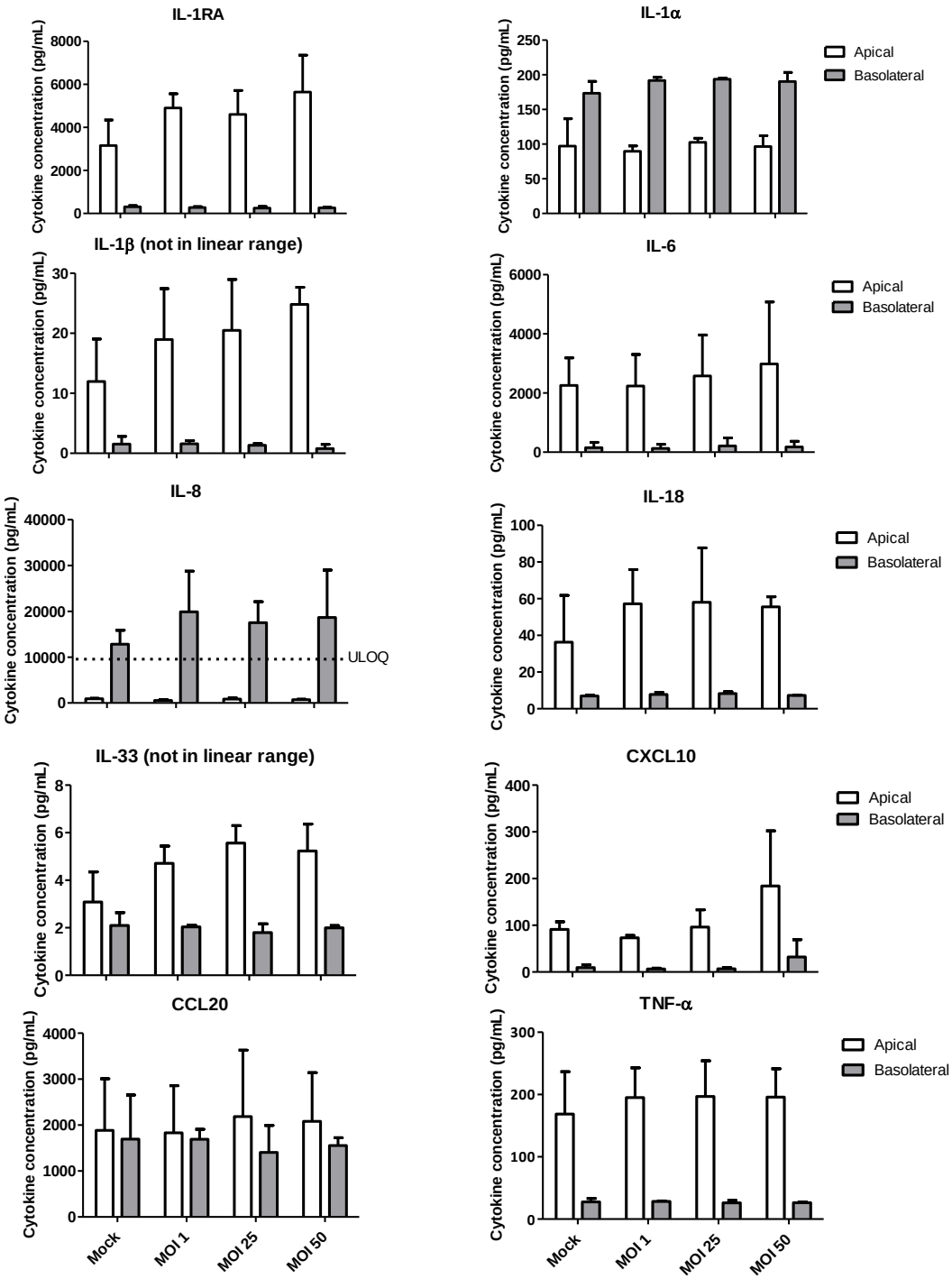

Figure 3.11. NTHi drives minimal epithelial inflammasome responses.

ALI-differentiated HBECs from COPD donors were infected apically with the indicated MOIs of exponential phase-grown bacteria, removing the apical stimulus after one hour. After 24 hours, apical (via apical washes) and basolateral supernatants were harvested for Luminex assay. Data represent the mean of two biological replicates ± SD from two independent experiments (COPD AB006302 and 02AB066702).

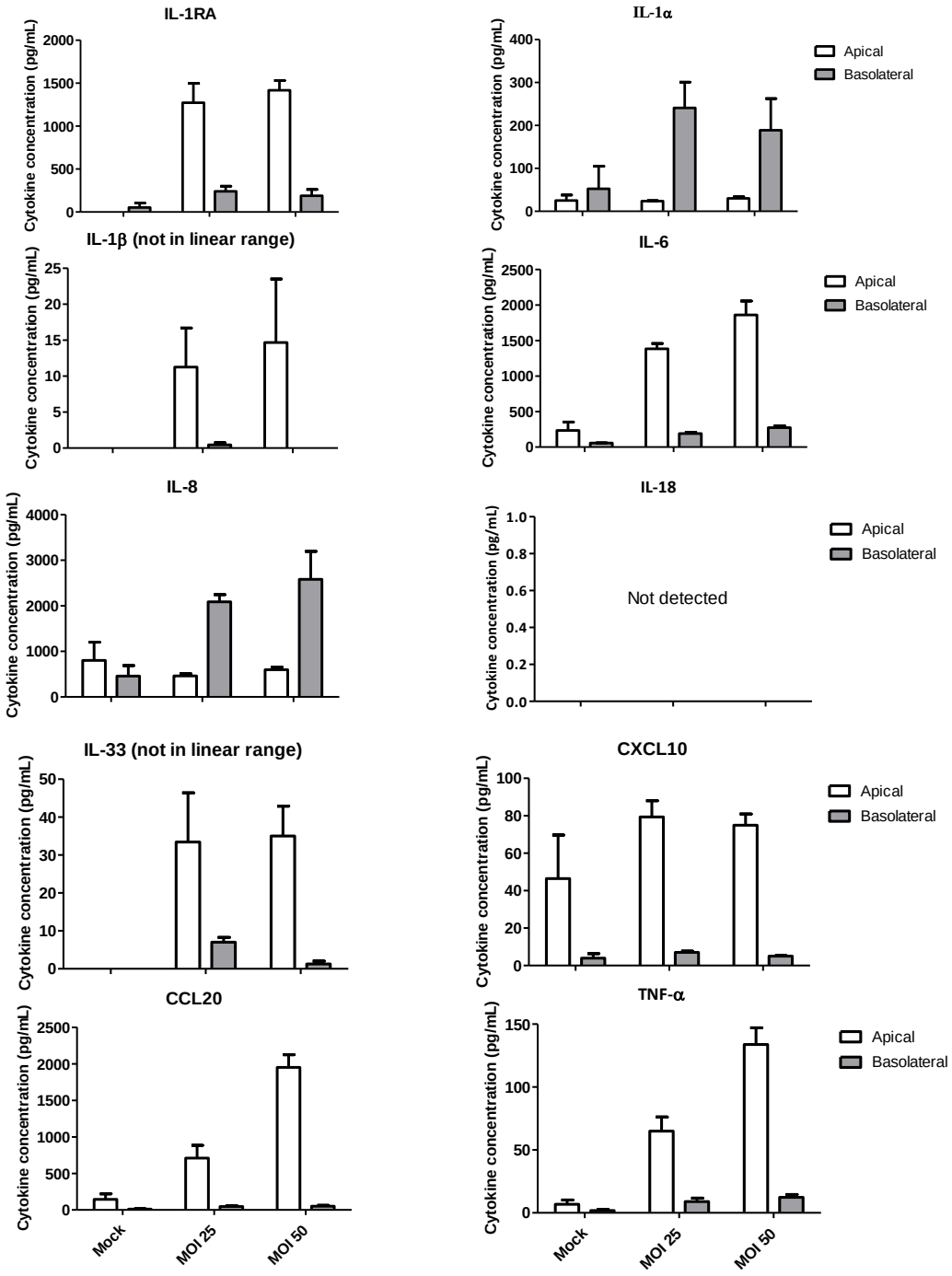

Figure 3.12. *P. aeruginosa* drives modest epithelial inflammasome responses.

ALI-differentiated HBECs from COPD donors were infected apically with the indicated MOIs of exponential phase-grown bacteria, removing the apical stimulus after one hour. After four hours, apical (via apical washes) and basolateral supernatants were harvested for Luminex assay. Data represent the mean of two biological replicates ± SD from two independent experiments (COPD AB006302 and 02AB066702).

3.7 NLRC4 and non-canonical inflammasome stimuli are unable to drive IL-1β secretion from BEAS-2B cells

In human macrophages, NAIP/NLRC4 responds to *P. aeruginosa* T3SS components (Grandjean et al., 2017). To assess whether the modest IL-1β and IL-33 secretion from HBECs were due to T3SS component-mediated NAIP/NLRC4 inflammasome activation, PrgI needle protein was transfected into BEAS-2B cells. In parallel, an attempt was made to activate the non-canonical inflammasome by LPS transfection. PrgI and LPS failed to induce responses in the absence of priming, however, pre-treatment with poly (I:C) caused cells to undergo cell death and release cytokines at four hours post transfection (**Figure 3.13**).

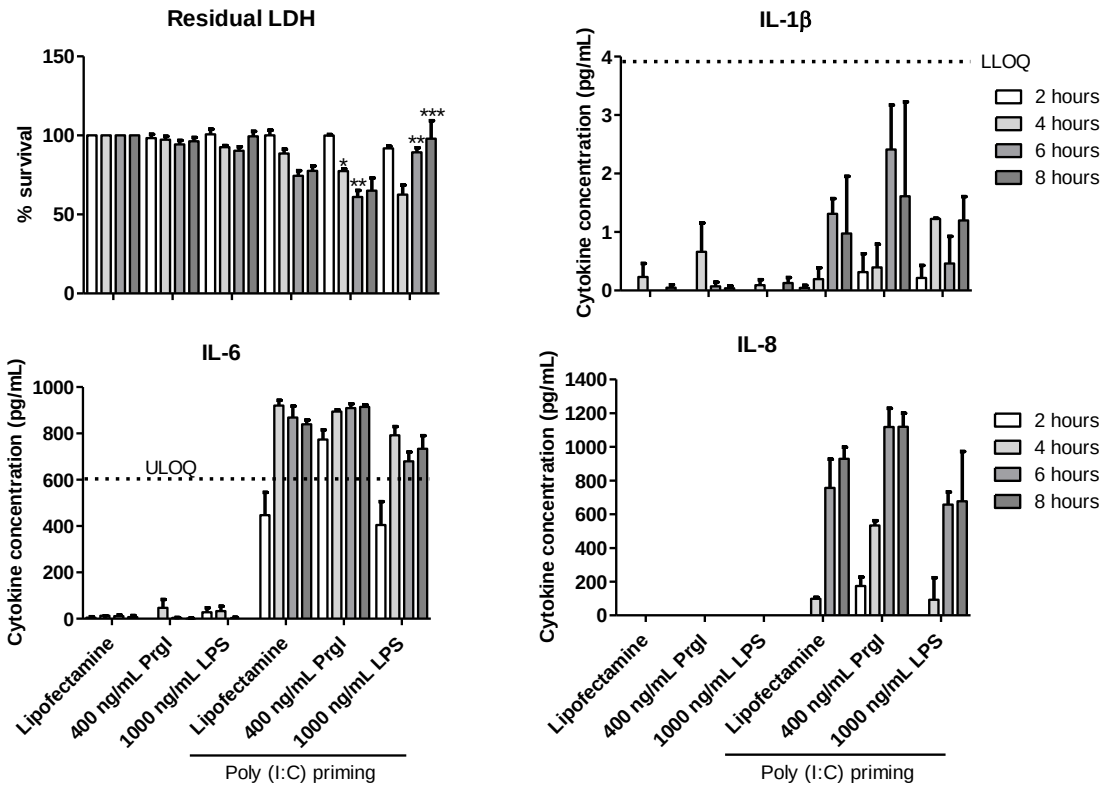

Figure 3.13. NLRC4 and the non-canonical inflammasome stimuli drive minimal inflammasome responses in BEAS-2B cells.

BEAS-2B cells were seeded and cultured overnight. Cells were treated with 10 µg/mL poly (I:C) for 24 hours. Unprimed or poly (I:C)-primed cells were treated with 400 ng PrgI or 1000 ng LPS for an additional two, four, six or eight hours. ELISAs were performed on the supernatants and the remaining cells were lysed for LDH. Data shown represent the mean of two – six technical replicates ± SEM from one experiment. One-way ANOVA with a Bonferroni post hoc test (Residual LDH only), relevant Lipofectamine control vs treatment groups, *p <0.05, **p <0.01, ***p <0.001.

At six hours, residual LDH continued to decline post PrgI transfection, however, LPS-transfected cells began to recover and Lipofectamine alone induced cell death. The cytokine data is largely inconclusive since secretion was high following poly (I:C) priming alone, however, the was some evidence that PrgI induced IL-1β (below LLOQ) and IL-8 release.

3.8 Discussion

The airway epithelium is now considered critical to the orchestration of respiratory inflammatory and immune responses. Little information is available, however, on the roles of inflammasome complexes within these cells, which may be assembled and activated in the cytosol following the engagement of intracellular PRRs.

To determine whether inflammasomes are relevant to AEC function, RT-qPCR and western blotting were performed using ALI-differentiated HBECs, then IHC was performed on tumour-adjacent lung tissue. Only low levels of NLRC4 were detected and, as previously reported, NLRP1 was abundantly expressed in the respiratory epithelium (**Figure 3.3**) (Kummer et al., 2007). Nuclear NLRP3 was observed in tissue HBECs, and the antibody specificity was confirmed by the ICC of NLRP3 KO THP-1 cells (**Figure 3.4**). This was not in line with the RNA data which showed minimal NLRP3 expression in HBECs derived from healthy patients (**Figure 3.1**). It has been suggested, however, that baseline NLRP3 expression may be elevated in lung malignancies, particularly in lung adenocarcinoma and in small cell lung cancers (Kong et al., 2015). This may explain the presence of NLRP3 in lung tissue resections from cancer patients and the discrepancies between previous publications (Kummer et al., 2007; Hirota et al., 2012; Rossios et al., 2018). The nuclear localisation of epithelial NLRP3 is perplexing and would warrant further investigation (**Figure 3.3**). It may have transcriptional functions similar to nuclear NLRP3 in T_H2 cells (Bruchard et al., 2015). The RT-qPCR data also demonstrated relatively low expression of AIM2 and CARD8, compared to NLRP1 (**Figure 3.1**). Low expression of AIM2 in HBECs from healthy donors has been confirmed by a recent publication (Tran et al., 2021). As evident by comparing whole cell lysates by western blot, NLRP1 is dominant in HBECs while CARD8 is dominant in THP-1 cells (**Figure 3.2**). This balance may have implications for the type of inflammasome which can be activated (discussed further in **Chapter 4**).

Inflammasome activation is typically preceded by TLR engagement which upregulates inflammasome components via NF-κB. Coupled with the restricted coreceptor expression and polarised TLR distribution, these data presented here suggest that low basal TLR expression may contribute to TLR2/4 hyporesponsiveness in HBECs (**Figure 3.1**). Conversely, activation of the highly expressed TLR3 with poly (I:C) effectively induced the *AIM2*, *CASP1* and *IL1B*

transcripts (**Figure 3.6**). In line with these findings, poly (I:C) was previously shown to be the most effective TLR ligand tested, and significantly induced genes such as *IL6*, *CXCL8* and *ICAM1* in BEAS-2B cells (Sha et al., 2004). Nevertheless, TLR3 priming of HBECs followed by nigericin treatment induced cell death but only IL-1β and IL-18 secretion at later timepoints (**Figure 3.7**). Here, nigericin-induced cell death was NLRP3-independent since no effect was observed with MCC950, which directly targets NLRP3 ATP hydrolysis (**Figure 3.8**) (Coll et al., 2019). A slight rescue of cell death was observed following pan-caspase inhibition with Z-VAD-FMK, possibly due to NLRP3-independent pyroptosis. More likely, however, the pore-forming activity of nigericin initiated necroptosis, since this was accompanied by the release of IL-1α and IL-33 which may predominantly be released via caspase-independent mechanisms (**Figure 3.7**) (Di Paolo and Shayakhmetov, 2016; Shlomovitz et al., 2019). Previous reports have suggested NLRP3 activation following environmental particle exposure, but these studies employed cell lines or found low levels of IL-1β release from primary cells (< 10 pg/mL), in parallel with the observations from this project (Mortaz et al., 2011; Hirota et al., 2012; Peeters et al., 2013).

Of the common respiratory bacteria tested, *M. catarrhalis* and NTHi were unable to drive inflammasome-regulated cytokine secretion, while *P. aeruginosa* induced only modest release of IL-1β and IL-33 from HBECs (**Figures 3.10**, **3.11** and **3.12**). *M. catarrhalis* has previously been shown to upregulate the *IL1B* transcript in pharyngeal epithelial cells and activate the NLRP3 inflammasome in macrophages (de Vries et al., 2013; Sha et al., 2014). One could speculate that, although *M. catarrhalis* may prime inflammasome activation, the lack of internalisation may deprive HBECs of Signal 2. Indeed, adherence but not invasion was observed in a pilot study with BEAS-2B cells which may have contributed to the minimal cytokine secretion (**Figure 3.9**). This does contrast with a report of *M. catarrhalis* micropinocytosis by BEAS-2B cells, however, the O35E strain employed previously may have been more invasive (Slevogt et al., 2007). The NTHi infection data is largely inconclusive due to cytokine responses to sBHI alone, however, IL-1β secretion increased slightly post MOI 50 inoculation (**Figure 3.11**). It has been shown that human lung tissues in culture release IL-1β and IL-18 when infected with NTHi (Rotta detto Loria et al., 2013). Although HBECs were detected in these

samples, the majority of IL-1β and IL-18 were likely derived from non-epithelial sources, such as macrophages via NLRP3 inflammasome activation. Indeed, PBMCs, BALF macrophages and BALF neutrophils secrete high levels of IL-1β when infected with NTHi in a caspase-1 or NLRP3-dependent manner (Chen et al., 2018a). Finally, *P. aeruginosa* was able to induce the modest release of IL-1β and IL-33, but surprisingly not the release of IL-18 (**Figure 3.12**). This may have been enhanced by a longer infection duration since HBEC cell lines only secrete IL-1β from 24 hours in response to this bacteria (Tang et al., 2012). To determine if *P. aeruginosa*-mediated cytokine production was due to functional NAIP/NLRC4 in HBECs, PrgI from *S. Typhimurium* was transfected into BEAS-2B cells (**Figure 3.13**). Cytosolic PrgI has previously been shown to activate the NAIP/NLRC4 inflammasome in myeloid cell lines and primary monocyte-derived macrophages (Yang et al., 2013; Gram et al., 2021). Although cell death was induced in BEAS-2B cells, IL-1β was only detected below the LLOQ. As a result, HBEC responses to *P. aeruginosa* may instead be due to NAIP/NLRC4 detection of a species-specific needle protein, rod protein or flagellin.

In summary, this chapter demonstrates that HBECs have a restricted repertoire of inflammasome components compared with immune cells. This may explain the rather limited responses to common respiratory bacteria. Stimulation with *M. catarrhalis*, NTHi or *P. aeruginosa* triggers a NLRP3 or NAIP/NLRC4-driven inflammasome in myeloid cells. In HBECs, however, the expression of these inflammasome sensors is low and they fail to respond to canonical inflammasome inducers such as nigericin and PrgI. ASC polarity, restricted sensor expression and/or defective signalling pathways may be regulatory mechanisms to mitigate spontaneous inflammasome assembly. This may be advantageous at this barrier site due to the large volume of non-pathogenic organisms, pathogens and urban particulate matter breathed in daily. AEC turnover is also relatively slow in comparison to other barrier epithelia (in rodents: 82 – 131 days in the airways compared to 3 – 5 days in the intestine), so frequent triggering of pyroptosis may be deleterious to barrier function (Blenkinsopp, 1967; Cheng and Leblond, 1974). Nevertheless, these results do indicate that HBECs may be important in antiviral responses due to the high expression of TLR3 and NLRP1 (see **Chapter 4**).

Chapter 4. NLRP1 in health and disease

4.1 Rationale

In **Chapter 4**, NLRP1 activation in HBECs was investigated and it was determined whether this pathway was dysregulated in obstructive airway diseases.

While this project was ongoing, pharmacological blockade of DPP8/9 was shown to activate the murine NLRP1b inflammasome (Okondo et al., 2017; Okondo et al., 2018). These studies primarily used the anti-cancer agent VBP which is a non-selective inhibitor of DPP4, DPP7, DPP8 and DPP9. It was demonstrated that DPP8 and DPP9 inhibition alone is sufficient for inflammasome activation since the DPP8/9 selective compound IG244 and double-knockout (DKO) THP-1 cells phenocopy the results of VBP (Okondo et al., 2017). More recently, it was shown that DPP8/9 inhibition in human cells activates NLRP1 in keratinocytes but CARD8 in myeloid and T cells (Johnson et al., 2018; Zhong et al., 2018; Linder et al., 2020). As a result, the VBP-induced inflammasome pathway was investigated in HBECs and it was determined if this was NLRP1 or CARD8 dependent.

Altered morphological and molecular processes are characteristic of the airway epithelium in both COPD and asthma, and these may impact salient functions (Carlier et al., 2021). There is also emerging evidence that epithelial inflammasomes may be linked to disease pathogenesis. It was recently shown that AIM2 expression is enhanced in HBECs from COPD patients compared with control patients (Tran et al., 2021). Moreover, HBEC3-KT cell stimulation with cigarette smoke induces the redistribution of AIM2 from the nuclear to the cytoplasmic compartment, presumably to facilitate dsDNA detection. There is also genetic evidence linking NLRP1 with the pathogenesis of COPD and asthma (Ozretić et al., 2019; Moecking et al., 2020). The functional consequences of NLRP1 activation were therefore investigated in basal and ALI-differentiated HBECs from healthy, asthmatic, and COPD patients.

4.2 IL-1β levels may be enhanced in COPD frequent exacerbators

To firstly investigate the relevance of inflammasome-relevant cytokines in disease, neat BALF from healthy smokers (no history of chronic respiratory disorders), COPD infrequent exacerbators (0 exacerbations in the previous year) and COPD frequent exacerbators (≥3 exacerbations in the previous year or ≥2 exacerbations

in each of the last two years) were analysed by Luminex assay. Although the concentrations of most cytokines were unchanged or low in these patient groups, likely due to harvesting large volumes pre- or post- exacerbation, IL-1α and TNF-α levels were enhanced in infrequent exacerbators while IL-1β levels were enhanced in frequent exacerbators compared with healthy smokers (**Figure 4.1**).

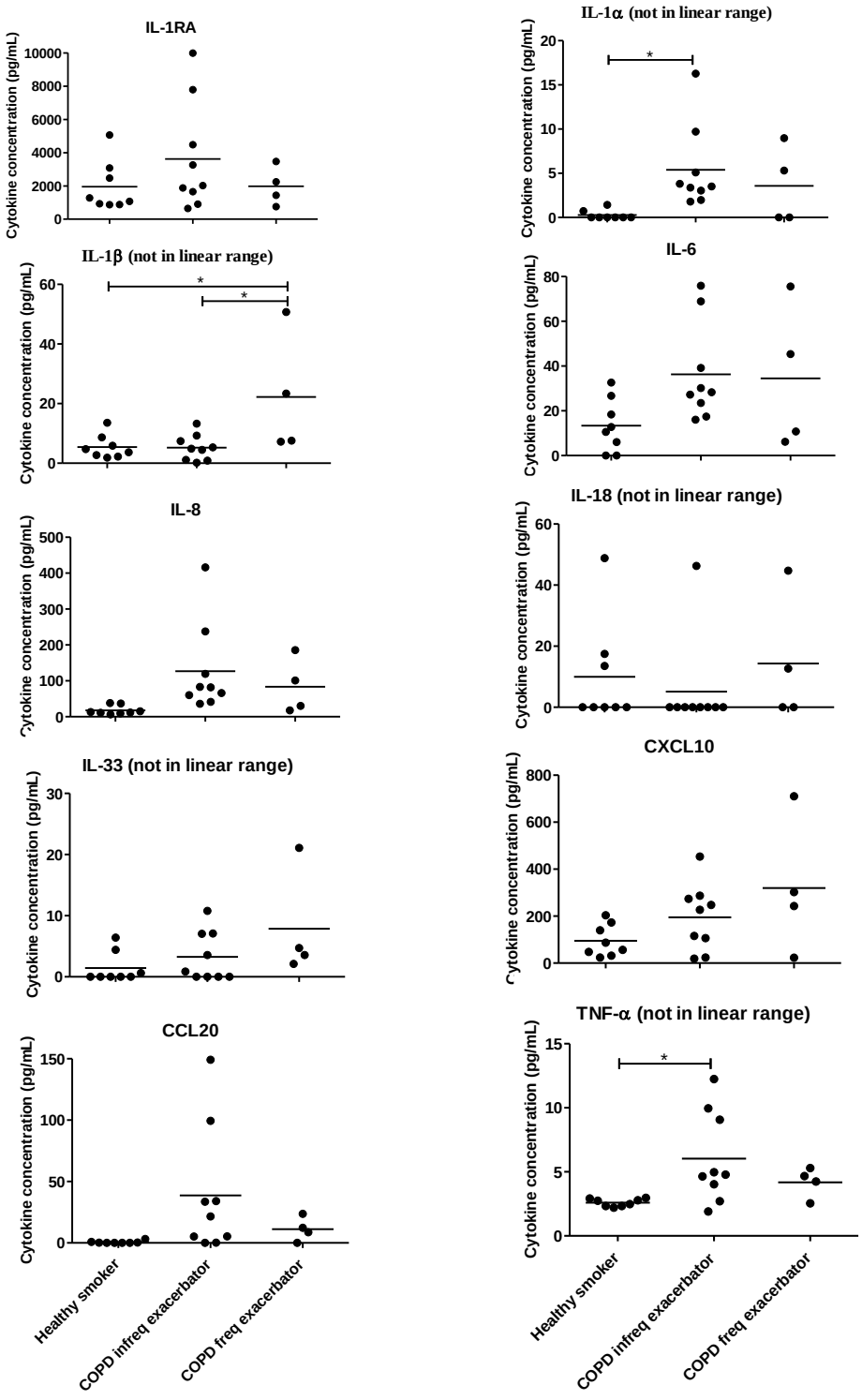

Figure 4.1. Cytokine profiles in the BALF from healthy smokers and COPD patients.

Equivalent volumes of BALF samples were assayed in triplicate using a Luminex assay. Data points represent individual donors with the mean; eight healthy smokers, nine COPD infrequent exacerbators and four COPD frequent exacerbators. One-way ANOVA with a Bonferroni post hoc test, *p <0.05.

4.3 VBP-induces inflammasome activation in HBEC3-KT and THP-1 cells

Since there was evidence demonstrating IL-1β secretion in the airways, the cellular source of this was investigated using a potent inflammatory stimulus which may mimic an exacerbation. The HBEC3-KT cell line was selected to investigate the kinetics of VBP-induced inflammasome activation, due to high NLRP1, DPP8 and DPP9 expression compared with other cell lines (The Human Protein Atlas, 2021c; b; a). Due to VBP catalysation at neutral pH, 0.1 % TFA was added to the culture media (Okondo et al., 2017). In HBEC3-KT cells, VBP induced ASC speck formation, cell death and cytokine release at 24 hours but not at four hours post-treatment (**Figure 4.2**).

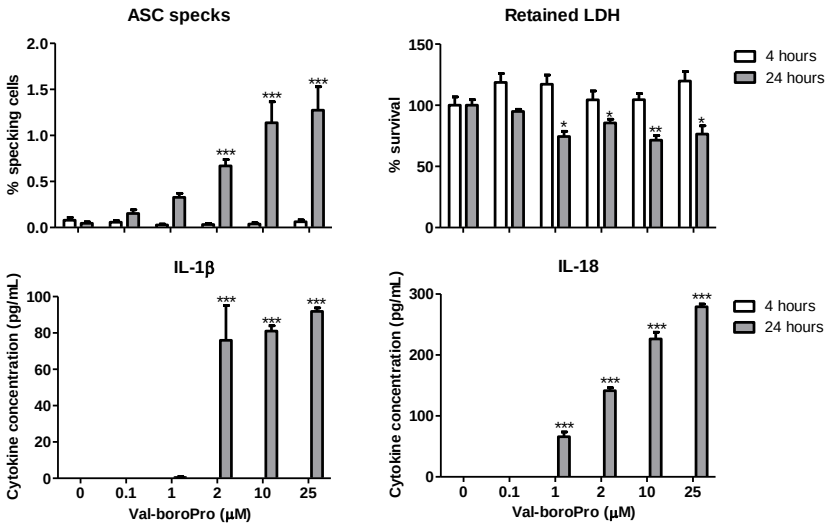

Figure 4.2. HBEC3-KT cells respond to VBP treatment at later timepoints.

HBEC3-KT cells were seeded and cultured overnight. Cells were treated with the indicated concentrations of VBP for four or 24 hours. ELISAs were performed on the supernatants and the remaining cells were lysed for LDH. Data represent the mean of six – 10 technical replicates ± SEM from one experiment. One-way ANOVA with a Dunnett's post hoc test, TFA control vs VBP treatment groups, *p <0.05, **p <0.01, or ***p <0.001.

Inflammasome responses were most prominent at ≥2 μM VBP, after which IL-1β secretion plateaued. As a result of these preliminary observations, 2 μM VBP was used in all subsequent experiments, in line with the concentration used to dose myeloid cells (Okondo et al., 2017; Johnson et al., 2018).

To compare the sensitivity of other cell lines to VBP, BEAS-2B and THP-1 cells were treated with a panel of inflammasome activators. In contrast with HBEC3-KT cells, this pilot experiment suggested that BEAS-2B cells were unable to respond to inflammasome induction, while THP-1 cells responded to LPS plus nigericin but only marginally to VBP (**Figure 4.3**).

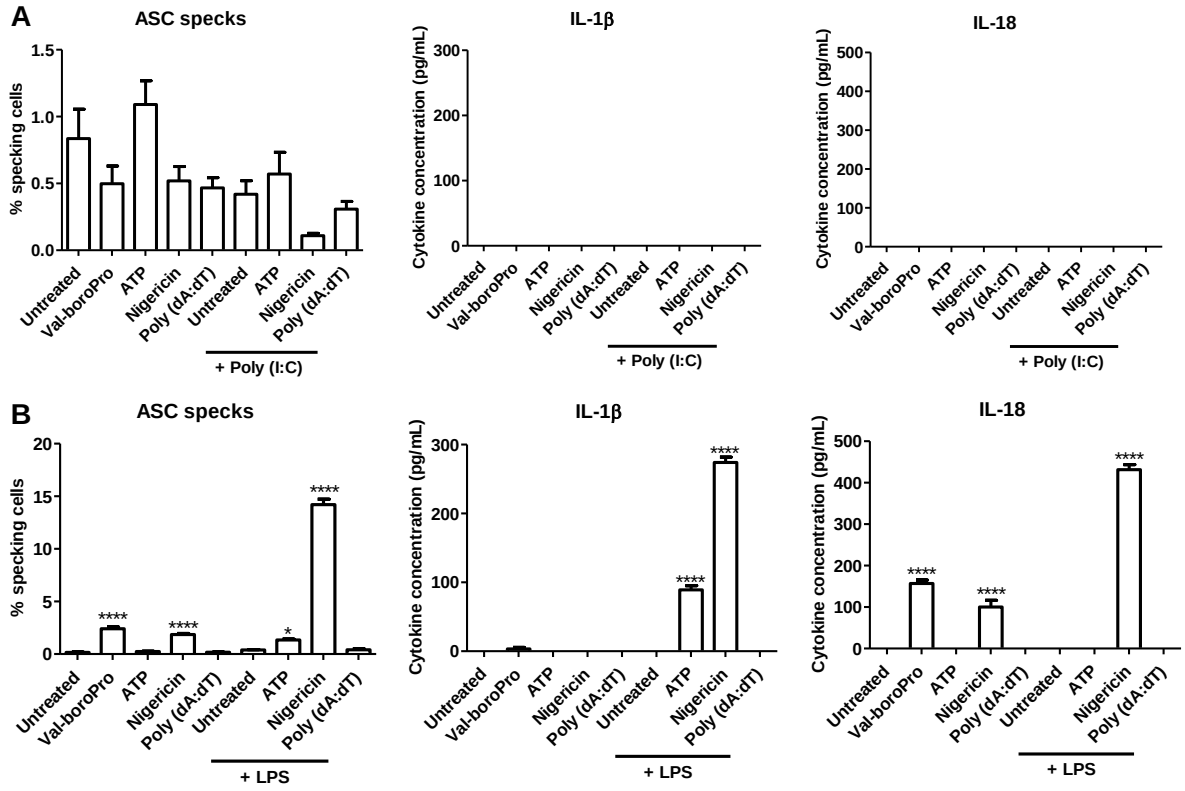

Figure 4.3. VBP and nigericin drive inflammasome responses in THP-1 cells but not in BEAS-2B cells.

(**A**) BEAS-2B cells were seeded and cultured for 48 hours. (**B**) THP-1 cells were differentiated with PMA overnight and then the media was replaced without PMA for 24 hours. (**A** and **B**) Cells were treated with 2 μM VBP, 10 μg/mL poly (I:C) or 200 ng/mL LPS. After 23 hours, primed cells were stimulated with 5 mM ATP, 10 μM nigericin or 5 μg/mL poly (dA:dT) for one hour. Cells were co-stained for ASC and Hoechst, then imaged by IF microscopy. Specks were quantified, ELISAs performed on the supernatants, and the remaining cells lysed for LDH. Data represent three – six technical replicates with the mean from one experiment. One-way ANOVA with a Bonferroni post hoc test, untreated vs treatment groups, *p <0.05, or ****p <0.0001.

4.4 VBP alone drives inflammasome responses in primary basal cells

Basal cells have been implicated in the development and maintenance of respiratory diseases, for example via the production of IL-1β, thus the inflammasome functions of these cells were further investigated (Araya et al., 2007; Byers et al., 2013). Primary cells were treated with a panel of inflammasome stimuli in the presence or absence of the TLR3 ligand poly (I:C) as the priming signal. Inflammasome activation following VBP treatment induced ASC specks in ~15 % cells from COPD patients, whereas NLRP3 or AIM2-activating stimuli were unable to induce any ASC specks and only VBP induced significant cell death alongside IL-1β and IL-18 release (**Figure 4.4**).

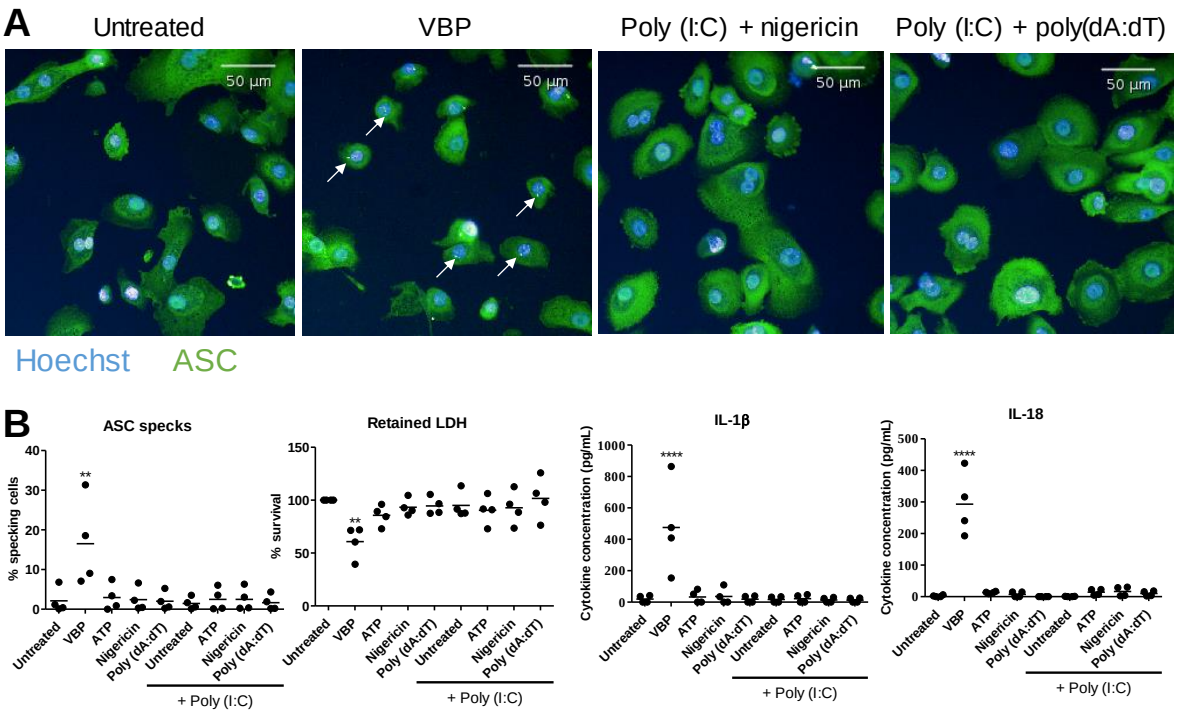

Figure 4.4. NLRP1 is activated in basal epithelial cells.

HBECs from COPD donors were seeded and cultured overnight. Basal cells were treated with 2 µM VBP or 10 µg/mL poly (I:C). After 23 hours, poly (I:C)-primed cells were stimulated with 5 mM ATP, 10 µM nigericin or 5 µg/mL poly (dA:dT) for one hour. (**A**) Cells were co-stained for ASC (green) and Hoechst (blue), then imaged by IF microscopy. Representative images from untreated, VBP, poly (I:C) + nigericin, or poly (I:C) + poly (dA:dT) treated cells are shown. Arrows indicate ASC specks. Scale bar: 50 µm. (**B**) Specks were quantified, ELISAs performed on the supernatants, and the remaining cells lysed for LDH. Data represent four individual donors with the mean from two independent experiments (COPD AB006302, 02AB066702, AB005801 and 0000415058). One-way ANOVA with a Bonferroni post hoc test, untreated vs treatment groups, **p <0.01, or ****p <0.0001.

There was some evidence implicating *P. aeruginosa* in inflammasome-dependent responses in ALI-differentiated HBECs but minimal responses were observed when the T3SS component PrgI alone was transfected into BEAS-2B cells (**Figures 3.12** and **3.13**). In comparison, transfecting PrgI into primary basal cells failed to activate NLRC4, while transfected LPS induced modest cell death although, as expected for

cells with little NLRP3, this was accompanied by negligible cytokine release (**Figure 4.5**).

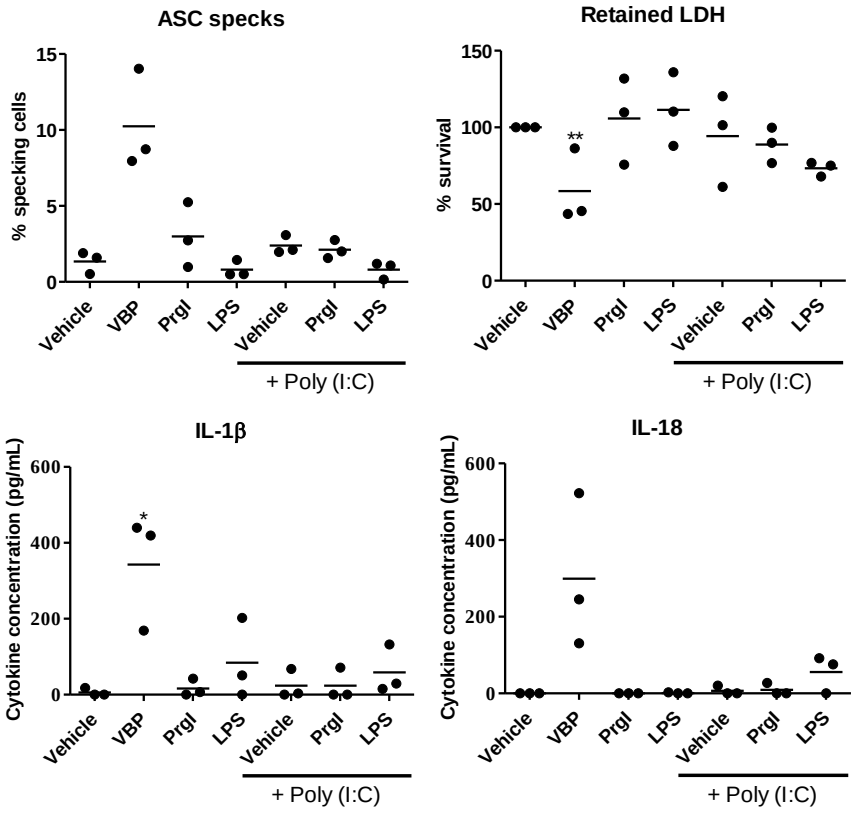

Figure 4.5. Basal epithelial cells are unable to activate NLRC4 or the non-canonical inflammasome.

HBECs from COPD donors were seeded and cultured overnight. Basal cells were treated with 10 µg/mL poly (I:C) for three hours. Unprimed or poly (I:C)-primed cells were treated with 2 µM VBP, 70 ng PrgI or 1000 ng LPS for an additional 24 hours. Cells were stained with anti-ASC for ASC speck IF, ELISAs performed on the supernatants, and the remaining cells were lysed for LDH. Data represent three individual donors with mean from two independent experiments (COPD 02AB066702, AB005801 and 0000415058). One-way ANOVA with a Bonferroni post hoc test, Lipofectamine vs treated groups, *p <0.05, or **p <0.01.

4.5 VBP-induced inflammasome activation is NLRP1-dependent

DPP8/9 inhibition activates the NLRP1 inflammasome, like the direct activation of mouse NLRP1B by anthrax lethal factor, by inducing proteasome-mediated 'functional degradation' (Chavarría-Smith and Vance, 2013; Sandstrom et al., 2019; Ball et al., 2020). Proteasomal degradation of the auto-inhibitory N-terminus

enables FIIND autoproteolysis and the liberation of the bioactive C-terminal fragment which recruits caspase-1. To investigate whether this pathway was also activated in HBECs, basal cells were pre-treated with NLRP3, caspase, proteasome, or cell death inhibitors prior to VBP treatment. Cells treated with the NLRP3 inhibitor MCC950 were not impaired in their ability to form ASC specks or undergo cell death (**Figure 4.6**).

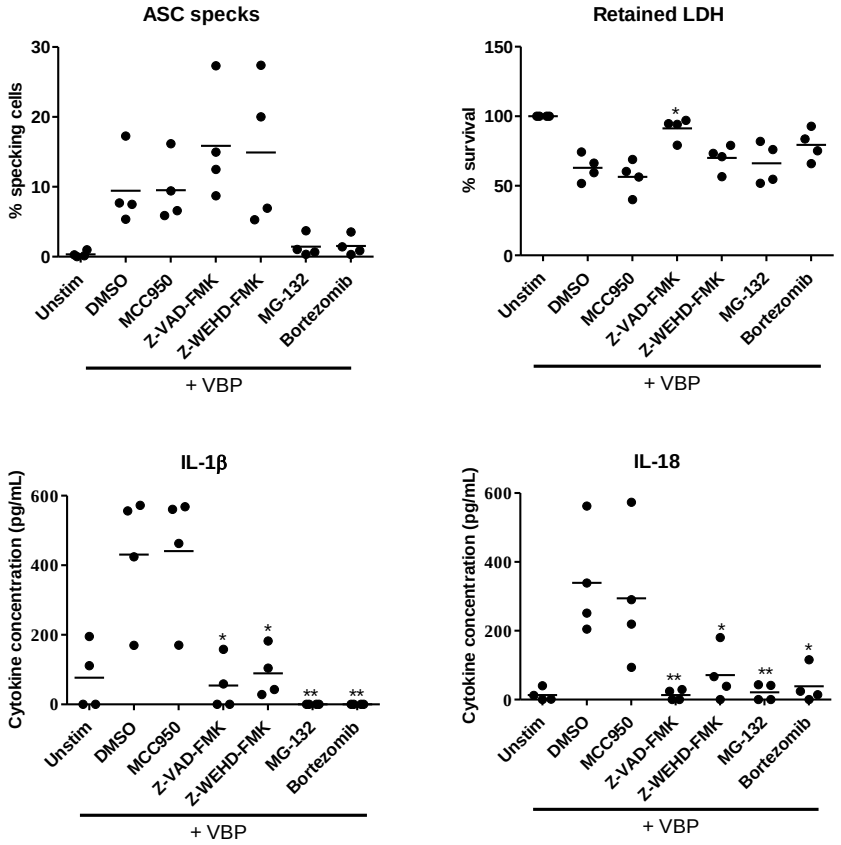

Figure 4.6. VBP-induced inflammasome activation is caspase or proteasome-dependent in basal epithelial cells.

Basal cells from COPD donors were seeded and cultured overnight. Cells were pre-treated with 1 µM MCC950, 20 µM Z-VAD-FMK, 20 µM Z-WEHD-FMK, 100 nM MG-132, or 100 nM bortezomib for one hour. HBECs were then treated with 2 µM VBP for 24 hours, which diluted the inhibitors two-fold. Cells were stained with anti-ASC for ASC IF, ELISAs performed on the supernatants, and the remaining cells were lysed for LDH. Data shown are four individual donors with the mean from two independent experiments (COPD AB006302, AB005801, 0000370751 and 0000415058). One-way ANOVA with a Bonferroni post hoc test, DMSO vs inhibitor-treated groups, *p <0.05, or **p <0.01.

Both the pan-caspase and caspase-1 inhibitors used reduced IL-1β and IL-18 secretion upon VBP treatment although the effect on ASC speck formation was minimal. Proteasomal inhibition with MG-132 or bortezomib reduced ASC speck formation and cytokine release but were unable to rescue VBP-induced cell death.

Despite the presence of ASC-forming inflammasomes, which implicates NLRP1 involvement since CARD8 fails to recruit ASC, this experiment preceded siRNA-mediated KD of NLRP1 or CARD8, to discount CARD8 contributions. To establish siRNA transfection conditions, GAPDH KD was performed using HBEC3-KT cells and the efficiency was assessed by western blot. Protein KD was achieved within 24 hours and was particularly prominent when cells remained exposed to the transfection mixtures (**Figure 4.7**).

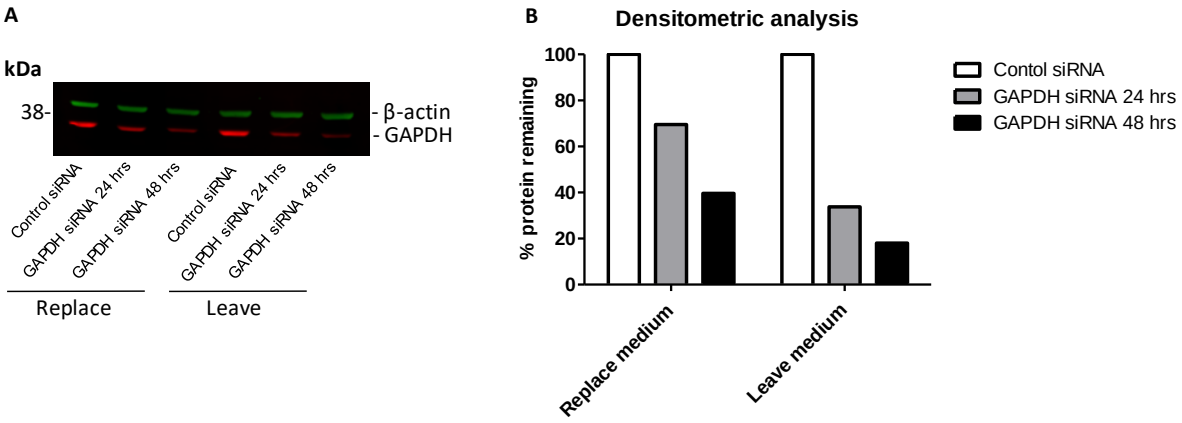

Figure 4.7. siRNA-mediated KD of GAPDH in HBEC3-KT cells.

Cells were incubated with control siRNA or GAPDH siRNA at 20 nM using Lipofectamine RNAiMAX for 24 or 48 hours. HBEC3-KT cells were lysed in RIPA buffer, proteins separated by SDS gel electrophoresis followed by transfer to a PVDF membrane. (**A**) Levels of ACTB (45 kDa) and GAPDH (~36 kDa) were detected using the relevant primary antibodies. Blot shown from one experiment consists of lysates from two pooled technical replicates. (**B**) Densitometric analysis of treatment bands compared with control bands, following normalisation to ACTB.

Quantification of protein bands by densitometric analysis revealed that leaving on the transfection mixes for 48 hours resulted in the greatest KD efficiency (~80 %). ACTB remained relatively consistent despite the different conditions, suggesting that Lipofectamine RNAiMAX was tolerated for 48 hours. These parameters were selected to KD NLRP1 and CARD8 in primary HBECs from multiple patients.

A clear reduction in NLRP1 protein levels was observed following transfection with NLRP1 siRNA, although this was less obvious for CARD8 expression following treatment with CARD8 siRNA (**Figure 4.8**).

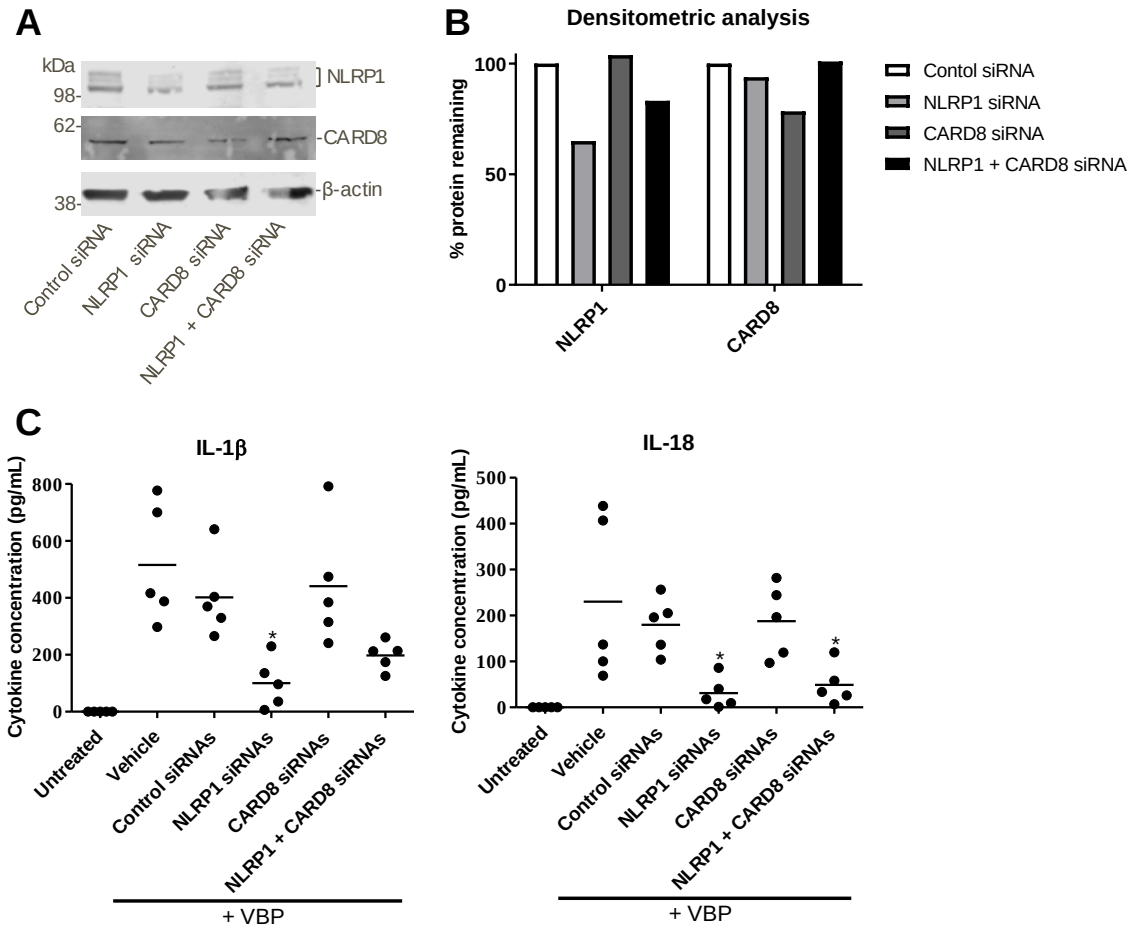

Figure 4.8. VBP-induced inflammasome activation is NLRP1-dependent in basal epithelial cells.

Basal cells from COPD donors were seeded and cultured overnight. Cells were incubated with vehicle control, control siRNA, NLRP1 siRNA, CARD8 siRNA or NLRP1 + CARD8 siRNA at 20 nM using Lipofectamine RNAiMAX for 48 hours before treatment with VBP for a further 24 hours. Cells were lysed in RIPA buffer, proteins separated by SDS gel electrophoresis followed by transfer to a PVDF membrane. (**A**) Levels of NLRP1 (~150 kDa) and CARD8 (~ 60 kDa) were detected using the relevant primary antibodies. Blot shown consists of three pooled donors (COPD AB005801, 0000370751 and 0000415058). (**B**) Densitometric analysis of treatment bands compared with control bands, following normalisation to ACTB. (**C**) ELISAs were performed on the supernatants. Data represent five individual donors with the mean from two independent experiments (COPD AB006302, 02AB066702, AB005801, 0000370751 and 0000415058). One-way ANOVA with a Bonferroni post hoc test, DMSO vs inhibitor-treated groups or control siRNA vs target siRNA-treated groups, *p <0.05.

KD of NLRP1 alone decreased IL-1β and IL-18 secretion upon VBP treatment, and this was not further reduced by synchronous CARD8 KD. In addition, CARD8 KD alone had no effect on cytokine production.

4.6 NLRP1 activation is enhanced in basal cells from COPD patients

Emerging evidence implicates inflammasomes in the development of chronic respiratory diseases. SNPs in NLRP1 may be implicated in COPD and asthma pathogenesis, but there remains a scarcity of functional data, particularly for epithelial cells (Ozretić et al., 2019; Moecking et al., 2020). The functional consequences of VBP-mediated NLRP1 activation were measured in basal cells by means of ASC speck formation, cell death and cytokine secretion. All cells were responsive to NLRP1 activation, but the sensitivities of cells from different patient groups varied markedly. Cells from COPD patients had enhanced ASC speck formation, increased cell death and IL-1β secretion in response to VBP in contrast to cells derived from healthy and asthmatic donors (**Figure 4.9**).

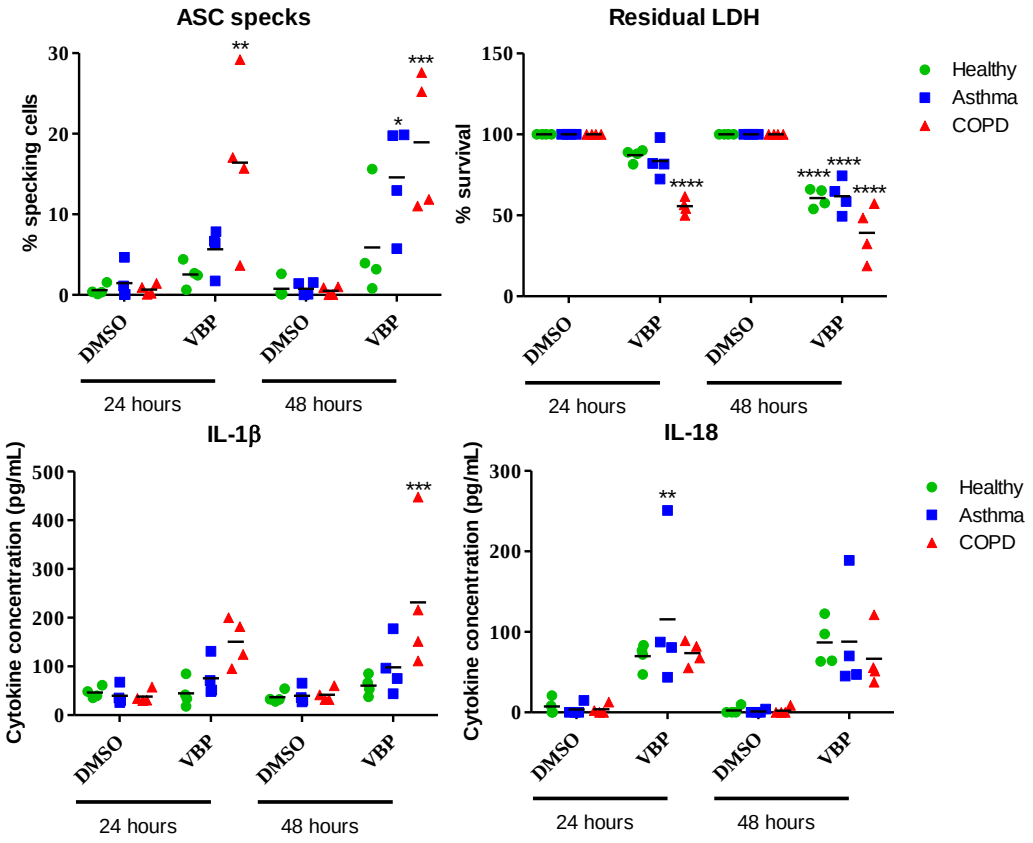

Figure 4.9. NLRP1 activation in basal cells from COPD donors leads to enhanced ASC speck formation, cell death and IL-1β secretion.

Basal cells from healthy, asthmatic or COPD donors were seeded and cultured overnight. Cells were treated with 2 μM VBP for 24 or 48 hours. Basal cells were stained with anti-ASC for ASC IF, ELISAs performed on the supernatants, and the remaining cells were lysed for LDH. Data represent four individual donors with the mean from four independent experiments (Healthy AB039401, 02AB061001, 02AB066901 and 0000333288; Asthma 02AB066501, 0000344668, 0000470633 and 0000534647; COPD AB006302, AB005801, 0000415058 and 0000370751). Two-way ANOVA with a Bonferroni post hoc test, DMSO-treated vs VBP-treated groups, *p <0.05, **p <0.01, ***p <0.001, or ****p <0.0001.

To determine if enhanced VBP-mediated inflammasome activation in cells from patients with COPD was caused by the elevated expression of *NLRP1*, endogenous RNA levels were investigated. *NLRP1*, but also the negative regulators *DPP8* and *DPP9*, were significantly upregulated in basal cells derived from COPD patients (**Figure 4.10**).

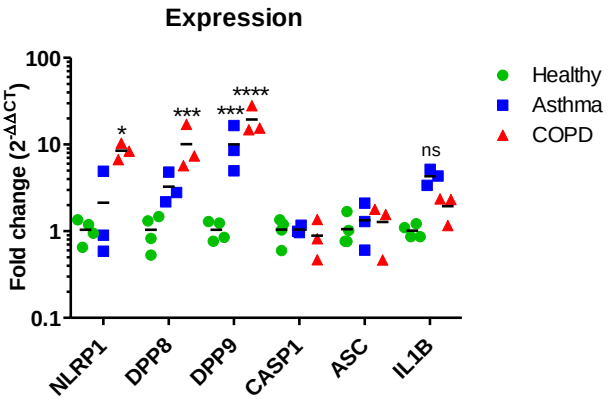

Figure 4.10. *NLRP1* levels are enhanced in COPD basal cells.

HBECs from healthy, asthmatic or COPD donors were seeded and cultured overnight. RNA was isolated from basal cells and reverse transcribed to cDNA. RT-qPCR was used to determine the fold change ($2^{-\Delta\Delta Ct}$) between healthy and disease-derived basal cells for *NLRP1*, *DPP8*, *DPP9*, *CASP1*, *ASC* and *IL1B*, following normalisation to the *ACTB* housekeeping gene. Data represent three – four individual donors with the mean from three – four independent experiments (Healthy AB039401, 02AB061001, 02AB066901 and 0000333288; Asthma AB049502, 02AB066501 and 0000534647; COPD AB006302, 02AB066702 and 0000415058). One-way ANOVA with a Bonferroni post hoc test, healthy vs disease groups, *p <0.05, ***p <0.001, or ****p <0.0001.

In addition to VBP, dsRNA has also been shown to activate the NLRP1 inflammasome (Bauernfried et al., 2021). As a result, poly (I:C), a dsRNA analogue, was transfected into primary HBECs using Lipofectamine 2000 as the transfection vehicle. Modest inflammasome responses were observed at 24 hours, and IL-1β levels were only marginally enhanced in cells from patients with COPD (**Figure 4.11**).

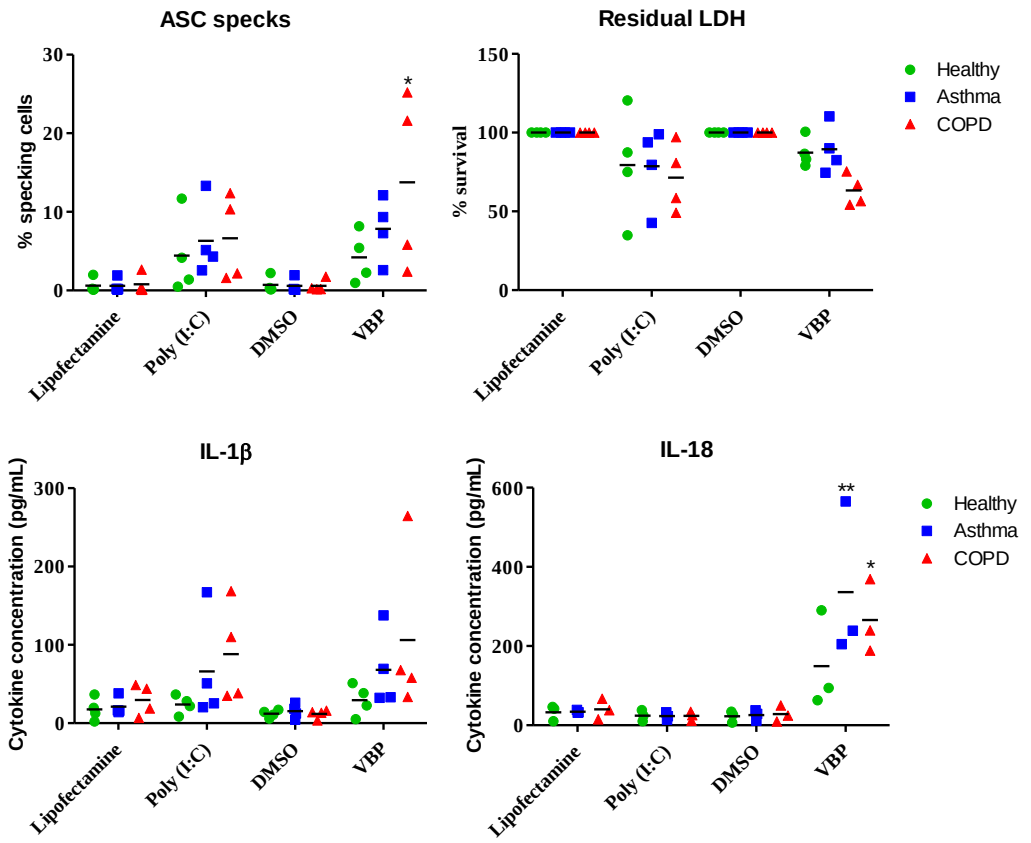

Figure 4.11. Poly (I:C) induces modest inflammasome responses in primary HBECs.

Basal cells from healthy, asthmatic or COPD donors were seeded and cultured overnight. Cells were transfected with 200 ng/mL poly (I:C) using Lipofectamine 2000 or directly stimulated with 2 μM VBP for 24 hours. Basal cells were stained with anti-ASC for ASC IF, ELISAs performed on the supernatants, and the remaining cells were lysed for LDH. Data shown are three – four individual donors with the mean from three – four independent experiments (Healthy AB039401, 02AB061001, 02AB066901 and [0000333288]; Asthma 02AB066501, [0000344668], 0000470633 and 0000534647; COPD [AB006302], AB005801, 0000415058 and 0000370751). One-way ANOVA with a Bonferroni post hoc test vs Lipofectamine only or DMSO control, *p <0.05, or **p <0.01.

4.7 NLRP1 activation is enhanced in ALI-differentiated HBECs from COPD patients

Given the polarised and multi-subtype composition of the airway epithelium *in vivo*, the relevance of these 2D findings was investigated in ALI-differentiated HBECs.

These cultures formed a pseudostratified layer and were characterised by a mixed population of basal (CD49f^{+} CD271^{+}), progenitor (CD66^{+} CD133^{+}), goblet (CD66^{+} CD133^{-}) and ciliated cells (CD66^{-} CD133^{+}) as determined by flow cytometry (**Figure 2.2**). ALI-differentiated cells were treated with VBP or HRV16, the latter of which activates the NLRP1 inflammasome via 3Cpro activity (Robinson et al., 2020; Tsu et al., 2021). Although to a lesser extent compared with VBP stimulation, HRV16 infection caused pro-inflammatory cytokine release, and this was most prominent in COPD donor cells (**Figure 4.12**).

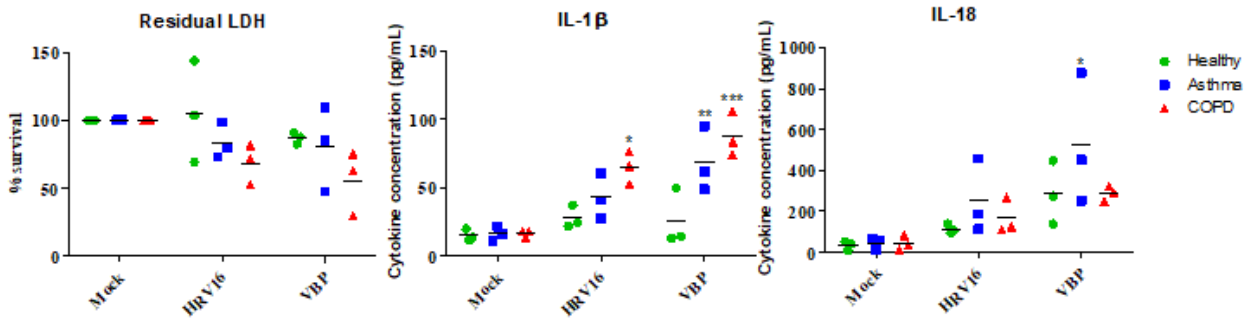

Figure 4.12. NLRP1 is activated in ALI-differentiated airway epithelial cells.

HBECs from healthy, asthmatic and COPD donors were cultured at the ALI for 28 days. Cells were incubated with HRV16 (MOI 1) or 2 µM VBP apically for one hour before removal. After a total of 48 hours, ELISAs were performed on supernatants collected via apical washes, and the remaining cells were lysed for LDH. Data shown are three individual donors with the mean from three independent experiments (Healthy 02AB061001, 02AB066901 and 0000333288; Asthma 0000344668, 0000470633 and 0000534647; COPD AB006302, 02AB066702 and 0000370751). One-way ANOVA with a Bonferroni post hoc test, mock vs treated groups, *p <0.05, **p <0.01, or ***p <0.001.

4.8 Discussion

There is emerging evidence that NLRP1 has functions in the barrier epithelium of the skin and the intestine (Zhong et al., 2016; Fenini et al., 2018; Tye et al., 2018; Zhong et al., 2018). It was unclear if this was also the case for HBECs, however, the findings from **Chapter 3** suggested that inflammasome sensors other than NLRP3 may be important. To this end, VBP was utilised as a tool to investigate the NLRP1/CARD8 axis in HBECs.

The kinetics of VBP-induced ASC formation, cell death and cytokine secretion were initially assessed in the HBEC3-KT cell line (**Figure 4.2**). Although the results from these cell line experiments were preliminary, they were in line with the precedent literature. As observed with other cell types, responses were delayed compared to NLRP3 activation in macrophages for example and peaked at 24 hours after stimulation (Okondo et al., 2017; Johnson et al., 2018). As speculated previously, a certain threshold of bioactive UPA-CARD may need to accumulate before subsequent inflammasome assembly (Mitchell et al., 2019). In contrast, the other epithelial cell line assayed, BEAS-2B cells, failed to respond to inflammasome induction, which may suggest low expression of NLRP1 or CARD8 (**Figure 4.3**). Indeed, HBEC3-KT cells were the only respiratory cell line screened to have high NLRP1 and DPP9 expression (The Human Protein Atlas, 2021c; b). In line with previous observations, VBP treatment of PMA-differentiated THP-1 cells induced ASC speck formation and IL-18 secretion, however, this was much lower than that induced by LPS plus nigericin (Okondo et al., 2017). VBP was unable to induce the release of IL-1β from THP-1 cells since CARD8 rather than NLRP1 is downstream of DPP8/9 inhibition in myeloid cells (Linder et al., 2020). Since basal cells from COPD patients have enhanced inflammatory profiles compared with control cells, these were used as a model to investigate inflammasome function (Araya et al., 2007; Byers et al., 2013). As mentioned above, VBP also activates CARD8 in myeloid cells and T cells, but unlike the closely related NLRP1, this molecule forms an ASC-independent inflammasome (Finger et al., 2012; Ball et al., 2020). VBP induced ASC speck formation in the basal epithelial cells, suggesting that NLRP1 is likely to be the effector of this molecule (**Figure 4.4**). In line with previous observations, pharmacological blockade revealed that VBP-induced responses were caspase-1 and proteasome-dependent but NLRP3-independent (**Figure 4.6**) (Okondo et al., 2018; Ball et al., 2020). The proteasome inhibitors used were unable to rescue cell death, however, potentially due to the potency of VBP and/or the propensity of proteasomal blockade to induce apoptosis (Nunes and Annunziata, 2017). siRNA-mediated KD confirmed the involvement of NLRP1, and this led to significantly reduced IL-1β and IL-18 secretion upon VBP treatment (**Figure 4.8**). Minimal effects on IL-1β release were observed following combined NLRP1 and CARD8 KD, most likely due to the lower concentration of NLRP1 siRNA used. Since

KD of CARD8 protein was less successful, these data were confirmed by CRISPR-Cas9 KO (**see Chapter 5**).

The elevated expression of NLRP1, which may be regulated by the increased expression of DPP8/9, presumably contributes to the enhanced inflammasome activation in cells from patients with COPD (**Figure 4.9** and **4.10**). Emerging evidence also suggests an involvement of the oxidoreductase, thioredoxin-1, the oxidised form of which can bind to and repress NLRP1 activity (Ball et al., 2021). Furthermore, thioredoxin-1 levels may be reduced in COPD, and its administration prevents inflammation and emphysema progression in murine exacerbation models (Tanabe et al., 2013; Zhou et al., 2020). At 48 hours post VBP treatment, delayed responses could also be observed in cells derived from asthmatic patients. In these cells, DPP9 expression was significantly enhanced compared with basal cells from healthy controls. This may reflect the overlap between asthma and COPD, and the progression from asthma to COPD in older sufferers (Brown et al., 1984; Backman et al., 1997). Indeed, NLRP1 is upregulated in ageing lungs, and this may help explain the prevalence of COPD in the elderly (de Vries et al., 2017). One may speculate, therefore, that enhanced responses may occur in cells derived from older asthmatic patients.

There was only slight evidence that IL-1β responses to poly (I:C) were enhanced in the disease (**Figure 4.11**). This may highlight the different mechanisms of activation and/or may have been an artefact of suboptimal transfection efficiencies (Bauernfried et al., 2021). Exaggerated responses in COPD could instead be recapitulated with ALI-differentiated HBECs, incorporating a physiological model of the respiratory epithelium and HRV16, the recently identified biological activator of NLRP1 (**Figure 4.12**) (Robinson et al., 2020; Tsu et al., 2021). It is plausible that HRV16-mediated NLRP1 activation may contribute to acute exacerbations of COPD, and that NLRP1 senses other pathogenic proteases, such as those from commonly infecting bacteria or viruses such as *Streptococcus* or coronaviruses, respectively.

In summary, this chapter provides evidence that NLRP1 is the dominant inflammasome in primary HBECs. VBP, but not activators of NLRP3, AIM2 or NAIP/NLRC4, induces robust inflammasome activation and this is dependent on

caspase or proteasome activity. NLRP1 was implicated as the specific inflammasome sensor since VBP induced ASC speck formation and IL-1β secretion, and responses were mollified by siRNA-mediated KD. A NLRP1 dependency was also confirmed independently by a recent publication (Robinson et al., 2020). Also presented here is the first functional evidence that NLRP1 responses are enhanced in basal and ALI-differentiated cells from COPD patients. Since this receptor is upregulated in COPD donors, who are particularly susceptible to exaggerated inflammation during viral infections, the NLRP1 inflammasome may be a novel therapeutic target for individuals with this challenging respiratory disease.

Chapter 5. The role of NLRP1 in epithelial differentiation

5.1 Rationale

In **Chapter 5**, the effects of chronic activation and genetic deletion of NLRP1 on HBEC differentiation were determined.

The involvement of NLRs in epithelial differentiation remains unexplored, however, evidence from other cell types suggests that they may play a role. In the context of non-immune cells, NLRP1 enhances the transdifferentiation of cardiac fibroblasts to myofibroblasts in the presence of TGF-β1 (Zong et al., 2018). Here, α-smooth muscle actin (α-SMA), a marker for cardiac myofibroblasts, was increased following NLRP1 overexpression but reduced following shRNA-mediated KD. There is also evidence that NOD1, NOD2 and NLRP3 influence adipocyte and osteogenic differentiation, following stimulation with receptor-specific ligands (Kim et al., 2010; J et al., 2013; Liu et al., 2020; Chen et al., 2021). Additionally, multiple reports have demonstrated the role of NLRP3 in immune cell differentiation. For example, NLRP3 positively regulates $CD4^+$ T cell differentiation into T_H2 cells but negatively regulates differentiation into T_{reg} cells (Bruchard et al., 2015; Park et al., 2019). In both cases, the nuclear activities of NLRP3 appeared to be important. Specifically, in rheumatoid arthritis, NLRP3 has been shown to drive T_H17 differentiation, while deficiency of this NLR leads to M2 microglia polarisation (Saresella et al., 2016; Zhao et al., 2018).

Since *NLRP1*, *DPP8* and *DPP9* expression were enhanced in cells from COPD patients in **Chapter 4**, and sufferers are known to have HBEC differentiation defects, it was reasonable to investigate the nexus between this NLR and differentiation of the pseudostratified columnar epithelium (Crystal, 2014).

5.2 Chronic NLRP1 activation arrests epithelial differentiation and leads to sustained cytokine release

To preliminarily investigate the roles of NLRP1 in differentiation, this NLR was chemically activated with VBP during ALI culture. In cells from both healthy and COPD patients, minimal differences could be observed on days seven and 14. At day 21, however, an increase in progenitor (CD66a/c/e^{+} CD133^{+}) and goblet cells (CD66a/c/e^{+} CD133^{-}), while a decrease in ciliated cells (CD66a/c/e^{-} CD133^{+}), could be observed in both patient groups following VBP treatment (**Figure 5.1**).

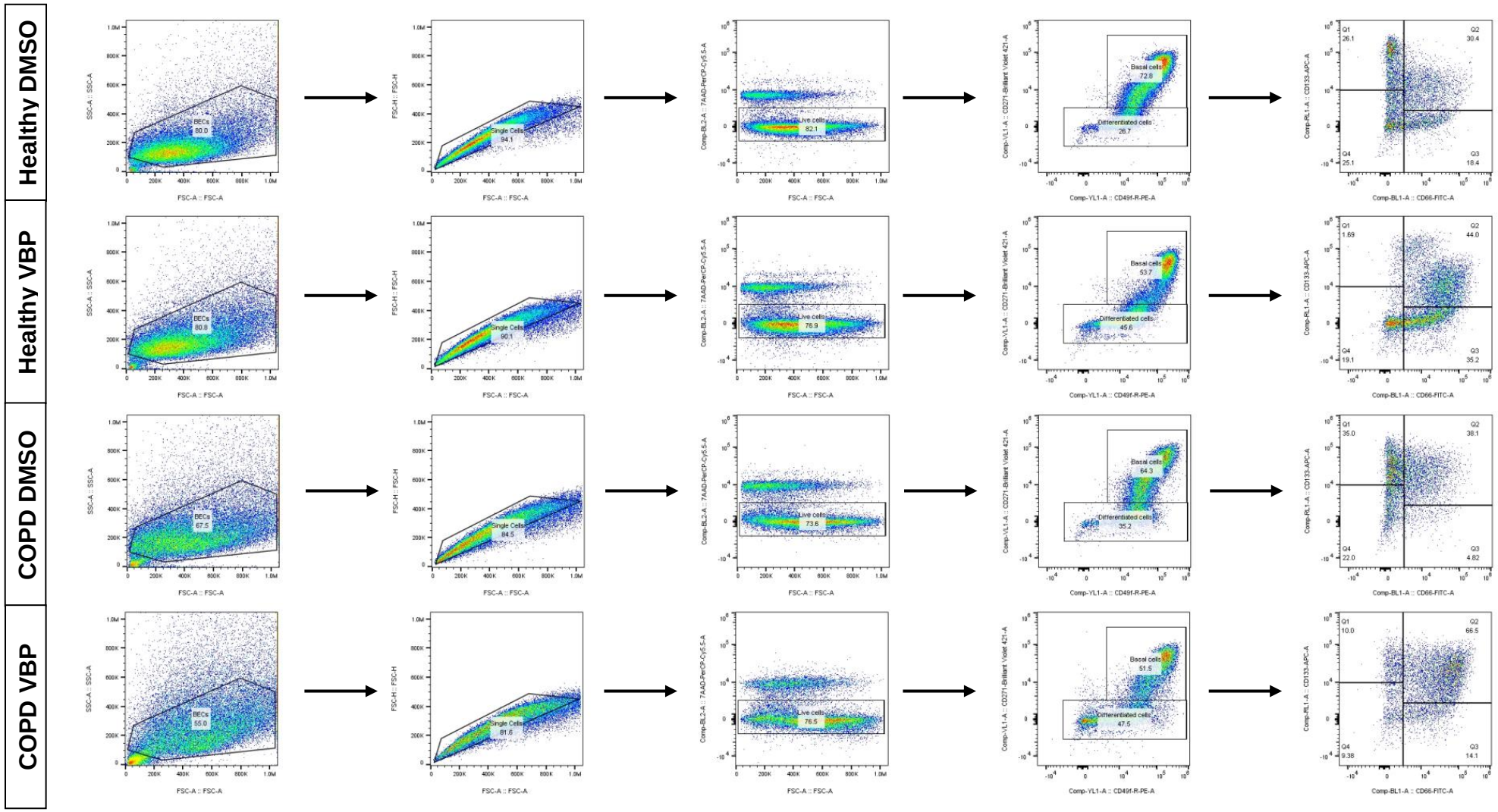
Healthy DMSO
Healthy VBP
COPD DMSO
COPD VBP
SSC-A :: SSC-A
FSC-A :: FSC-A
BECs
80.0
FSC-H :: FSC-H
Single Cells
94.1
Comp-BL2-A :: 7AAD-PerCP-Cy5.5-A
Live cells
82.1
Comp-YL1-A :: CD271-Brilliant Violet 421-A
Basal cells
72.8
Differentiated cells
26.7
Comp-YL1-A :: CD49f-R-PE-A
Comp-RL1-A :: CD133-APC-A
Comp-BL1-A :: CD66-FITC-A
Q1
26.1
Q2
30.4
Q4
25.1
Q3
18.4
BECs
80.8
Single Cells
90.1
Live cells
76.9
Basal cells
53.7
Differentiated cells
45.6
Q1
1.69
Q2
44.0
Q4
19.1
Q3
35.2
BECs
67.5
Single Cells
84.5
Live cells
73.6
Basal cells
64.3
Differentiated cells
35.2
Q1
35.0
Q2
38.1
Q4
22.0
Q3
4.82
BECs
55.0
Single Cells
81.6
Live cells
76.5
Basal cells
51.5
Differentiated cells
47.5
Q1
10.0
Q2
66.5
Q4
9.38
Q3
14.1

Figure 5.1. Progenitor/secretory cell populations are enhanced upon chronic VBP exposure.

Following initiation of ALI, culture media containing 2 μM VBP was replenished every other day for 21 days. To determine the presence of basal cells ($CD49f^+$ $CD271^+$), progenitor cells ($CD66a/c/e^+$ $CD133^+$), goblet cells ($CD66a/c/e^+$ $CD133^-$) and ciliated cells ($CD66a/c/e^-$ $CD133^+$), dissociated cells were stained with anti-CD49f, anti-CD271, anti-CD66a/c/e and anti-CD133 for flow-cytometric analysis. Live, single cells were gated based on FSC, SSC and 7AAD-negativity. FACS plots are shown for one healthy and one COPD donor from one experiment (Healthy 18TL127524; COPD 0000370751).

To confirm that NLRP1 was activated in these cultures, IL-1β and IL-18 levels were measured in the basolateral compartment. Chronic treatment with VBP induced sustained cytokine release and, as observed in **Chapter 4**, levels were greater in the HBECs from the COPD patient as opposed to the healthy control (**Figure 5.2**).

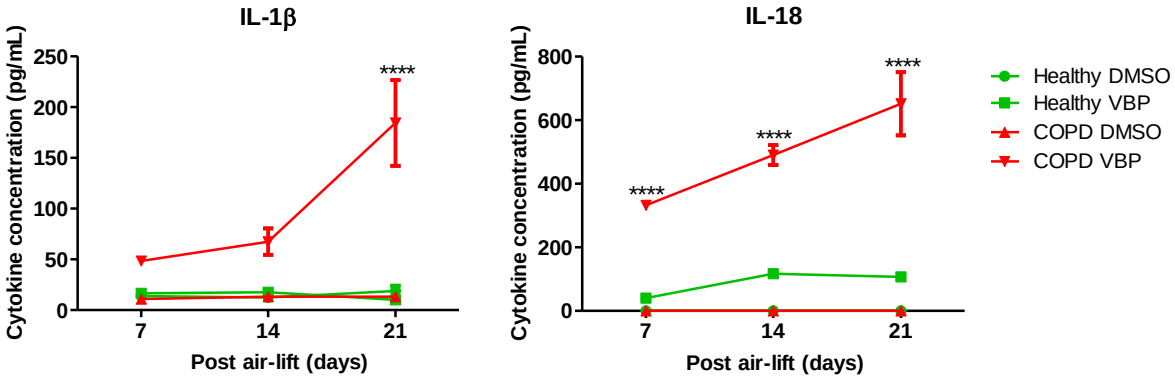

Figure 5.2. Chronic dosing of ALI-differentiating HBECs with VBP induces sustained cytokine secretion.

HBECs from one healthy and one COPD donor were seeded onto Transwells, and ALI was initiated after two days. Culture media containing 2 μM VBP was replenished every other day for 21 days. ELISAs were performed on the basolateral supernatants collected on days seven, 14 and 21. Data shown are the mean of six technical replicates ± SEM from one experiment (Healthy 18TL127524; COPD 0000370751). One-way ANOVA with a Bonferroni post hoc test, relevant DMSO control vs VBP treatment, ****p <0.0001.

5.3 Deletion of NLRP1 protects cells from VBP

To specifically investigate the functions of NLRP1 in epithelial differentiation, NLRP1 KO HBECs were generated using RNP electroporation. An attempt was also made to KO CARD8, which has low expression in HBECs (**Figures 3.1** and **3.2**). Following electroporation with target-specific RNPs, NLRP1 protein levels were abolished in basal cells from three healthy and three COPD donors, however, CARD8 expression remained unchanged (**Figure 5.3**).

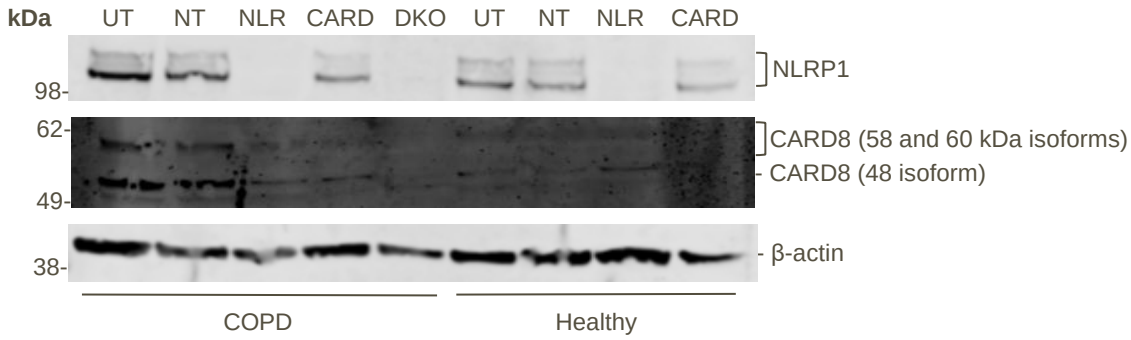

Figure 5.3. NLRP1 protein levels are abolished in KO basal cells.

Basal cells cultured under submerged conditions were transfected with pooled NLRP1 or pooled CARD8 crRNA (50 μM final concentration) and cultured for seven days until confluency. Cells were lysed in RIPA buffer, proteins separated by SDS gel electrophoresis, followed by transfer to a PVDF membrane. Levels of NLRP1 (~150 kDa) and CARD8 isoforms (48, 58 and 60 kDa) were detected using the relevant primary antibodies. Representative blot shown from three independent experiments consists of lysates from two donors (COPD 02AB066702; Healthy 000333288). UT, untreated. NT, non-targeting. NLR, NLRP1 KO. CARD, CARD8 KO. DKO, NLRP1 and CARD8 KO.

To confirm the results from **Chapter 4** and to functionally validate KO cells, VBP was used to assess NLRP1 activity. As previously suggested, KO of NLRP1 protects HBECs from the activities of VBP, and as shown above, ASC speck formation and IL-1β release were enhanced in cells from COPD donors (**Figure 5.4**).

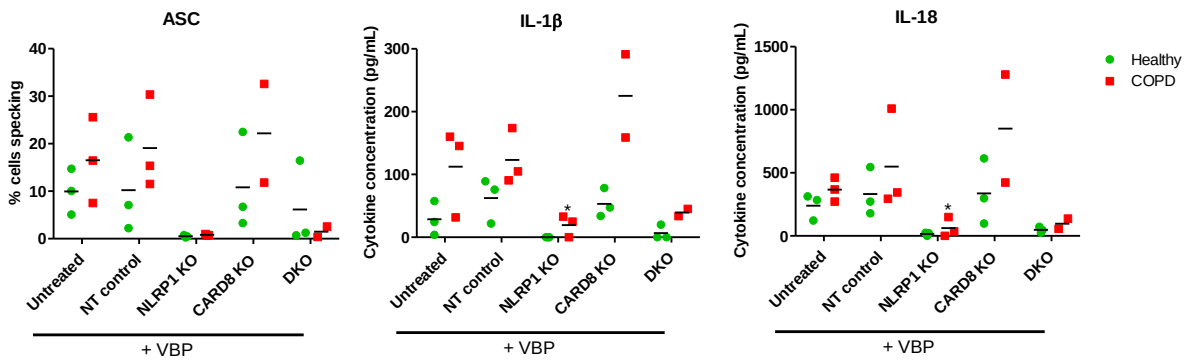

Figure 5.4. NLRP1 KO abrogates ASC speck formation and cytokine secretion.

KO basal cells from healthy or COPD donors were seeded and cultured overnight. Cells were treated with 2 μM VBP for 48 hours. Basal cells were stained with anti-ASC for ASC IF and ELISAs performed on the supernatants. Data points represent two-three individual donors with the mean from two – three independent experiments (Healthy 02AB061001, 02AB066901 and 0000333288; COPD [AB006302], 02AB066702 and 0000370751). One-way ANOVA with a Dunnett's post hoc test (excluding groups with two donors), relevant NT control vs crRNA-treated groups, *p <0.05. NT, non-targeting. DKO, NLRP1 and CARD8 KO.

To further confirm the specificity of the crRNA used, KO cells were treated with poly (I:C) to activate TLR3, and the secretion of IL-6 was measured. IL-6 secretion from healthy patient-derived HBECs was maintained across all conditions. NLRP1 KO cells from COPD donors released slightly higher levels of IL-6 upon TLR3 activation, however, this did not achieve statistical significance (**Figure 5.5**).

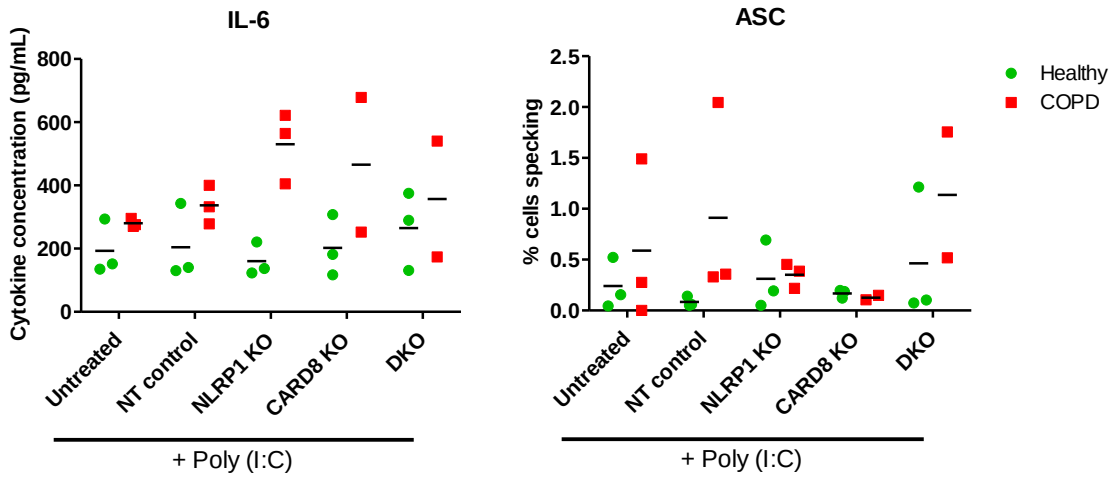

Figure 5.5. Deletion of NLRP1 may enhance poly (I:C)-induced IL-6 secretion in cells from COPD patients.

KO basal cells from healthy or COPD donors were seeded and cultured overnight. Cells were treated with 10 µg/mL poly (I:C) for 48 hours. Basal cells were stained with anti-ASC for ASC IF and ELISAs performed on the supernatants. Data shown are two-three individual donors with the mean from two – three independent experiments (Healthy 02AB061001, 02AB066901 and 0000333288; COPD [AB006302], 02AB066702 and 0000370751). One-way ANOVA with a Dunnett's post hoc test (excluding groups with two donors), relevant NT control vs crRNA-treated groups. NT, non-targeting. DKO, NLRP1 and CARD8 KO.

5.4 Deletion of NLRP1 has minimal impact on barrier formation

To determine if NLRP1 KO cells were impaired in their ability to form AJCs, TEER was recorded every six days commencing on day two post-ALI induction. As expected, cells from COPD donors returned lower TEER measurements compared with those from control cells, however, there was a marginal impact on TEER between treatments (**Figure 5.6**).

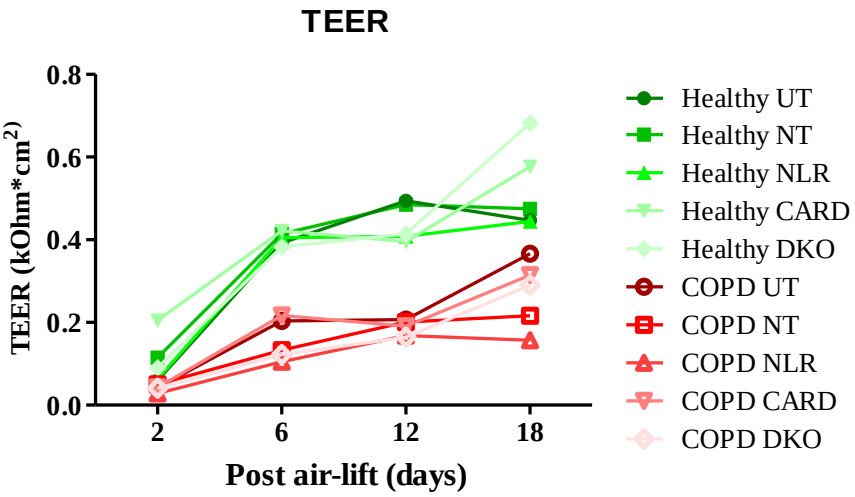

Figure 5.6. Deletion of NLRP1 has no impact on barrier formation.

KO HBECs from healthy and COPD donors were cultured at the ALI for 21 days. TEER was measured on days two, six, 12 and 18. TEER values in Ohms were blank subtracted, multiplied by the culture surface area, and then divided by 1000 to convert to kOhms. Data shown are the mean of two donors from two independent experiments (Healthy 02AB066901 and 0000333288; COPD 02AB066702 and 0000370751). UT, untreated. NT, non-targeting. NLR, NLRP1 KO. CARD, CARD8 KO. DKO, NLRP1 and CARD8 KO.

5.5 NLRP1 and CARD8 protein levels are reduced following ALI culture

To investigate NLRP1 and CARD8 levels after differentiation, KO cells were seeded onto Transwells and differentiated at the ALI for 21 days. Cells were then lysed, and western blots were performed using pooled donors. As shown above, KO of NLRP1 was achieved in submerged basal cells, however, KO of both NLRP1 and CARD8 were observed in ALI-differentiated cells (**Figure 5.7**).

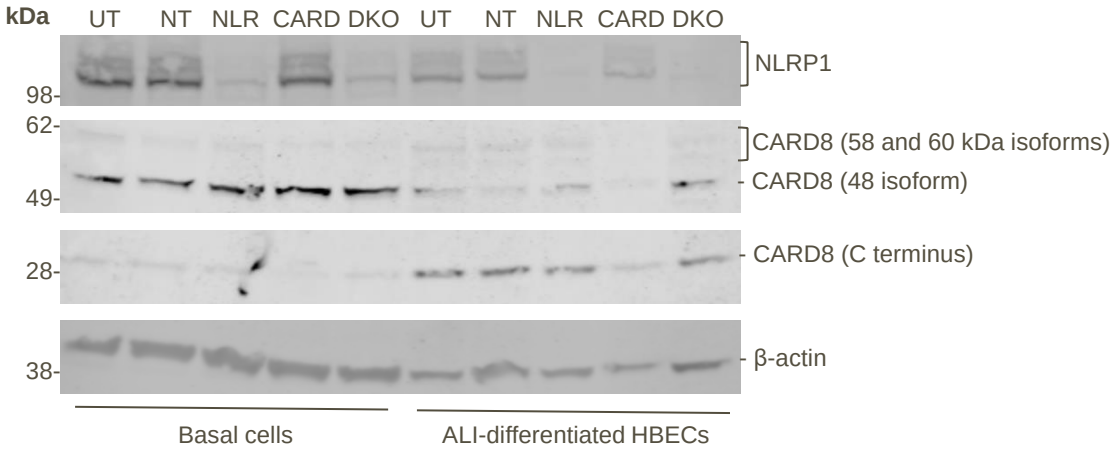

Figure 5.7. NLRP1 and CARD8 protein levels are reduced following ALI culture of KO cells.

Basal cells from healthy donors were transfected with pooled NLRP1 or pooled CARD8 crRNA (50 μM final concentration) and cultured for seven days until confluency and then lysed. Alternatively, KO HBECs were cultured at the ALI for 21 days then lysed. Proteins were separated by SDS gel electrophoresis, followed by transfer to a PVDF membrane. Levels of NLRP1 (~150 kDa), CARD8 isoforms (48, 58 and 60 kDa) and CARD8 C-terminus (~28 kDa) were detected using the relevant primary antibodies. Representative blot shown consists of lysates from three pooled donors from three independent experiments (Healthy 02AB061001, 02AB066901 and 0000333288). UT, untreated. NT, non-targeting. NLR, NLRP1 KO. CARD, CARD8 KO. DKO, NLRP1 and CARD8 KO.

5.6 KO of NLRP1 may reduce the progenitor cell pool

To investigate the cell subtype composition of NLRP1 KO HBECs, cells differentiated at the ALI were stained for flow cytometry analysis. CD49f and CD271 positivity were used to discriminate between basal and differentiated cells (Rock et al., 2009). Of these differentiated cells, CD66 and CD133 were then used to identify progenitor, goblet, and ciliated cells (GlaxoSmithKline, unpublished data). On day 35 post-ALI initiation, there were no differences in HBEC populations in the one healthy donor analysed (**Figure 5.8**).

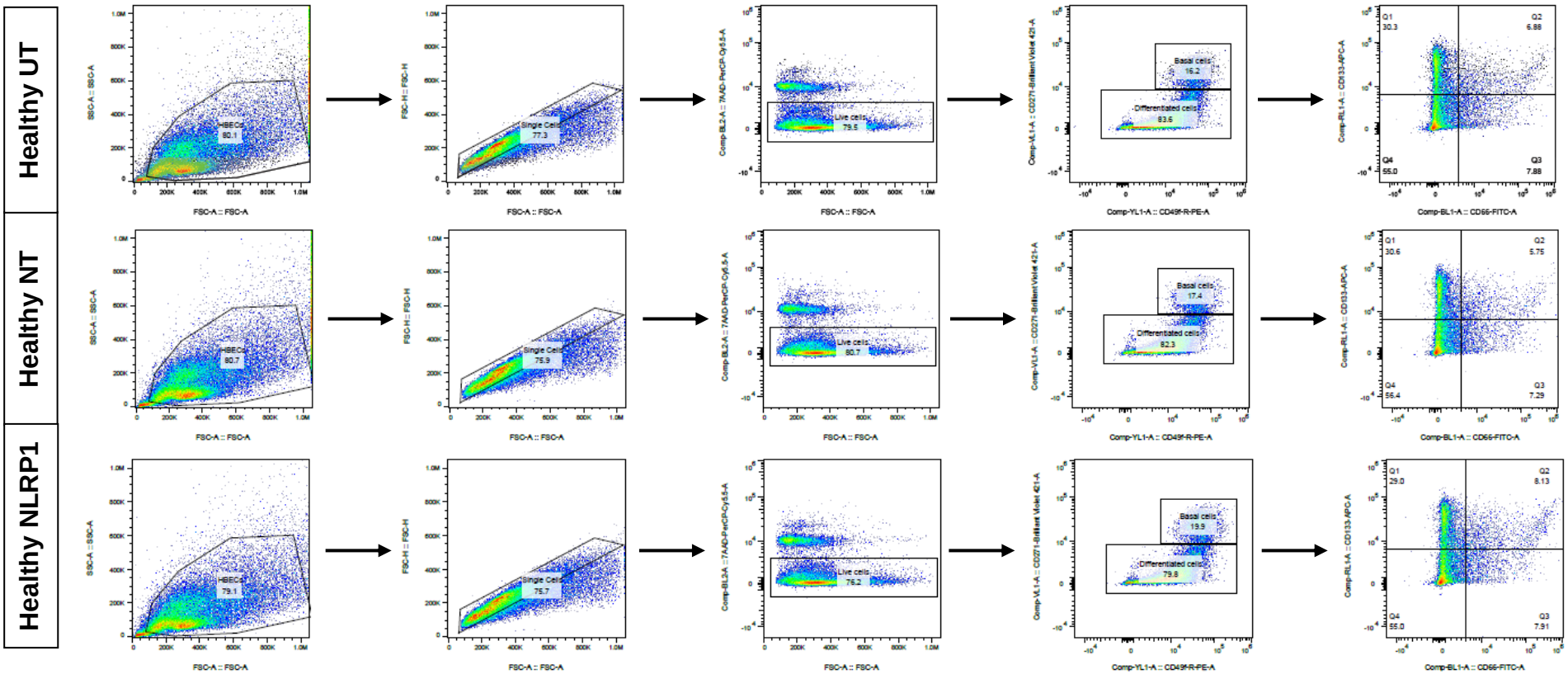
Healthy UT
Healthy NT
Healthy NLRP1
HBEC's
80.1
Single Cells
77.3
Live cells
79.5
Basal cells
16.2
Differentiated cells
83.6
Q1
30.3
Q2
6.88
Q4
55.0
Q3
7.88
HBEC's
80.7
Single Cells
75.9
Live cells
80.7
Basal cells
17.4
Differentiated cells
82.3
Q1
30.6
Q2
5.75
Q4
56.4
Q3
7.29
HBEC's
79.1
Single Cells
75.7
Live cells
76.2
Basal cells
19.9
Differentiated cells
79.8
Q1
29.0
Q2
8.13
Q4
55.0
Q3
7.91

Figure 5.8. HBEC cell populations were unaltered following NLRP1 KO at later timepoints.

Following the initiation of ALI, culture media was replenished every other day for 35 days. To determine the presence of basal cells ($CD49f^+$ $CD271^+$), progenitor cells ($CD66a/c/e^+$ $CD133^+$), goblet cells ($CD66a/c/e^+$ $CD133^-$) and ciliated cells ($CD66a/c/e^-$ $CD133^+$), dissociated cells were stained with anti-CD49f, anti-CD271, anti-CD66a/c/e and anti-CD133 for flow-cytometric analysis. Live, single cells were gated based on FSC, SSC and 7AAD-negativity. FACS plots are shown from one donor from one experiment (Healthy 0000333288). UT, untreated. NT, non-targeting. NLRP1, NLRP1 KO.

Since previous observations revealed the greatest decline in basal cell percentages and the greatest increase in goblet cell percentages at day 21, it is plausible that most HBECs may have already committed to cell fate decisions by day 35 (Gras et al., 2017). Consequently, HBECs from three healthy and three COPD patients were analysed at this timepoint. On day 21 post-ALI initiation, progenitor cell populations ($CD66^{+}$ $CD133^{+}$) were slightly reduced while double-negative cells ($CD66^{-}$ $CD133^{-}$) were slightly enhanced following NLRP1 KO, particularly in the COPD group (**Figure 5.9**).

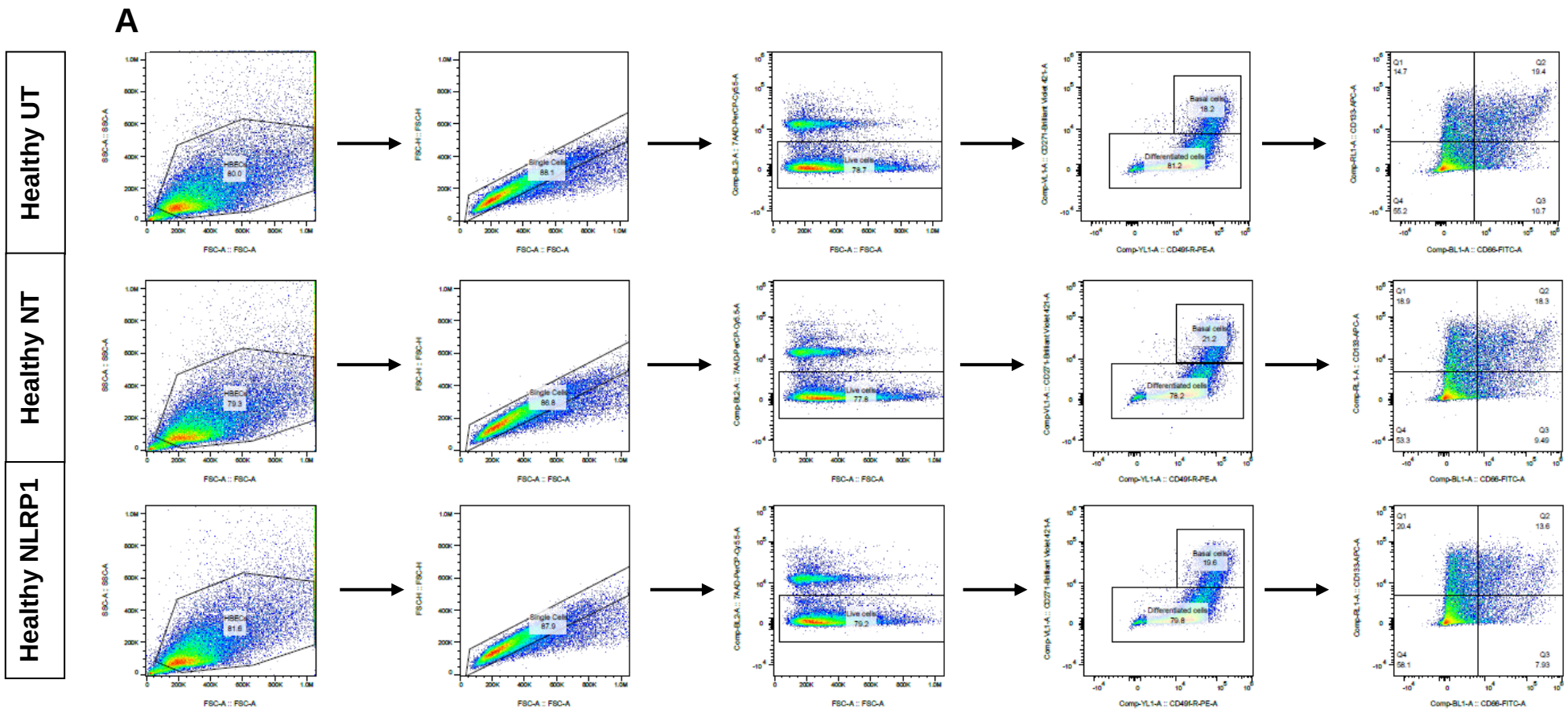
A
Healthy UT
Healthy NT
Healthy NLRP1
HBEC
80.0
Single Cells
88.1
Live cells
78.7
Basal cells
18.2
Differentiated cells
81.2
Q1
14.7
Q2
19.4
Q4
55.2
Q3
10.7
HBEC
79.3
Single Cells
86.8
Live cells
77.8
Basal cells
21.2
Differentiated cells
78.2
Q1
18.9
Q2
18.3
Q4
53.3
Q3
9.49
HBEC
81.6
Single Cells
87.9
Live cells
79.2
Basal cells
19.6
Differentiated cells
79.8
Q1
20.4
Q2
13.6
Q4
58.1
Q3
7.93
FSC-A :: FSC-A
FSC-H :: FSC-H
Comp-YL1-A :: CD49f-R-PE-A
Comp-BL1-A :: CD66-FITC-A

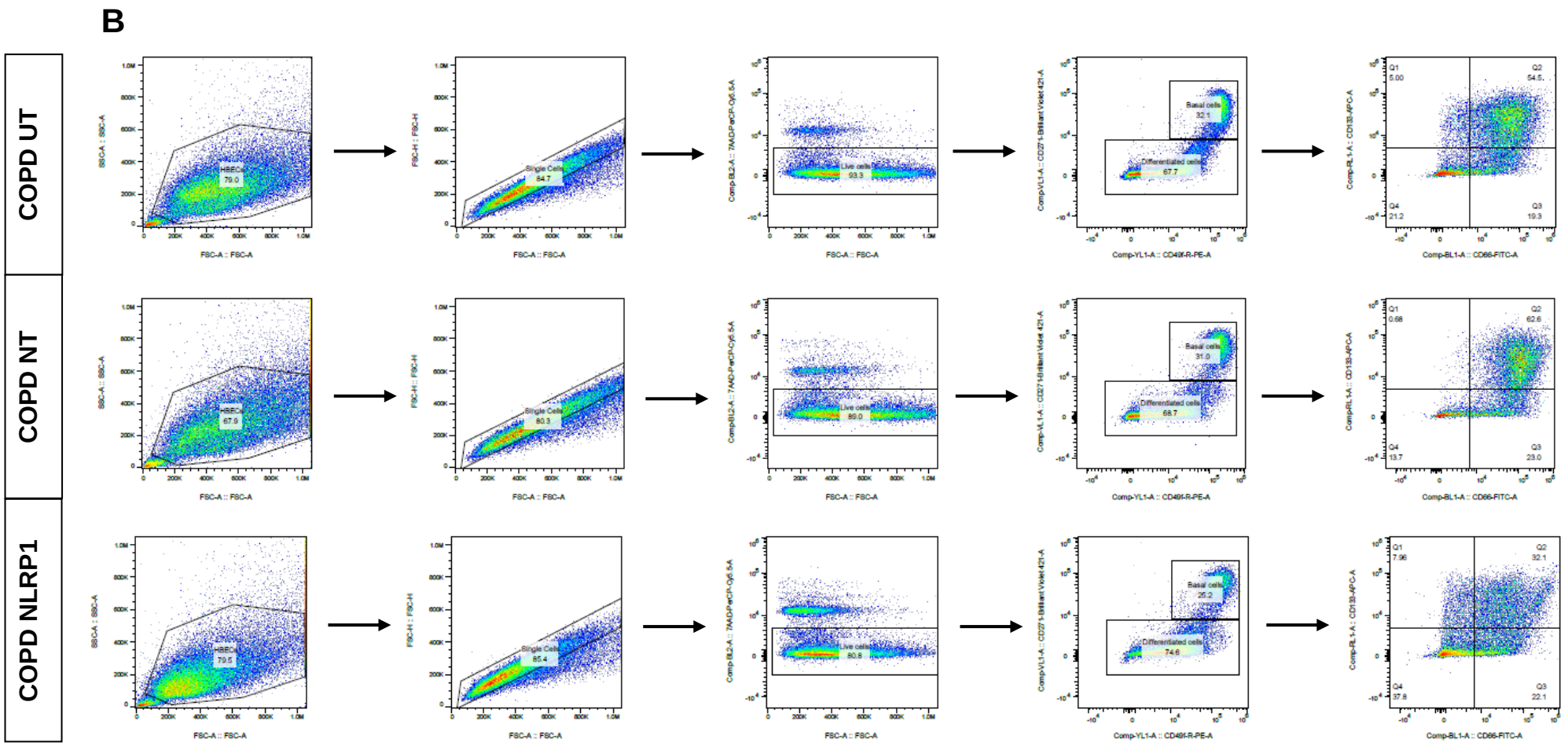
B
COPD UT
COPD NT
COPD NLRP1
FSC-A :: FSC-A
FSC-H :: FSC-H
Comp-BL2-A :: 7AAD-PerCP-Cy5.5A
Comp-VL1-A :: CD271-Brilliant Violet 421-A
Comp-YL1-A :: CD49f-R-PE-A
Comp-RL1-A :: CD133-APC-A
Comp-BL1-A :: CD66-FITC-A
HSEC
79.0
Single Cells
84.7
Live cells
93.3
Basal cells
32.1
Differentiated cells
67.7
Q1
5.00
Q2
54.5
Q4
21.2
Q3
19.3
HSEC
67.9
Single Cells
80.3
Live cells
89.0
Basal cells
31.0
Differentiated cells
68.7
Q1
0.68
Q2
62.6
Q4
13.7
Q3
23.0
HSEC
79.5
Single Cells
85.4
Live cells
80.8
Basal cells
25.2
Differentiated cells
74.6
Q1
7.96
Q2
32.1
Q4
37.8
Q3
22.1

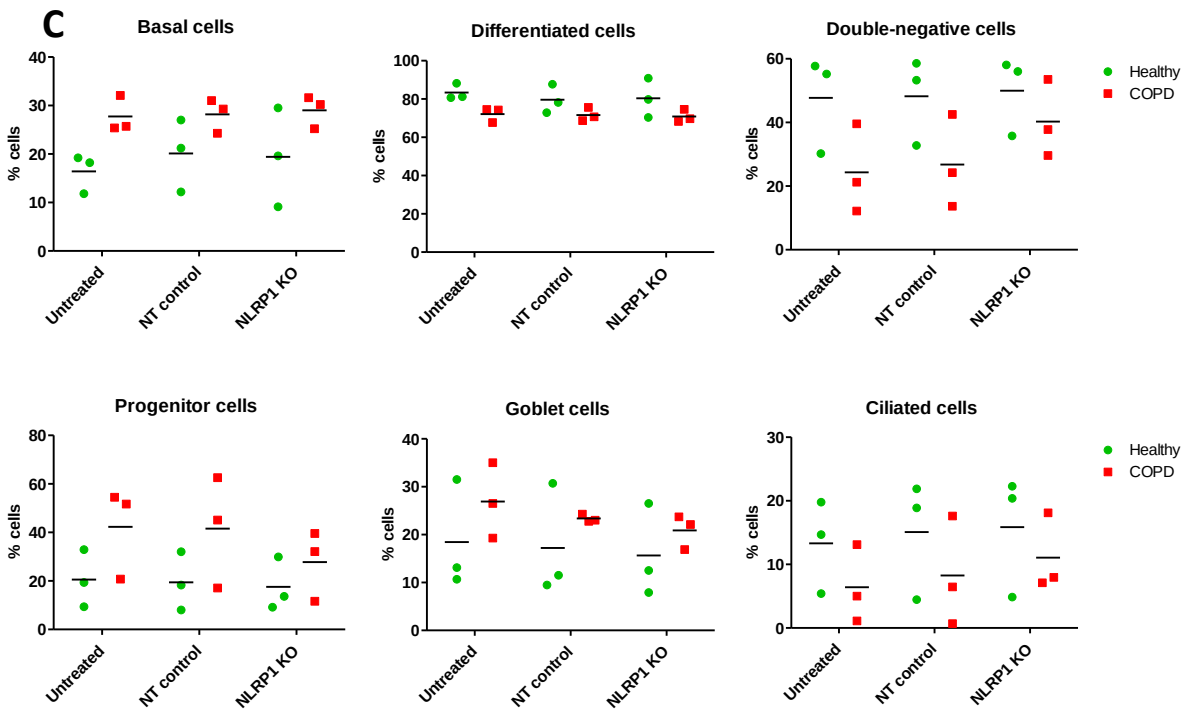

Figure 5.9. KO of NLRP1 induces a modest reduction of progenitor cells and a modest enhancement of double-negative cells.

Following the initiation of ALI, culture media was replenished every other day for 21 days. To determine the presence of basal cells ($CD49f^+$ $CD271^+$), progenitor cells ($CD66a/c/e^+$ $CD133^+$), goblet cells ($CD66a/c/e^+$ $CD133^-$) and ciliated cells ($CD66a/c/e^-$ $CD133^+$), dissociated cells were stained with anti-CD49f, anti-CD271, anti-CD66a/c/e and anti-CD133 for flow-cytometric analysis. Live, single cells were gated based on FSC, SSC and 7AAD-negativity. Representative FACS plots are shown from (**A**) one healthy donor (Healthy 02AB061001) and (**B**) one COPD donor (COPD AB006302). (**C**) Percentage cell data were plotted. Data shown are three individual donors with the mean from three independent experiments (Healthy 02AB061001, 02AB066901 and 0000333288; COPD AB006302, 02AB066702 and 0000370751). UT, untreated. NT, non-targeting. NLRP1, NLRP1 KO.

To confirm this inference using published cell markers, KRT4 and KRT13 were utilised as markers for progenitor and basal cells, respectively (Plasschaert et al., 2018; Ruiz García et al., 2019). Initially, cell lysates were pooled and then protein levels were analysed by western blot. In healthy and COPD donor cells, KRT4 expression was reduced, however, KRT13 remained stable across all conditions (**Figure 5.10**).

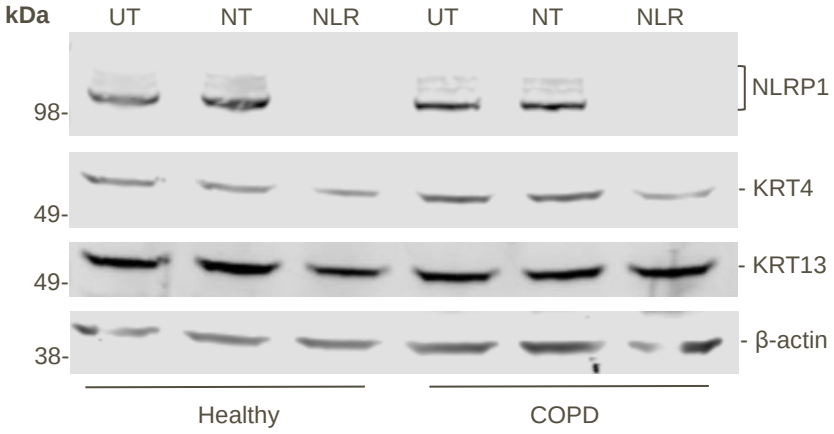

Figure 5.10. Deletion of NLRP1 reduces KRT4 but not KRT13 expression.

Basal cells from healthy and COPD donors were transfected with pooled NLRP1 crRNA (50 μM final concentration) and cultured for seven days until confluency. KO HBECs were then cultured at the ALI for 21 days. Cells were lysed in RIPA lysis buffer, proteins separated by SDS gel electrophoresis, followed by transfer to a PVDF membrane. Levels of NLRP1 (~150 kDa), KRT4 (56 kDa) and KRT13 (50 kDa) were detected using the relevant primary antibodies. Representative blot shown consists of lysates from three pooled donors from three independent experiments (Healthy 02AB061001, 02AB066901 and 0000333288; COPD AB006302, 02AB066702 and 0000370751). UT, untreated. NT, non-targeting. NLR, NLRP1 KO.

To validate these observations and to confirm the cellular localisation, FFPE cells were subjected to IF staining. In line with the western blot data, decreased KRT4 staining was observed in NLRP1 KO cells (**Figure 5.11**).

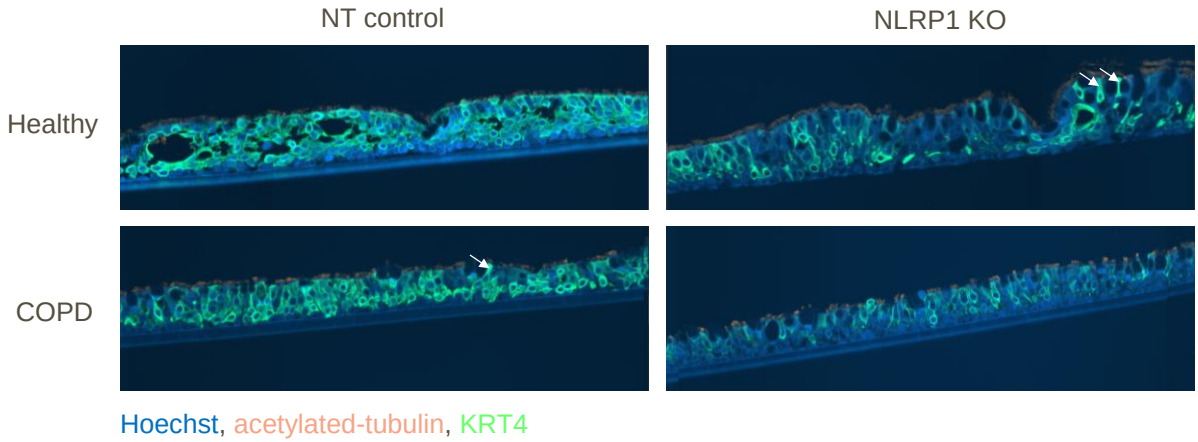

Figure 5.11. Deletion of NLRP1 reduces KRT4 expression in the pseudostratified columnar cell layer.

KO HBECs from healthy and COPD donors were cultured at the ALI for 21 days. Cells were then fixed before embedding in paraffin. Sections of 4 µm were prepared using a microtome and then stained with anti-acetylated tubulin (ciliated cells) and anti-KRT4 (progenitor cells). Nuclei were counterstained with Hoechst. Representative images are shown from two donors from three independent experiments (Healthy 02AB061001; COPD AB006302). Arrows indicate cells with the characteristic club cell morphology and an enlarged luminal surface. NT, non-targeting.

5.7 Discussion

The advent of scRNA-seq approaches has challenged the classical model of airway epithelial differentiation, and novel cell subtypes (such as ionocytes) and transitional states (such as mucous ciliated cells) have now been identified (Plasschaert et al., 2018; Vieira Braga et al., 2019). Recent evidence also suggests that Notch activity alone is not responsible for the comprehensive differentiated cell repertoire and that other molecular players may be involved, such as Hedgehog and SRY-related HMG-box proteins (Belgacemi et al., 2020; Eenjes et al., 2021). Since **Chapter 3** and **Chapter 4** demonstrated NLRP1 expression and functionality in primary HBECs, in this chapter the roles of NLRP1 in epithelial differentiation were examined.

Initially, the effects of chronic NLRP1 inflammasome activation were determined by dosing differentiating HBECs with VBP (**Figure 5.1**). These preliminary data indicated that sustained inflammasome activation inhibited epithelial differentiation

at the progenitor and goblet cell stages. An overall reduction in ciliated cells was also observed, potentially due to blockade of progenitor/club cell differentiation or goblet cell transdifferentiation (Ruiz García et al., 2019; Vieira Braga et al., 2019). In line with the results from **Chapter 4**, VBP induced greater IL-1β secretion from the cells from the COPD patient compared with those derived from the healthy control (**Figure 5.2**). IL-1β levels continued to increase throughout the culture period which may suggest a self-perpetuating mechanism via autocrine or paracrine induction of IL-1R1. Indeed, primary HBECs express IL-1R1, but not the decoy receptor IL-1R2, which may enhance signalling (Coulter et al., 1999). In disconnect with the observations from **Chapter 4**, IL-18 release from cells derived from the COPD patient was also elevated in this assay. This may have been due to the longer treatment duration or due to inter-donor variability. Induced persistent NLRP1 activation may model recurrent exacerbations in COPD patients, in response to NLRP1-activating stimuli such as HRV16 (Robinson et al., 2020). Indeed, frequent exacerbators have elevated sputum IL-1β levels compared with infrequent exacerbators (Fu et al., 2015). One may therefore speculate that recurrent viral infection drives pathological airway remodelling to a progenitor and goblet cell phenotype, which may contribute to inflammation and mucus hypersecretion in COPD (Crystal, 2014).

To determine the consequences of NLRP1 deletion on epithelial differentiation, KO cells were generated using a previously established protocol (Rapiteanu et al., 2020). Successful KO of NLRP1 was achieved in submerged basal cells while KO of both NLRP1 and CARD8 were observed in basal and ALI-differentiated cells (**Figures 5.3** and **5.7**). This may indicate greater CARD8 protein stability despite the lower baseline levels of expression (**Figures 3.1** and **3.2**), and this has been observed at least in terms of binding with DPP9 (Taabazuing et al., 2020). In line with previous observations, deletion of NLRP1 protects HBECs from the activities of VBP (**Figure 5.4**) (Robinson et al., 2020). Further demonstrated here is that IL-1β release was curtailed in NLRP1 KO cells and, in comparison with **Chapter 4**, ASC speck formation plus IL-1β levels were enhanced in cells from COPD donors. LDH data would be required to determine the involvement of impaired cell death, however, there was some evidence that NLRP1 KO HBECs from COPD patients were hyper-responsive to TLR3-activating stimuli (**Figure 5.5**).

Following air-lifting, NLRP1 KO cells were not impaired in their ability to form AJCs (**Figure 5.6**). Compared with control cells, those from COPD donors returned lower TEER measurements, in-line with observations that barrier function may be compromised in the disease (Aghapour et al., 2018). Subsequent immunostaining revealed that cell layers from healthy donors had an increased thickness when compared to those from COPD patients (**Figure 5.11**). Consequently, this may also have contributed to the lower TEER values in disease. At day 21 post-ALI initiation, progenitor cell populations ($CD66^+$ $CD133^+$) were slightly reduced following NLRP1 KO, particularly in the COPD group (**Figure 5.9**). This correlated with decreased KRT4 expression which is copious in suprabasal cell progenitors and club cells (**Figure 5.11**) (Plasschaert et al., 2018; Ruiz García et al., 2019). A similar reduction could not be observed with KRT13, which is expressed at earlier pseudotimes and is predominantly localised to basal cells (**Figure 5.10**). Concomitant with the decreased progenitor cell pool, an increase in $CD66^-$ $CD133^-$ airways cells and a potential slight increase in $CD66^-$ $CD133^+$ ciliated cells were observed (**Figure 5.9**). Due to inter-donor variability, KO of NLRP1 in cells from additional patients may be required to achieve statistical significance. The $CD66^-$ $CD133^-$ population is currently undefined but likely consists of tuft cells, ionocytes and pulmonary neuroendocrine cells (Montoro et al., 2018).

In summary, this chapter illustrates the novel role of NLRP1 in epithelial differentiation. Upon NLRP1 inflammasome activation, progenitor and goblet cells are increased while ciliated cells are reduced. Conversely, following the genetic deletion of NLRP1, progenitor cells are modestly decreased while a slight increase of ciliated cells is observed. This progenitor population consists of suprabasal cell progenitors and club cells which are characterised by KRT4 expression. Selective modulation of NLRP1 in disorders characterised by differentiation defects, such as COPD or asthma, may present a novel therapeutic target.

Chapter 6. General discussion and future perspectives

6.1 NLRP1 in airway defence

The airway epithelium fulfils an integral role in host defence against pathogens. It limits infection through the mucus-lined epithelial barrier, via the mucociliary 'escalator', and by facilitating the coughing reflex. Antimicrobial peptides and reactive oxygen/nitrogen intermediates produced by the epithelium also create an unconducive milieu for pathogen survival. If these initial defences are inefficient, AECs may also secrete cytokines and chemokines to attract inflammatory cells and modify their activity, plus growth factors to repair the damaged epithelium.

NLRP1 represents an additional tool in the AEC toolkit and may be particularly important in driving antiviral immunity, in the absence of other functional inflammasomes. In addition to cleaving the viral polyprotein during replication, HRV-3Cpro also cleaves human NLRP1 leading to inflammasome assembly (Robinson et al., 2020). Consequently, primary HBECs infected with HRV16 form ASC oligomers and secrete IL-1β and lL-18. In **Chapter 4**, it was observed that HRV-induced cell death was limited when compared with chemically induced NLRP1 activation with VBP, which likely represent a more potent stimulus. HRV has been shown to induce limited cytotoxicity when compared with other respiratory viruses such as influenza or RSV (Jacobs et al., 2013). This may suggest that physiological NLRP1 activation in HBECs is associated with minimal cell death and/or may occur in a subset of epithelial cells. Indeed, in **Chapter 3** it was demonstrated that ASC expression is restricted to basal cells under resting conditions. This may be particularly important in the airways where regeneration of the respiratory epithelium typically necessitates several weeks and could leave the underlying tissues vulnerable to airborne pathogens or particulate matter. Indeed, HBECs cultured on denuded rodent tracheas reconstitute a fully differentiated pseudostratified columnar epithelium after ~28 days (Castillon et al., 2002; Escotte et al., 2004). dsRNA, which may exist in the cytoplasm due to the genomic RNA of dsRNA viruses or the dsRNA intermediates of ssRNA viruses, has also been shown to be detected by NLRP1 in the HBEC3-KT cell line (Bauernfried et al., 2021). In parallel with this, delivery of dsRNA into primary basal cells results in inflammasome activation, although this was again modest when compared with VBP. Nevertheless, it is plausible to suggest that HBEC NLRP1 evolved as a broad-

spectrum sensor of viral replication, incorporating different mechanisms of activation to safeguard epithelial responsiveness.

Subsequent steps would be required to investigate the potential synchronous activation of NLRP1 with the RIG-I inflammasome. RIG-I has previously been identified as a sensor of dsRNA and HRV, resulting in caspase-activating platform assembly via ASC engagement (Poeck et al., 2010; Slater et al., 2010). As a result, it may be prudent to generate NLRP1/RIG-I DKO cells using CRISPR-Cas9, to investigate their interactions in HBECs. It may also be advisable to confirm that the findings in primary HBECs are due to 3Cpro alone, perhaps through the generation and transfection of recombinant HRV-3Cpro or the use of the 3Cpro inhibitor rupintrivir (Binford et al., 2007). Lipofectamine delivery into human tracheal epithelial cells has previously resulted in low transfection efficiencies of < 25 % (Maurisse et al., 2010). Instead, optimal transfection of primary HBECs with 3Cpro may be achieved by utilising Amaxa electroporation, which showed promise with RNP delivery as described above. The novel, severe acute respiratory syndrome coronavirus 2 (SARS-CoV-2) also expresses a 3C-like protease (M^{pro}) (Jin et al., 2020). As a result, an ongoing collaboration with the University of Cambridge is investigating this virus in the context of NLRP1 inflammasome activation. Data is preliminary but suggested that SARS-CoV-2 infection failed to induce significant ASC speck formation in basal cells due to the absence of angiotensin-converting enzyme 2 (ACE2) (**Figure 6.1**).

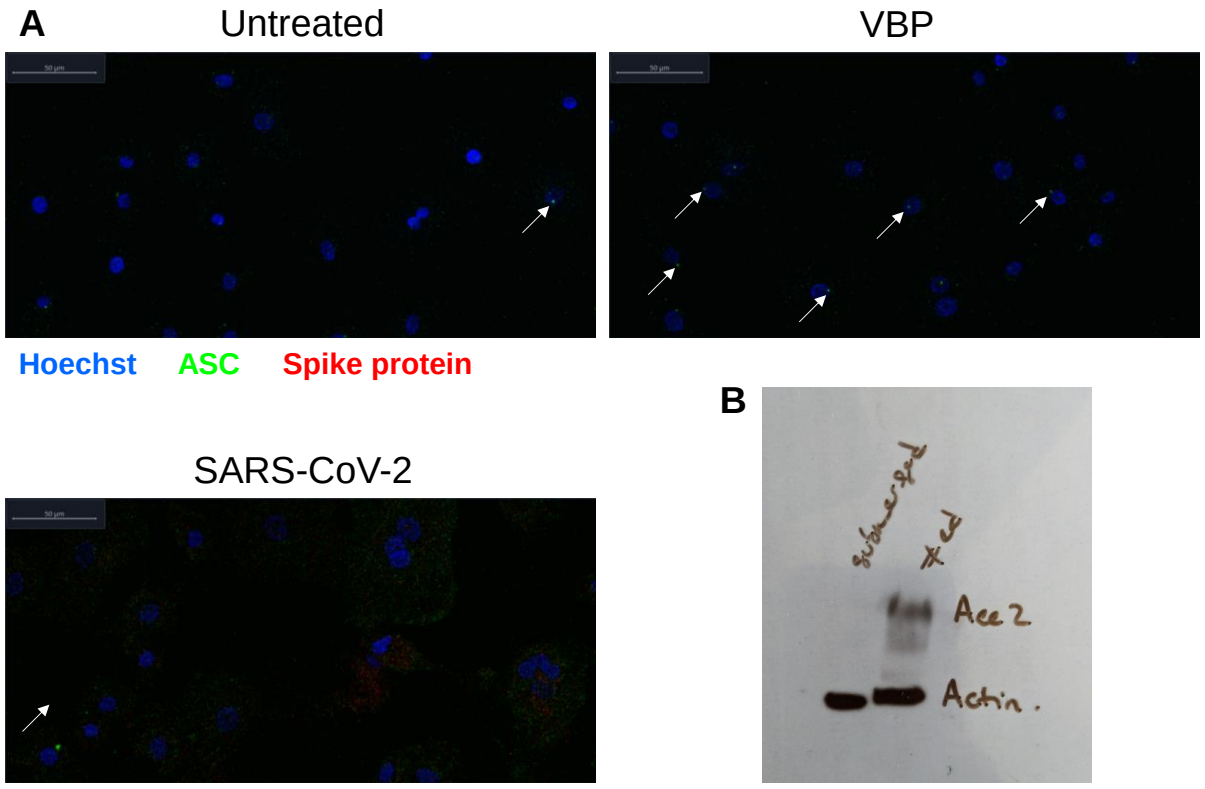

Figure 6.1. SARS-CoV-2 variant B.1.1.7 is unable to induce ASC speck formation in basal cells due to the absence of ACE2.

(**A**) HBECs were seeded and cultured overnight. Cells were incubated with 2 μM VBP or SARS-CoV-2 (MOI 1) for 24 hours. Cells were co-stained for ASC (green), spike protein (red) and Hoechst (blue), then imaged by IF microscopy. Representative images from one donor are shown (COPD AB006302). Images were acquired using a Zeiss LSM 710 confocal microscope. Arrows indicate ASC specks. Scale bar: 50 μm. (**B**) Basal cells were cultured for seven days until confluency or cultured at the ALI for 21 days and then lysed. Proteins were separated by SDS gel electrophoresis, followed by transfer to a PVDF membrane. Levels of ACE2 (~120 kDa) were detected using the relevant primary antibody. Blot shown consists of lysates from one experiment.

Like SARS-CoV, ACE2 is the crucial entry receptor for SARS-CoV-2 following spike protein priming by transmembrane serine protease 2 (TMPRSS2) (Hoffmann et al., 2020). In line with the literature, ACE2 expression was enhanced in ALI-differentiated HBECs, most likely corresponding with the emergence of ciliated cells (Lee et al., 2020). Infection of fully differentiated HBECs with the B.1.1.7 (Alpha), B.1.351 (Beta) and B.1.617.2 (Delta) variants is ongoing.

6.2 NLRP1 in airway disease

Long-acting β2-adrenoceptor agonists (LABAs) are considered the mainstay of COPD treatment, while asthmatic patients typically undergo inhaled corticosteroid with LABA therapy (Gross and Barnes, 2017). Although these medicines may control symptoms, they fail to modify the underlying disease processes, leading to subsequent exacerbations. Severe COPD and asthma which are refractory to standard therapies are also areas of high unmet need.

One potential solution is to ameliorate the inflammatory pathways in chronic respiratory disorders using anti-cytokine therapies. Despite positive safety data, many of these require further investigation and/or have achieved inconclusive results in the clinic. For example, anti-IL-1β blockade with canakinumab reduced circulating cytokine levels and induced delayed asthmatic responses, however, this study was limited to a small sample size of 16 patients with mild disease (Pascoe S., 2006). In trials with COPD patients, statistical power was not demonstrated for the lung function endpoints examined following canakinumab treatment (NCT00581945), and anti-IL-1R1 therapy using MEDI8968 failed to reduce acute exacerbations (Calverley et al., 2017). The anti-IL-18R, MEDI2338, has also shown to be well tolerated in COPD sufferers (NCT01322594), but efficacy studies are absent. Clinical trials of anti-IL-33 biologics are underway for asthma (NCT04570657) and COPD (NCT04701983); however, initial data suggests that these may be less effective than dual cytokine blockade (NCT03387852).

The previously observed lack of clinical efficacy may have been due to complex and compensatory cytokine networks. It may be more advantageous, therefore, to target upstream inflammasome sensors, which may also facilitate the targeting of specific cell types. Although in their infancy compared with NLRP3 inhibitors, due to a dearth of tool compounds, the development of NLRP1-modulating therapies may present opportunities for the treatment of diseases involving the epithelium or keratinocytes (Schwaid and Spencer, 2021). In the context of COPD, where NLRP1 expression is enhanced in HBECs (see **Chapter 4**) and protein SNPs may impact salient functions, it may be astute to inhibit inflammasome activation (Ozretić et al., 2019). There have been some advances in this area with the identification of Orf63 from Kaposi's sarcoma–associated herpesvirus as a dual NLRP1 and NLRP3 inflammasome inhibitor (Gregory et al., 2011). Conversely, it may be preferred to

enhance NLRP1 activity in some malignancies. VBP, which inhibits DPP8/9 and activates the NLRP1 inflammasome, has shown some efficacy in non-small cell lung cancer patients due to enhancing host immunity coupled with fibroblast activation protein blockade (Eager et al., 2009). Phase III trials were terminated, however, due to reduced survival in the treatment group (NCT00290017), potentially due to the broad spectrum of inhibition. As a result, there is a current need for NLRP1-selective molecules. One approach to drug discovery may be the utilisation of Scintillation Proximity Assays (SPAs), where ligands were previously screened for their ability to displace a radiolabelled ATP analogue from NLRP1 (Harris et al., 2015).

Subsequent experiments could be performed to determine if, in addition to NLRP1 overexpression in HBECs, other mechanisms are responsible for the exaggerated phenotype in COPD. Recent data has indicated that thioredoxin-1 negatively regulates the NLRP1 inflammasome and that levels may be reduced in respiratory diseases (Barnes, 2020; Zhou et al., 2020; Ball et al., 2021). It may be prudent, therefore, to pre-treat HBECs derived from COPD donors with recombinant thioredoxin-1 before NLRP1 activation, to determine if inflammasome responses can be rescued to control levels. In addition, contemporary evidence has confirmed that although NLRP1 repression is mediated by DPP8/9 binding, DPP9 catalytic activity is required to fully restrain inflammasome activation (Hollingsworth et al., 2021; Huang et al., 2021). *In silico* support has revealed targets of DPP8/9, several of which are found in epithelial cells, such as cathepsin Z, and would warrant further investigation as intermediate regulators of the NLRP1 inflammasome pathway (**Figure 6.2; Table 6.1**):

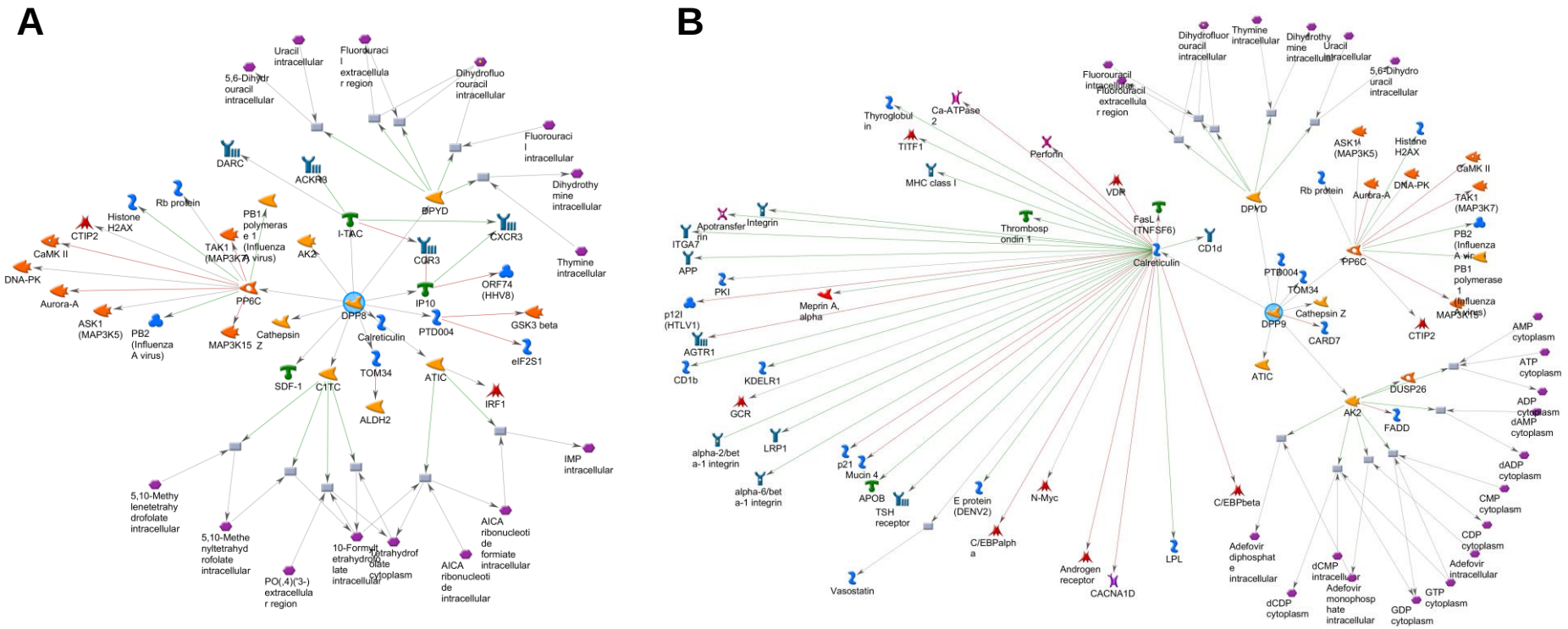

Figure 6.2. Interactome of proteins downstream of DPP8 and DPP9.

GeneGo MetaCore from Clarivate Analytics was used to analyse the downstream targets of (**A**) DPP8 and (**B**) DPP9. Arrows indicate activatory (green), inhibitory (red) or unspecified (grey) interactions.

Table 6.1. Summary of published DPP8/9 substrates.

Where known, the effect of protease cleavage, the substrate localisation and substrate function are indicated. Adapted from multiple sources (Ajami et al., 2008; Wilson et al., 2013; Zhang et al., 2015).

Protease	Target	Aliases	Effect	Epithelial	Myeloid	Cytoplasmic	Function
DPP8/9	IP10	CXCL10	Inactivation	Yes	Yes	Yes	Chemotactic
DPP8	SDF-1	CXCL12	Inactivation	No	No	Yes	Chemotactic
DPP8	ITAC	CXCL11	Inactivation	Yes	Yes	Yes	Chemotactic
DPP8	C1TC	MTHFD1	?	Yes	Yes	Yes	Glyoxylate and dicarboxylate metabolism
DPP8/9	ATIC	PurH	?	Yes	Yes	Yes	Purine metabolism
DPP8/9	Cathepsin Z	Cathepsin X/P	?	Yes	Yes	Lysosomes	Proteolysis
DPP8/9	PP6C	PPP6C	?	Yes	Yes	Yes	Protein dephosphorylation
DPP8/9	AK2		PTM	Yes	Yes	No	Purine metabolism
DPP8/9	TOM34	TOMM34	?	Yes	Yes	Yes	Protein targeting and mitochondrial import
DPP8/9	DPYD	DPD	?	Yes	Yes	Yes	Pyrimidine metabolism
DPP8/9	PTD004	OLA1	?	Yes	Yes	Yes	ATP catabolism
DPP8/9	Calreticulin	Calregulin	Translocation?	Yes	Yes	Yes	Antigen processing and presentation

6.3 NLRP1 in airway differentiation

It is now postulated that chronic respiratory disorders arise and are maintained due to the dysregulated differentiation of airway basal cells. Chronic insult with cigarette smoke in COPD or allergens in asthma may result in derangement of the respiratory architecture due to basal cell hyperplasia, squamous metaplasia, goblet cell hyperplasia, ciliopathies, and the loss of functional AJCs (Crystal, 2014; Heijink et al., 2020). Restoration of appropriate differentiation pathways may therefore represent an attractive target as a “disease-modifying” therapy for these conditions.

Chapter 5 provides the first evidence that NLRP1 is involved in the differentiation of the pseudostratified columnar respiratory epithelium. While chronic NLRP1 activation with VBP enhances progenitor and goblet cell differentiation, genetic deletion of NLRP1 appears to reduce the progenitor cell pool and increase the double-negative cell pool (and potentially also ciliated cell numbers). Recurrent infections with biological activators of NLRP1, such as HRV16, may drive basal cell hyperplasia and squamous metaplasia in COPD and contribute to the high cytokine

burden in the disease (Araya et al., 2007). This mechanism may be self-perpetuating since regions of epithelial derangement express high levels of IL-1β which has been demonstrated to further induce basal cell hyperplasia via NF-κB (Herfs et al., 2012). Together this suggests that NLRP1 activation upon HRV infection may be an inciting incident in the development of pathological airway remodelling.

Subsequent experiments could confirm the physiological relevance of chronic NLRP1 activation by employing recurrent HRV16 infection as opposed to VBP. VBP is a potent inhibitor of DPP4 (IC_{50} = < 4 nM), as well as DPP8 (IC_{50} = 4 nM) and DPP9 (IC_{50} = 11 nM), therefore effects disconnected from NLRP1 cannot be discounted in these assays (Lankas et al., 2005). Instead, a more specific approach could be the utilisation of CRISPR-Ca9 to generate NLRP1-activating mutations by gene KI. Several of these mutations have been described in patients and typically lead to inflammatory phenotypes such as familial keratosis lichenoides chronica (FKLC), but also aberrant cell proliferation in the case of multiple self-healing palmoplantar carcinoma (MSPC) and juvenile-onset recurrent respiratory papillomatosis (JRRP) (Zhong et al., 2016; Drutman et al., 2019).

As demonstrated above with the flow cytometry panel employed, further donors may be required to achieve statistical significance due to inter-donor variability. Additional characterisation of differentiated HBEC subtypes is also necessary, particularly in light of new transitional cell states, such as deuterosomal cells and mucous ciliated cells (Davis and Wypych, 2021). In cell sections, $KRT4^+$ cells which were morphologically akin to club cells were observed, however, confirmation would be required using specific markers such as SCGB1A1. SCGB1A1 expression is reduced in both biopsy specimens and cultured cells from COPD patients, and SCGB1A1 KO in mice leads to enhanced cigarette smoke-induced emphysema and peribronchiolar fibrosis (Gamez et al., 2015; Laucho-Contreras et al., 2015). As a result, club cells may hold promise as a cell subtype potentially under negative regulation by NLRP1 in airway diseases. The $CD66^-$ $CD133^-$ cell population, which showed the greatest enhancement following NLRP1 KO, is currently under investigation.

Overall, selective modulation of NLRP1 may present a novel therapeutic angle for the treatment of chronic respiratory conditions, which are growing in prevalence in line with Western lifestyles. COPD is the third leading cause of mortality globally, and while asthma mortality rates have waned, it remains a significant burden in terms of morbidity, particularly in the paediatric population (Serebrisky and Wiznia, 2019; World Health Organization, 2020). For these conditions, NLRP1 inhibitors may fulfil the role of "disease-modifying" agents and restore epithelial homeostasis (**Figure 6.3**).

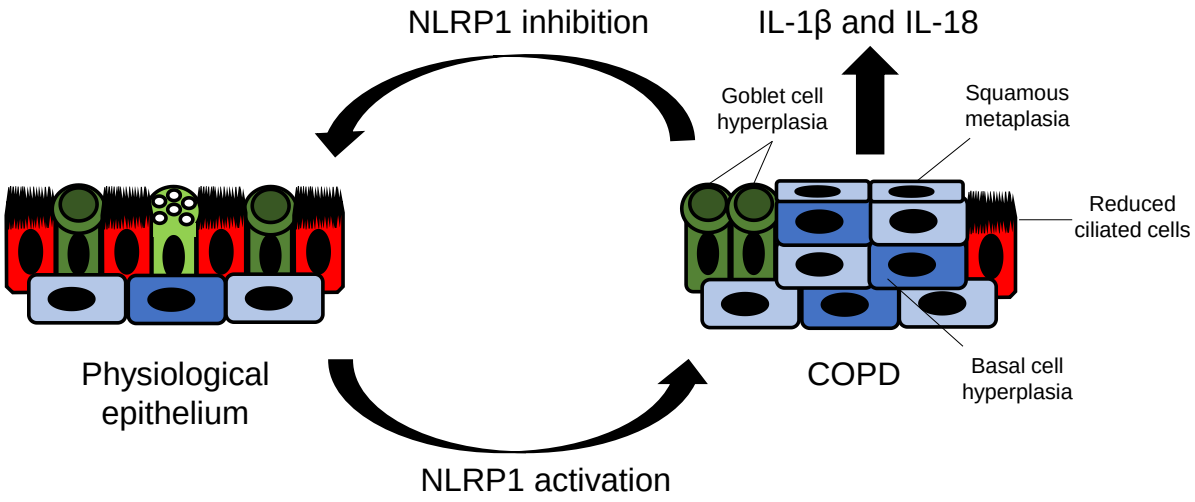

Figure 6.3. Proposed role of NLRP1 in the differentiation of HBECs.

Recurrent activation of the NLRP1 inflammasome may induce pathological remodelling of the airway epithelium in COPD. NLRP1 inhibitors may represent a novel class of "disease-modifying" agents with the potential of treating disorders involving epithelial derangement and restoring physiological function.

Chapter 7. References

Aghapour, M., Raee, P., Moghaddam, S.J., Hiemstra, P.S., and Heijink, I.H. (2018). Airway Epithelial Barrier Dysfunction in Chronic Obstructive Pulmonary Disease: Role of Cigarette Smoke Exposure. *American Journal of Respiratory Cell and Molecular Biology* 58(2), 157-169. doi: 10.1165/rcmb.2017-0200TR.

Ajami, K., Pitman, M.R., Wilson, C.H., Park, J., Menz, R.I., Starr, A.E., et al. (2008). Stromal cell-derived factors 1alpha and 1beta, inflammatory protein-10 and interferon-inducible T cell chemo-attractant are novel substrates of dipeptidyl peptidase 8. *FEBS Lett* 582(5), 819-825. doi: 10.1016/j.febslet.2008.02.005.

Akira, S., and Takeda, K. (2004). Toll-like receptor signalling. *Nature Reviews Immunology* 4(7), 499-511. doi: 10.1038/nri1391.

Ali, J., Summer, W.G., Levitzky, M.G., Summer, W., and Levitzky, M. (2010). *Pulmonary Pathophysiology.* McGraw-Hill Professional Publishing.

Allen, I.C., Scull, M.A., Moore, C.B., Holl, E.K., McElvania-TeKippe, E., Taxman, D.J., et al. (2009). The NLRP3 Inflammasome Mediates In Vivo Innate Immunity to Influenza A Virus through Recognition of Viral RNA. *Immunity* 30(4), 556-565. doi: https://doi.org/10.1016/j.immuni.2009.02.005.

Andrei, C., Margiocco, P., Poggi, A., Lotti, L.V., Torrisi, M.R., and Rubartelli, A. (2004). Phospholipases C and A2 control lysosome-mediated IL-1β secretion: Implications for inflammatory processes. *Proceedings of the National Academy of Sciences of the United States of America* 101(26), 9745-9750. doi: 10.1073/pnas.0308558101.

Anthonisen, N.R., Manfreda, J., Warren, C.P., Hershfield, E.S., Harding, G.K., and Nelson, N.A. (1987). Antibiotic therapy in exacerbations of chronic obstructive pulmonary disease. *Ann Intern Med* 106(2), 196-204. doi: 10.7326/0003-4819-106-2-196.

Araya, J., Cambier, S., Markovics, J.A., Wolters, P., Jablons, D., Hill, A., et al. (2007). Squamous metaplasia amplifies pathologic epithelial-mesenchymal interactions in COPD patients. *J Clin Invest* 117(11), 3551-3562. doi: 10.1172/jci32526.

Backman, K.S., Greenberger, P.A., and Patterson, R. (1997). Airways Obstruction in Patients With Long-term Asthma Consistent With Irreversible Asthma'. *Chest* 112(5), 1234-1240. doi: https://doi.org/10.1378/chest.112.5.1234.

Badaoui, M., Zoso, A., Idris, T., Bacchetta, M., Simonin, J., Lemeille, S., et al. (2020). Vav3 Mediates Pseudomonas aeruginosa Adhesion to the Cystic Fibrosis Airway Epithelium. *Cell Rep* 32(1), 107842. doi: 10.1016/j.celrep.2020.107842.

Bafadhel, M., McKenna, S., Terry, S., Mistry, V., Reid, C., Haldar, P., et al. (2011). Acute exacerbations of chronic obstructive pulmonary disease: identification of biologic clusters and their biomarkers. *Am J Respir Crit Care Med* 184(6), 662-671. doi: 10.1164/rccm.201104-0597OC.

Bai, B., Yang, Y., Wang, Q., Li, M., Tian, C., Liu, Y., et al. (2020). NLRP3 inflammasome in endothelial dysfunction. *Cell Death & Disease* 11(9), 776. doi: 10.1038/s41419-020-02985-x.

Ball, D.P., Taabazuing, C.Y., Griswold, A.R., Orth, E.L., Rao, S.D., Kotliar, I.B., et al. (2020). Caspase-1 interdomain linker cleavage is required for pyroptosis. *Life science alliance* 3(3), e202000664. doi: 10.26508/lsa.202000664.

Ball, D.P., Wang, A.E., Warren, C.D., Wang, Q., Griswold, A.R., Rao, S.D., et al. (2021). Oxidized thioredoxin-1 restrains the NLRP1 inflammasome. *bioRxiv*, 2021.2009.2020.461118. doi: 10.1101/2021.09.20.461118.

Bals, R., and Hiemstra, P.S. (2004). Innate immunity in the lung: how epithelial cells fight against respiratory pathogens. *Eur Respir J* 23(2), 327-333.

Bals, R., Wang, X., Zasloff, M., and Wilson, J.M. (1998). The peptide antibiotic LL-37/hCAP-18 is expressed in epithelia of the human lung where it has broad antimicrobial activity at the airway surface. *Proc Natl Acad Sci U S A* 95(16), 9541-9546.

Barnes, P.J. (2020). Oxidative stress-based therapeutics in COPD. *Redox Biology* 33, 101544. doi: https://doi.org/10.1016/j.redox.2020.101544.

Bauernfeind, F., and Hornung, V. (2013). Of inflammasomes and pathogens--sensing of microbes by the inflammasome. *EMBO molecular medicine* 5(6), 814-826. doi: 10.1002/emmm.201201771.

Bauernfried, S., Scherr, M.J., Pichlmair, A., Duderstadt, K.E., and Hornung, V. (2021). Human NLRP1 is a sensor for double-stranded RNA. 371(6528), eabd0811. doi: 10.1126/science.abd0811 %J Science.

Bautista, M.V., Chen, Y., Ivanova, V.S., Rahimi, M.K., Watson, A.M., and Rose, M.C. (2009). IL-8 regulates mucin gene expression at the posttranscriptional level in lung epithelial cells. *J Immunol* 183(3), 2159-2166. doi: 10.4049/jimmunol.0803022.

Becker, M.N., Diamond, G., Verghese, M.W., and Randell, S.H. (2000). CD14-dependent lipopolysaccharide-induced beta-defensin-2 expression in human tracheobronchial epithelium. *J Biol Chem* 275(38), 29731-29736. doi: 10.1074/jbc.M000184200.

Beilharz, M., De Nardo, D., Latz, E., and Franklin, B.S. (2016). Measuring NLR Oligomerization II: Detection of ASC Speck Formation by Confocal Microscopy and Immunofluorescence. *Methods Mol Biol* 1417, 145-158. doi: 10.1007/978-1-4939-3566-6_9.

Belgacemi, R., Luczka, E., Ancel, J., Diabasana, Z., Perotin, J.-M., Germain, A., et al. (2020). Airway epithelial cell differentiation relies on deficient Hedgehog signalling in COPD. *EBioMedicine* 51, 102572-102572. doi: 10.1016/j.ebiom.2019.11.033.

Bergsbaken, T., Fink, S.L., and Cookson, B.T. (2009). Pyroptosis: Host cell death and inflammation. *Nature Reviews Microbiology* 7(2), 99-109. doi: 10.1038/nrmicro2070.

Bianco, F., Pravettoni, E., Colombo, A., Schenk, U., Möller, T., Matteoli, M., et al. (2005). Astrocyte-derived ATP induces vesicle shedding and IL-1β release from microglia. *Journal of Immunology* 174(11), 7268-7277.

Binford, S.L., Weady, P.T., Maldonado, F., Brothers, M.A., Matthews, D.A., and Patick, A.K. (2007). In vitro resistance study of rupintrivir, a novel inhibitor of human rhinovirus 3C protease. *Antimicrobial agents and chemotherapy* 51(12), 4366-4373. doi: 10.1128/AAC.00905-07.

Birchenough, G.M.H., Nyström, E.E.L., Johansson, M.E.V., and Hansson, G.C. (2016). A sentinel goblet cell guards the colonic crypt by triggering Nlrp6-dependent Muc2 secretion. *Science* 352(6293), 1535-1542. doi: 10.1126/science.aaf7419.

Blenkinsopp, W.K. (1967). Proliferation of respiratory tract epithelium in the rat. *Exp Cell Res* 46(1), 144-154. doi: 10.1016/0014-4827(67)90416-8.

Bochkov, Y.A., Watters, K., Ashraf, S., Griggs, T.F., Devries, M.K., Jackson, D.J., et al. (2015). Cadherin-related family member 3, a childhood asthma susceptibility gene product, mediates rhinovirus C binding and replication. *Proc Natl Acad Sci U S A* 112(17)**,** 5485-5490. doi: 10.1073/pnas.1421178112.

Boers, J.E., Ambergen, A.W., and Thunnissen, F.B.J.M. (1998). Number and Proliferation of Basal and Parabasal Cells in Normal Human Airway Epithelium. *American Journal of Respiratory and Critical Care Medicine* 157(6)**,** 2000-2006. doi: 10.1164/ajrccm.157.6.9707011.

Boon, M., Wallmeier, J., Ma, L., Loges, N.T., Jaspers, M., Olbrich, H., et al. (2014). MCIDAS mutations result in a mucociliary clearance disorder with reduced generation of multiple motile cilia. *Nature Communications* 5(1)**,** 4418. doi: 10.1038/ncomms5418.

Borthwick, L.A. (2016). The IL-1 cytokine family and its role in inflammation and fibrosis in the lung. *Seminars in Immunopathology* 38(4)**,** 517-534. doi: 10.1007/s00281-016-0559-z.

Botelho, F.M., Bauer, C.M.T., Finch, D., Nikota, J.K., Zavitz, C.C.J., Kelly, A., et al. (2011). IL-1α/IL-1R1 Expression in Chronic Obstructive Pulmonary Disease and Mechanistic Relevance to Smoke-Induced Neutrophilia in Mice. *PLOS ONE* 6(12)**,** e28457. doi: 10.1371/journal.pone.0028457.

Bou Saab, J., Losa, D., Chanson, M., and Ruez, R. (2014). Connexins in respiratory and gastrointestinal mucosal immunity. *FEBS Lett* 588(8)**,** 1288-1296. doi: 10.1016/j.febslet.2014.02.059.

Boyden, E.D., and Dietrich, W.F. (2006). Nalp1b controls mouse macrophage susceptibility to anthrax lethal toxin. *Nature Genetics* 38(2)**,** 240-244. doi: 10.1038/ng1724.

Brown, P.J., Greville, H.W., and Finucane, K.E. (1984). Asthma and irreversible airflow obstruction. *Thorax* 39(2)**,** 131-136. doi: 10.1136/thx.39.2.131.

Bruchard, M., Rebé, C., Derangère, V., Togbé, D., Ryffel, B., Boidot, R., et al. (2015). The receptor NLRP3 is a transcriptional regulator of TH2 differentiation. *Nature Immunology* 16(8)**,** 859-870. doi: 10.1038/ni.3202.

Bryant, C., and Fitzgerald, K.A. (2009). Molecular mechanisms involved in inflammasome activation. *Trends Cell Biol* 19(9)**,** 455-464. doi: 10.1016/j.tcb.2009.06.002.

Byers, D.E., Alexander-Brett, J., Patel, A.C., Agapov, E., Dang-Vu, G., Jin, X., et al. (2013). Long-term IL-33–producing epithelial progenitor cells in chronic obstructive lung disease. *The Journal of Clinical Investigation* 123(9)**,** 3967-3982. doi: 10.1172/JCI65570.

Calderazzo, M.A., Trujillo-Torralbo, M.-B., Finney, L.J., Singanayagam, A., Bakhsoliani, E., Padmanaban, V., et al. (2019). Inflammation and infections in unreported chronic obstructive pulmonary disease exacerbations. *International journal of chronic obstructive pulmonary disease* 14**,** 823-832. doi: 10.2147/COPD.S191946.

Calverley, P.M.A., Sethi, S., Dawson, M., Ward, C.K., Finch, D.K., Penney, M., et al. (2017). A randomised, placebo-controlled trial of anti-interleukin-1 receptor 1 monoclonal antibody MEDI8968 in chronic obstructive pulmonary disease. *Respiratory research* 18(1)**,** 153-153. doi: 10.1186/s12931-017-0633-7.

Carlier, F.M., de Fays, C., and Pilette, C. (2021). Epithelial Barrier Dysfunction in Chronic Respiratory Diseases. *Frontiers in Physiology* 12(861). doi: 10.3389/fphys.2021.691227.

Castillon, N., Hinnrasky, J., Zahm, J.-M., Kaplan, H., Bonnet, N., Corlieu, P., et al. (2002). Polarized Expression of Cystic Fibrosis Transmembrane Conductance Regulator and Associated Epithelial Proteins during the Regeneration of Human Airway Surface Epithelium in Three-Dimensional Culture. *Laboratory Investigation* 82(8)**,** 989-998. doi: 10.1097/01.LAB.0000022221.88025.43.

Cayrol, C., and Girard, J.P. (2009). The IL-1-like cytokine IL-33 is inactivated after maturation by caspase-1. *Proceedings of the National Academy of Sciences of the United States of America* 106(22)**,** 9021-9026. doi: 10.1073/pnas.0812690106.

Chavarría-Smith, J., and Vance, R.E. (2013). Direct Proteolytic Cleavage of NLRP1B Is Necessary and Sufficient for Inflammasome Activation by Anthrax Lethal Factor. *PLOS Pathogens* 9(6)**,** e1003452. doi: 10.1371/journal.ppat.1003452.

Chazal, M., Beauclair, G., Gracias, S., Najburg, V., Simon-Lorière, E., Tangy, F., et al. (2018). RIG-I Recognizes the 5' Region of Dengue and Zika Virus Genomes. *Cell Rep* 24(2)**,** 320-328. doi: 10.1016/j.celrep.2018.06.047.

Chen, A.C.H., Tran, H.B., Xi, Y., Yerkovich, S.T., Baines, K.J., Pizzutto, S.J., et al. (2018a). Multiple inflammasomes may regulate the interleukin-1-driven inflammation in protracted bacterial bronchitis. *ERJ open research* 4(1)**,** 00130-02017. doi: 10.1183/23120541.00130-2017.

Chen, Y., Qin, X., An, Q., Yi, J., Feng, F., Yin, D., et al. (2018b). Mesenchymal Stromal Cells Directly Promote Inflammation by Canonical NLRP3 and Non-canonical Caspase-11 Inflammasomes. *EBioMedicine* 32**,** 31-42. doi: 10.1016/j.ebiom.2018.05.023.

Chen, Y., Yang, Q., Lv, C., Chen, Y., Zhao, W., Li, W., et al. (2021). NLRP3 regulates alveolar bone loss in ligature-induced periodontitis by promoting osteoclastic differentiation. *Cell Proliferation* 54(2)**,** e12973. doi: https://doi.org/10.1111/cpr.12973.

Chenery, A.L., Alhallaf, R., Agha, Z., Ajendra, J., Parkinson, J.E., Cooper, M.M., et al. (2019). Inflammasome-Independent Role for NLRP3 in Controlling Innate Antihelminth Immunity and Tissue Repair in the Lung. *The Journal of Immunology* 203(10)**,** 2724. doi: 10.4049/jimmunol.1900640.

Cheng, H., and Leblond, C.P. (1974). Origin, differentiation and renewal of the four main epithelial cell types in the mouse small intestine V. Unitarian theory of the origin of the four epithelial cell types. 141(4)**,** 537-561. doi: 10.1002/aja.1001410407.

Chu, Z.L., Pio, F., Xie, Z., Welsh, K., Krajewska, M., Krajewski, S., et al. (2001). A novel enhancer of the Apaf1 apoptosome involved in cytochrome c-dependent caspase activation and apoptosis. *The Journal of biological chemistry* 276(12)**,** 9239-9245. doi: 10.1074/jbc.m006309200.

Coll, R.C., Hill, J.R., Day, C.J., Zamoshnikova, A., Boucher, D., Massey, N.L., et al. (2019). MCC950 directly targets the NLRP3 ATP-hydrolysis motif for inflammasome inhibition. *Nature Chemical Biology* 15(6)**,** 556-559. doi: 10.1038/s41589-019-0277-7.

Coulter, K.R., Wewers, M.D., Lowe, M.P., and Knoell, D.L. (1999). Extracellular Regulation of Interleukin (IL)-1 β through Lung Epithelial Cells and Defective

IL-1 Type II Receptor Expression. *American Journal of Respiratory Cell and Molecular Biology* 20(5)**,** 964-975. doi: 10.1165/ajrcmb.20.5.3458.

Cozens, A.L., Yezzi, M.J., Kunzelmann, K., Ohrui, T., Chin, L., Eng, K., et al. (1994). CFTR expression and chloride secretion in polarized immortal human bronchial epithelial cells. *Am J Respir Cell Mol Biol* 10(1)**,** 38-47. doi: 10.1165/ajrcmb.10.1.7507342.

Crystal, R.G. (2014). Airway basal cells. The "smoking gun" of chronic obstructive pulmonary disease. *American journal of respiratory and critical care medicine* 190(12)**,** 1355-1362. doi: 10.1164/rccm.201408-1492PP.

D'Osualdo, A., Weichenberger, C.X., Wagner, R.N., Godzik, A., Wooley, J., and Reed, J.C. (2011). CARD8 and NLRP1 Undergo Autoproteolytic Processing through a ZU5-Like Domain. *PLOS ONE* 6(11)**,** e27396. doi: 10.1371/journal.pone.0027396.

Davis, J.D., and Wypych, T.P. (2021). Cellular and functional heterogeneity of the airway epithelium. *Mucosal Immunology* 14(5)**,** 978-990. doi: 10.1038/s41385-020-00370-7.

De Falco, G., Terlizzi, M., Sirignano, M., Commodo, M., D'Anna, A., Aquino, R.P., et al. (2017). Human peripheral blood mononuclear cells (PBMCs) from smokers release higher levels of IL-1-like cytokines after exposure to combustion-generated ultrafine particles. *Sci Rep* 7**,** 43016. doi: 10.1038/srep43016.

de Vries, M., Faiz, A., Woldhuis, R.R., Postma, D.S., de Jong, T.V., Sin, D.D., et al. (2017). Lung tissue gene-expression signature for the ageing lung in COPD. *Thorax*. doi: 10.1136/thoraxjnl-2017-210074.

de Vries, S.P., Bootsma, H.J., Hays, J.P., and Hermans, P.W. (2009). Molecular aspects of Moraxella catarrhalis pathogenesis. *Microbiol Mol Biol Rev* 73(3)**,** 389-406, Table of Contents. doi: 10.1128/mmbr.00007-09.

de Vries, S.P.W., Eleveld, M.J., Hermans, P.W.M., and Bootsma, H.J. (2013). Characterization of the molecular interplay between Moraxella catarrhalis and human respiratory tract epithelial cells. *PloS one* 8(8)**,** e72193-e72193. doi: 10.1371/journal.pone.0072193.

Delgado, O., Kaisani, A.A., Spinola, M., Xie, X.J., Batten, K.G., Minna, J.D., et al. (2011). Multipotent capacity of immortalized human bronchial epithelial cells. *PLoS One* 6(7)**,** e22023. doi: 10.1371/journal.pone.0022023.

DeMeo, D.L., and Silverman, E.K. (2004). α1-Antitrypsin deficiency • 2: Genetic aspects of α1-antitrypsin deficiency: Phenotypes and genetic modifiers of emphysema risk. *Thorax* 59(3)**,** 259-264. doi: 10.1136/thx.2003.006502.

Di Paolo, N.C., and Shayakhmetov, D.M. (2016). Interleukin 1α and the inflammatory process. *Nature Immunology* 17(8)**,** 906-913. doi: 10.1038/ni.3503.

Dinarello, C.A. (1994). The interleukin-1 family: 10 years of discovery. *FASEB Journal* 8(15)**,** 1314-1325.

Dinarello, C.A., Novick, D., Kim, S., and Kaplanski, G. (2013). Interleukin-18 and IL-18 binding protein. *Frontiers in Immunology* 4(OCT). doi: 10.3389/fimmu.2013.00289.

Dripps, D.J., Brandhuber, B.J., Thompson, R.C., and Eisenberg, S.P. (1991). Interleukin-1 (IL-1) receptor antagonist binds to the 80-kDa IL-1 receptor but does not initiate IL-1 signal transduction. *J Biol Chem* 266(16)**,** 10331-10336.

Drutman, S.B., Haerynck, F., Zhong, F.L., Hum, D., Hernandez, N.J., Belkaya, S., et al. (2019). Homozygous NLRP1 gain-of-function mutation in

siblings with a syndromic form of recurrent respiratory papillomatosis. *Proceedings of the National Academy of Sciences* 116(38)**,** 19055-19063. doi: 10.1073/pnas.1906184116.

Duell, B.L., Su, Y.-C., and Riesbeck, K. (2016). Host–pathogen interactions of nontypeable Haemophilus influenzae: from commensal to pathogen. *FEBS Letters* 590(21)**,** 3840-3853. doi: https://doi.org/10.1002/1873-3468.12351.

Dvorak, A., Tilley, A.E., Shaykhiev, R., Wang, R., and Crystal, R.G. (2011). Do airway epithelium air-liquid cultures represent the in vivo airway epithelium transcriptome? *Am J Respir Cell Mol Biol* 44(4)**,** 465-473. doi: 10.1165/rcmb.2009-0453OC.

Eager, R.M., Cunningham, C.C., Senzer, N., Richards, D.A., Raju, R.N., Jones, B., et al. (2009). Phase II trial of talabostat and docetaxel in advanced non-small cell lung cancer. *Clin Oncol (R Coll Radiol)* 21(6)**,** 464-472. doi: 10.1016/j.clon.2009.04.007.

Eenjes, E., Buscop-van Kempen, M., Boerema-de Munck, A., Edel, G.G., Benthem, F., de Kreij-de Bruin, L., et al. (2021). SOX21 modulates SOX2-initiated differentiation of epithelial cells in the extrapulmonary airways. *Elife* 10. doi: 10.7554/eLife.57325.

Escotte, S., Catusse, C., Coraux, C., and Puchelle, E. (2004). Reconstitution of human airway tissue in the humanized xenograft model. *Journal of Cystic Fibrosis* 3**,** 63-65. doi: 10.1016/j.jcf.2004.05.014.

Evavold, C.L., Ruan, J., Tan, Y., Xia, S., Wu, H., and Kagan, J.C. (2018). The Pore-Forming Protein Gasdermin D Regulates Interleukin-1 Secretion from Living Macrophages. *Immunity* 48(1)**,** 35-44.e36. doi: https://doi.org/10.1016/j.immuni.2017.11.013.

Ewald Sarah, E., Chavarria-Smith, J., Boothroyd John, C., and Adams, J.H. (2014). NLRP1 Is an Inflammasome Sensor for Toxoplasma gondii. *Infection and Immunity* 82(1)**,** 460-468. doi: 10.1128/IAI.01170-13.

Fang, R., Uchiyama, R., Sakai, S., Hara, H., Tsutsui, H., Suda, T., et al. (2019). ASC and NLRP3 maintain innate immune homeostasis in the airway through an inflammasome-independent mechanism. *Mucosal Immunology* 12(5)**,** 1092-1103. doi: 10.1038/s41385-019-0181-1.

Faure, E., Kwong, K., and Nguyen, D. (2018). Pseudomonas aeruginosa in Chronic Lung Infections: How to Adapt Within the Host? *Frontiers in Immunology* 9. doi: 10.3389/fimmu.2018.02416.

Fenini, G., Grossi, S., Contassot, E., Biedermann, T., Reichmann, E., French, L.E., et al. (2018). Genome Editing of Human Primary Keratinocytes by CRISPR/Cas9 Reveals an Essential Role of the NLRP1 Inflammasome in UVB Sensing. *Journal of Investigative Dermatology* 138(12)**,** 2644-2652. doi: https://doi.org/10.1016/j.jid.2018.07.016.

Fettelschoss, A., Kistowska, M., LeibundGut-Landmann, S., Beer, H.-D., Johansen, P., Senti, G., et al. (2011). Inflammasome activation and IL-1β target IL-1α for secretion as opposed to surface expression. *Proceedings of the National Academy of Sciences* 108(44)**,** 18055-18060. doi: 10.1073/pnas.1109176108.

Finger, J.N., Lich, J.D., Dare, L.C., Cook, M.N., Brown, K.K., Duraiswami, C., et al. (2012). Autolytic proteolysis within the function to find domain (FIIND) is required for NLRP1 inflammasome activity. *J Biol Chem* 287(30)**,** 25030-25037. doi: 10.1074/jbc.M112.378323.

Fliegauf, M., Benzing, T., and Omran, H. (2007). When cilia go bad: cilia defects and ciliopathies. *Nature Reviews Molecular Cell Biology* 8**,** 880. doi: 10.1038/nrm2278

https://www.nature.com/articles/nrm2278#supplementary-information.

Franklin, B.S., Bossaller, L., De Nardo, D., Ratter, J.M., Stutz, A., Engels, G., et al. (2014). The adaptor ASC has extracellular and 'prionoid' activities that propagate inflammation. *Nature Immunology* 15(8)**,** 727-737. doi: 10.1038/ni.2913.

Fu, J.-j., McDonald, V.M., Baines, K.J., and Gibson, P.G. (2015). Airway IL-1β and Systemic Inflammation as Predictors of Future Exacerbation Risk in Asthma and COPD. *Chest* 148(3)**,** 618-629. doi: https://doi.org/10.1378/chest.14-2337.

Fulcher, M.L., and Randell, S.H. (2013). "Human Nasal and Tracheo-Bronchial Respiratory Epithelial Cell Culture," in *Epithelial Cell Culture Protocols: Second Edition,* eds. S.H. Randell & M.L. Fulcher. (Totowa, NJ: Humana Press), 109-121.

Gamez, A.S., Gras, D., Petit, A., Knabe, L., Molinari, N., Vachier, I., et al. (2015). Supplementing Defect in Club Cell Secretory Protein Attenuates Airway Inflammation in COPD. *CHEST* 147(6)**,** 1467-1476. doi: 10.1378/chest.14-1174.

Garcia-Vidal, C., Almagro, P., Romaní, V., Rodríguez-Carballeira, M., Cuchi, E., Canales, L., et al. (2009). Pseudomonas aeruginosa in patients hospitalised for COPD exacerbation: a prospective study. *European Respiratory Journal* 34(5)**,** 1072-1078. doi: 10.1183/09031936.00003309.

Gavino, A.C., Chung, J.S., Sato, K., Ariizumi, K., and Cruz, P.D., Jr. (2005). Identification and expression profiling of a human C-type lectin, structurally homologous to mouse dectin-2. *Exp Dermatol* 14(4)**,** 281-288. doi: 10.1111/j.0906-6705.2005.00312.x.

Geddes, B.J., Wang, L., Huang, W.-J., Lavellee, M., Manji, G.A., Brown, M., et al. (2001). Human CARD12 Is a Novel CED4/Apaf-1 Family Member That Induces Apoptosis. *Biochemical and Biophysical Research Communications* 284(1)**,** 77-82. doi: https://doi.org/10.1006/bbrc.2001.4928.

Ghimire, L., Paudel, S., Jin, L., Baral, P., Cai, S., and Jeyaseelan, S. (2018). NLRP6 negatively regulates pulmonary host defense in Gram-positive bacterial infection through modulating neutrophil recruitment and function. *PLoS pathogens* 14(9)**,** e1007308-e1007308. doi: 10.1371/journal.ppat.1007308.

Gindele, J.A., Kiechle, T., Benediktus, K., Birk, G., Brendel, M., Heinemann, F., et al. (2020). Intermittent exposure to whole cigarette smoke alters the differentiation of primary small airway epithelial cells in the air-liquid interface culture. *Scientific Reports* 10(1)**,** 6257. doi: 10.1038/s41598-020-63345-5.

Gorfu, G., Cirelli Kimberly, M., Melo Mariane, B., Mayer-Barber, K., Crown, D., Koller Beverly, H., et al. Dual Role for Inflammasome Sensors NLRP1 and NLRP3 in Murine Resistance to Toxoplasma gondii. *mBio* 5(1)**,** e01117-01113. doi: 10.1128/mBio.01117-13.

Gour, N., Lajoie, S., Smole, U., White, M., Hu, D., Goddard, P., et al. (2018). Dysregulated invertebrate tropomyosin-dectin-1 interaction confers susceptibility to allergic diseases. *Sci Immunol* 3(20). doi: 10.1126/sciimmunol.aam9841.

Grainger, C.I., Greenwell, L.L., Lockley, D.J., Martin, G.P., and Forbes, B. (2006). Culture of Calu-3 cells at the air interface provides a representative model of the airway epithelial barrier. *Pharm Res* 23(7)**,** 1482-1490. doi: 10.1007/s11095-006-0255-0.

Gram, A.M., Wright, J.A., Pickering, R.J., Lam, N.L., Booty, L.M., Webster, S.J., et al. (2021). Salmonella Flagellin Activates NAIP/NLRC4 and Canonical NLRP3 Inflammasomes in Human Macrophages. 206(3)**,** 631-640. doi: 10.4049/jimmunol.2000382 %J The Journal of Immunology.

Grandjean, T., Boucher, A., Thepaut, M., Monlezun, L., Guery, B., Faudry, E., et al. (2017). The human NAIP-NLRC4-inflammasome senses the Pseudomonas aeruginosa T3SS inner-rod protein. *Int Immunol* 29(8)**,** 377-384. doi: 10.1093/intimm/dxx047.

Gras, D., Petit, A., Charriot, J., Knabe, L., Alagha, K., Gamez, A.S., et al. (2017). Epithelial ciliated beating cells essential for ex vivo ALI culture growth. *BMC Pulmonary Medicine* 17(1)**,** 80. doi: 10.1186/s12890-017-0423-5.

Greenfeder, S.A., Nunes, P., Kwee, L., Labow, M., Chizzonite, R.A., and Ju, G. (1995). Molecular cloning and characterization of a second subunit of the interleukin 1 receptor complex. *J Biol Chem* 270(23)**,** 13757-13765.

Gregory, S.M., Davis, B.K., West, J.A., Taxman, D.J., Matsuzawa, S., Reed, J.C., et al. (2011). Discovery of a viral NLR homolog that inhibits the inflammasome. *Science* 331(6015)**,** 330-334. doi: 10.1126/science.1199478.

Griswold, A.R., Ball, D.P., Bhattacharjee, A., Chui, A.J., Rao, S.D., Taabazuing, C.Y., et al. (2019). DPP9's Enzymatic Activity and Not Its Binding to CARD8 Inhibits Inflammasome Activation. *ACS Chemical Biology* 14(11)**,** 2424-2429. doi: 10.1021/acschembio.9b00462.

Gross, N.J., and Barnes, P.J. (2017). New Therapies for Asthma and Chronic Obstructive Pulmonary Disease. *American Journal of Respiratory and Critical Care Medicine* 195(2)**,** 159-166. doi: 10.1164/rccm.201610-2074PP.

Groß, O., Yazdi, Amir S., Thomas, Christina J., Masin, M., Heinz, Leonhard X., Guarda, G., et al. (2012). Inflammasome Activators Induce Interleukin-1α Secretion via Distinct Pathways with Differential Requirement for the Protease Function of Caspase-1. *Immunity* 36(3)**,** 388-400. doi: https://doi.org/10.1016/j.immuni.2012.01.018.

Guillot, L., Medjane, S., Le-Barillec, K., Balloy, V., Danel, C., Chignard, M., et al. (2004). Response of human pulmonary epithelial cells to lipopolysaccharide involves Toll-like receptor 4 (TLR4)-dependent signaling pathways: evidence for an intracellular compartmentalization of TLR4. *J Biol Chem* 279(4)**,** 2712-2718. doi: 10.1074/jbc.M305790200.

Guo, H., Callaway, J.B., and Ting, J.P.Y. (2015). Inflammasomes: mechanism of action, role in disease, and therapeutics. *Nature medicine* 21(7)**,** 677-687. doi: 10.1038/nm.3893.

Harris, P.A., Duraiswami, C., Fisher, D.T., Fornwald, J., Hoffman, S.J., Hofmann, G., et al. (2015). High throughput screening identifies ATP-competitive inhibitors of the NLRP1 inflammasome. *Bioorg Med Chem Lett* 25(14)**,** 2739-2743. doi: 10.1016/j.bmcl.2015.05.032.

Hayakawa, H., Hayakawa, M., Kume, A., and Tominaga, S.I. (2007). Soluble ST2 blocks interleukin-33 signaling in allergic airway inflammation. *Journal of Biological Chemistry* 282(36)**,** 26369-26380. doi: 10.1074/jbc.M704916200.

Heijink, I.H., Kuchibhotla, V.N.S., Roffel, M.P., Maes, T., Knight, D.A., Sayers, I., et al. (2020). Epithelial cell dysfunction, a major driver of asthma development. *Allergy* 75(8)**,** 1902-1917. doi: https://doi.org/10.1111/all.14421.

Herfs, M., Hubert, P., Poirrier, A.L., Vandevenne, P., Renoux, V., Habraken, Y., et al. (2012). Proinflammatory cytokines induce bronchial hyperplasia and squamous metaplasia in smokers: implications for chronic obstructive pulmonary disease therapy. *Am J Respir Cell Mol Biol* 47(1)**,** 67-79. doi: 10.1165/rcmb.2011-0353OC.

Hertzog, J., Dias Junior, A.G., Rigby, R.E., Donald, C.L., Mayer, A., Sezgin, E., et al. (2018). Infection with a Brazilian isolate of Zika virus generates RIG-I stimulatory RNA and the viral NS5 protein blocks type I IFN induction and signaling. *Eur J Immunol* 48(7)**,** 1120-1136. doi: 10.1002/eji.201847483.

Hewitt, R.J., and Lloyd, C.M. (2021). Regulation of immune responses by the airway epithelial cell landscape. *Nature Reviews Immunology* 21(6)**,** 347-362. doi: 10.1038/s41577-020-00477-9.

Heyl, K.A., Klassert, T.E., Heinrich, A., Muller, M.M., Klaile, E., Dienemann, H., et al. (2014). Dectin-1 is expressed in human lung and mediates the proinflammatory immune response to nontypeable Haemophilus influenzae. *MBio* 5(5)**,** e01492-01414. doi: 10.1128/mBio.01492-14.

Hiemstra, P.S., McCray, P.B., and Bals, R. (2015). The innate immune function of airway epithelial cells in inflammatory lung disease. *European Respiratory Journal* 45(4)**,** 1150. doi: 10.1183/09031936.00141514.

Hirota, J.A., Hirota, S.A., Warner, S.M., Stefanowicz, D., Shaheen, F., Beck, P.L., et al. (2012). The airway epithelium nucleotide-binding domain and leucine-rich repeat protein 3 inflammasome is activated by urban particulate matter. *Journal of Allergy and Clinical Immunology* 129(4)**,** 1116-1125.e1116. doi: https://doi.org/10.1016/j.jaci.2011.11.033.

Hofer, F., Gruenberger, M., Kowalski, H., Machat, H., Huettinger, M., Kuechler, E., et al. (1994). Members of the low density lipoprotein receptor family mediate cell entry of a minor-group common cold virus. *Proceedings of the National Academy of Sciences* 91(5)**,** 1839-1842. doi: 10.1073/pnas.91.5.1839.

Hoffmann, M., Kleine-Weber, H., Schroeder, S., Krüger, N., Herrler, T., Erichsen, S., et al. (2020). SARS-CoV-2 Cell Entry Depends on ACE2 and TMPRSS2 and Is Blocked by a Clinically Proven Protease Inhibitor. *Cell* 181(2)**,** 271-280.e278. doi: https://doi.org/10.1016/j.cell.2020.02.052.

Hollingsworth, L.R., Sharif, H., Griswold, A.R., Fontana, P., Mintseris, J., Dagbay, K.B., et al. (2021). DPP9 sequesters the C terminus of NLRP1 to repress inflammasome activation. *Nature* 592(7856)**,** 778-783. doi: 10.1038/s41586-021-03350-4.

Hornung, V., Ablasser, A., Charrel-Dennis, M., Bauernfeind, F., Horvath, G., Caffrey, D.R., et al. (2009). AIM2 recognizes cytosolic dsDNA and forms a caspase-1-activating inflammasome with ASC. *Nature* 458(7237)**,** 514-518. doi: 10.1038/nature07725.

Hoshino, T., Kato, S., Oka, N., Imaoka, H., Kinoshita, T., Takei, S., et al. (2007). Pulmonary inflammation and emphysema: Role of the cytokines IL-18 and IL-13. *American Journal of Respiratory and Critical Care Medicine* 176(1)**,** 49-62. doi: 10.1164/rccm.200603-316OC.

Hou, C., Zhao, H., Liu, L., Li, W., Zhou, X., Lv, Y., et al. (2011). High mobility group protein B1 (HMGB1) in asthma: Comparison of patients with chronic

obstructive pulmonary disease and healthy controls. *Molecular Medicine* 17(7-8)**,** 807-815. doi: 10.2119/molmed.2010.00173.

Huang, M., Zhang, X., Toh, G.A., Gong, Q., Wang, J., Han, Z., et al. (2021). Structural and biochemical mechanisms of NLRP1 inhibition by DPP9. *Nature* 592(7856)**,** 773-777. doi: 10.1038/s41586-021-03320-w.

Imaoka, H., Hoshino, T., Takei, S., Kinoshita, T., Okamoto, M., Kawayama, T., et al. (2008). Interleukin-18 production and pulmonary function in COPD. *European Respiratory Journal* 31(2)**,** 287-297. doi: 10.1183/09031936.00019207.

Ioannidis, I., Ye, F., McNally, B., Willette, M., and Flaño, E. (2013). Toll-Like Receptor Expression and Induction of Type I and Type III Interferons in Primary Airway Epithelial Cells. *Journal of Virology* 87(6)**,** 3261. doi: 10.1128/JVI.01956-12.

Ito, S., Hara, Y., and Kubota, T. (2014). CARD8 is a negative regulator for NLRP3 inflammasome, but mutant NLRP3 in cryopyrin-associated periodic syndromes escapes the restriction. *Arthritis Research & Therapy* 16(1)**,** R52. doi: 10.1186/ar4483.

J, S.P., Hu, P., Burke, S.J., Collier, J.J., Chen, J., and Zhao, L. (2013). The effects of NOD activation on adipocyte differentiation. *Obesity (Silver Spring)* 21(4)**,** 737-747. doi: 10.1002/oby.20275.

Jacobs, S.E., Lamson, D.M., St George, K., and Walsh, T.J. (2013). Human rhinoviruses. *Clinical microbiology reviews* 26(1)**,** 135-162. doi: 10.1128/CMR.00077-12.

Jakiela, B., Brockman-Schneider, R., Amineva, S., Lee, W.-M., and Gern, J.E. (2008). Basal Cells of Differentiated Bronchial Epithelium Are More Susceptible to Rhinovirus Infection. *American Journal of Respiratory Cell and Molecular Biology* 38(5)**,** 517-523. doi: 10.1165/rcmb.2007-0050OC.

Janowski, A.M., Colegio, O.R., Hornick, E.E., McNiff, J.M., Martin, M.D., Badovinac, V.P., et al. (2016). NLRC4 suppresses melanoma tumor progression independently of inflammasome activation. *The Journal of clinical investigation* 126(10)**,** 3917-3928. doi: 10.1172/JCI86953.

Jha, S., Brickey, W.J., and Ting, J.P. (2017). Inflammasomes in Myeloid Cells: Warriors Within. *Microbiol Spectr* 5(1). doi: 10.1128/microbiolspec.MCHD-0049-2016.

Jia, H.P., Kline, J.N., Penisten, A., Apicella, M.A., Gioannini, T.L., Weiss, J., et al. (2004). Endotoxin responsiveness of human airway epithelia is limited by low expression of MD-2. *Am J Physiol Lung Cell Mol Physiol* 287(2)**,** L428-437. doi: 10.1152/ajplung.00377.2003.

Jin, Z., Du, X., Xu, Y., Deng, Y., Liu, M., Zhao, Y., et al. (2020). Structure of Mpro from SARS-CoV-2 and discovery of its inhibitors. *Nature* 582(7811)**,** 289-293. doi: 10.1038/s41586-020-2223-y.

Johnson, D.C., Taabazuing, C.Y., Okondo, M.C., Chui, A.J., Rao, S.D., Brown, F.C., et al. (2018). DPP8/DPP9 inhibitor-induced pyroptosis for treatment of acute myeloid leukemia. *Nature Medicine* 24(8)**,** 1151-1156. doi: 10.1038/s41591-018-0082-y.

Kang, M.J., Homer, R.J., Gallo, A., Lee, C.G., Crothers, K.A., Cho, S.J., et al. (2007). IL-18 is induced and IL-18 receptor α plays a critical role in the pathogenesis of cigarette smoke-induced pulmonary emphysema and inflammation. *Journal of Immunology* 178(3)**,** 1948-1959.

Karp, P.H., Moninger, T.O., Weber, S.P., Nesselhauf, T.S., Launspach, J.L., Zabner, J., et al. (2002). An in vitro model of differentiated human airway epithelia. Methods for establishing primary cultures. *Methods Mol Biol* 188**,** 115-137. doi: 10.1385/1-59259-185-x:115.

Kato, H., Takeuchi, O., Sato, S., Yoneyama, M., Yamamoto, M., Matsui, K., et al. (2006). Differential roles of MDA5 and RIG-I helicases in the recognition of RNA viruses. *Nature* 441(7089)**,** 101-105. doi: 10.1038/nature04734.

Kayagaki, N., Stowe, I.B., Lee, B.L., O'Rourke, K., Anderson, K., Warming, S., et al. (2015). Caspase-11 cleaves gasdermin D for non-canonical inflammasome signalling. *Nature* 526(7575)**,** 666-671. doi: 10.1038/nature15541.

Keatings, V.M., Collins, P.D., Scott, D.M., and Barnes, P.J. (1996). Differences in interleukin-8 and tumor necrosis factor-alpha in induced sputum from patients with chronic obstructive pulmonary disease or asthma. *Am J Respir Crit Care Med* 153(2)**,** 530-534. doi: 10.1164/ajrccm.153.2.8564092.

Kerur, N., Veettil, M.V., Sharma-Walia, N., Bottero, V., Sadagopan, S., Otageri, P., et al. (2011). IFI16 acts as a nuclear pathogen sensor to induce the inflammasome in response to Kaposi Sarcoma-associated herpesvirus infection. *Cell Host Microbe* 9(5)**,** 363-375. doi: 10.1016/j.chom.2011.04.008.

Kim, B., Lee, Y., Kim, E., Kwak, A., Ryoo, S., Bae, S.H., et al. (2013). The Interleukin-1α Precursor is Biologically Active and is Likely a Key Alarmin in the IL-1 Family of Cytokines. *Front Immunol* 4**,** 391. doi: 10.3389/fimmu.2013.00391.

Kim, H.-S., Shin, T.-H., Yang, S.-R., Seo, M.-S., Kim, D.-J., Kang, S.-K., et al. (2010). Implication of NOD1 and NOD2 for the Differentiation of Multipotent Mesenchymal Stem Cells Derived from Human Umbilical Cord Blood. *PLOS ONE* 5(10)**,** e15369. doi: 10.1371/journal.pone.0015369.

Kiyokawa, H., and Morimoto, M. (2020). Notch signaling in the mammalian respiratory system, specifically the trachea and lungs, in development, homeostasis, regeneration, and disease. *Development, Growth & Differentiation* 62(1)**,** 67-79. doi: https://doi.org/10.1111/dgd.12628.

Kong, H., Wang, Y., Zeng, X., Wang, Z., Wang, H., and Xie, W. (2015). Differential expression of inflammasomes in lung cancer cell lines and tissues. *Tumour Biol* 36(10)**,** 7501-7513. doi: 10.1007/s13277-015-3473-4.

Kopan, R., and Ilagan, M.X. (2009). The canonical Notch signaling pathway: unfolding the activation mechanism. *Cell* 137(2)**,** 216-233. doi: 10.1016/j.cell.2009.03.045.

Kostadinova, E., Chaput, C., Gutbier, B., Lippmann, J., Sander, L.E., Mitchell, T.J., et al. (2016). NLRP3 protects alveolar barrier integrity by an inflammasome-independent increase of epithelial cell adherence. *Scientific Reports* 6(1)**,** 30943. doi: 10.1038/srep30943.

Kummer, J.A., Broekhuizen, R., Everett, H., Agostini, L., Kuijk, L., Martinon, F., et al. (2007). Inflammasome Components NALP 1 and 3 Show Distinct but Separate Expression Profiles in Human Tissues Suggesting a Site-specific Role in the Inflammatory Response. *Journal of Histochemistry & Cytochemistry* 55(5)**,** 443-452. doi: 10.1369/jhc.6A7101.2006.

Lankas, G.R., Leiting, B., Roy, R.S., Eiermann, G.J., Beconi, M.G., Biftu, T., et al. (2005). Dipeptidyl peptidase IV inhibition for the treatment of type 2 diabetes: potential importance of selectivity over dipeptidyl peptidases 8 and 9. *Diabetes* 54(10)**,** 2988-2994. doi: 10.2337/diabetes.54.10.2988.

Laucho-Contreras, M.E., Polverino, F., Gupta, K., Taylor, K.L., Kelly, E., Pinto-Plata, V., et al. (2015). Protective role for club cell secretory protein-16 (CC16) in the development of COPD. *European Respiratory Journal* 45(6)**,** 1544-1556. doi: 10.1183/09031936.00134214.

Lee, H.M., Yuk, J.M., Shin, D.M., and Jo, E.K. (2009). Dectin-1 is inducible and plays an essential role for mycobacteria-induced innate immune responses in airway epithelial cells. *J Clin Immunol* 29(6)**,** 795-805. doi: 10.1007/s10875-009-9319-3.

Lee, I.T., Nakayama, T., Wu, C.-T., Goltsev, Y., Jiang, S., Gall, P.A., et al. (2020). ACE2 localizes to the respiratory cilia and is not increased by ACE inhibitors or ARBs. *Nature Communications* 11(1)**,** 5453. doi: 10.1038/s41467-020-19145-6.

Lee, S., Ishitsuka, A., Noguchi, M., Hirohama, M., Fujiyasu, Y., Petric, P.P., et al. (2019). Influenza restriction factor MxA functions as inflammasome sensor in the respiratory epithelium. *Sci Immunol* 4(40). doi: 10.1126/sciimmunol.aau4643.

Lee, S.M.Y., Kok, K.-H., Jaume, M., Cheung, T.K.W., Yip, T.-F., Lai, J.C.C., et al. (2014). Toll-like receptor 10 is involved in induction of innate immune responses to influenza virus infection. *Proceedings of the National Academy of Sciences* 111(10)**,** 3793-3798. doi: doi:10.1073/pnas.1324266111.

Lefrançais, E., Roga, S., Gautier, V., Gonzalez-de-Peredo, A., Monsarrat, B., Girard, J.P., et al. (2012). IL-33 is processed into mature bioactive forms by neutrophil elastase and cathepsin G. *Proceedings of the National Academy of Sciences of the United States of America* 109(5)**,** 1673-1678. doi: 10.1073/pnas.1115884109.

Levy, D.E., Marié, I.J., and Durbin, J.E. (2011). Induction and function of type I and III interferon in response to viral infection. *Current Opinion in Virology* 1(6)**,** 476-486. doi: https://doi.org/10.1016/j.coviro.2011.11.001.

Lieber, M., Smith, B., Szakal, A., Nelson-Rees, W., and Todaro, G. (1976). A continuous tumor-cell line from a human lung carcinoma with properties of type II alveolar epithelial cells. *Int J Cancer* 17(1)**,** 62-70. doi: 10.1002/ijc.2910170110.

Lillehoj, E.P., Guang, W., Hyun, S.W., Liu, A., Hegerle, N., Simon, R., et al. (2019). Neuraminidase 1–mediated desialylation of the mucin 1 ectodomain releases a decoy receptor that protects against Pseudomonas aeruginosa lung infection. *Journal of Biological Chemistry* 294(2)**,** 662-678. doi: https://doi.org/10.1074/jbc.RA118.006022.

Lillehoj, E.P., Kato, K., Lu, W., and Kim, K.C. (2013). Cellular and molecular biology of airway mucins. *International review of cell and molecular biology* 303**,** 139-202. doi: 10.1016/B978-0-12-407697-6.00004-0.

Lin, H., Li, H., Cho, H.-J., Bian, S., Roh, H.-J., Lee, M.-K., et al. (2007). Air-Liquid Interface (ALI) Culture of Human Bronchial Epithelial Cell Monolayers as an in vitro Model for Airway Drug Transport Studies. *Journal of Pharmaceutical Sciences* 96(2)**,** 341-350. doi: https://doi.org/10.1002/jps.20803.

Linder, A., Bauernfried, S., Cheng, Y., Albanese, M., Jung, C., Keppler, O.T., et al. (2020). CARD8 inflammasome activation triggers pyroptosis in human T cells. *The EMBO Journal* 39(19)**,** e105071. doi: https://doi.org/10.15252/embj.2020105071.

Liu, P., Jamaluddin, M., Li, K., Garofalo, R.P., Casola, A., and Brasier, A.R. (2007). Retinoic Acid-Inducible Gene I Mediates Early Antiviral Response and Toll-

Like Receptor 3 Expression in Respiratory Syncytial Virus-Infected Airway Epithelial Cells. *Journal of Virology* 81(3)**,** 1401-1411. doi: 10.1128/jvi.01740-06.

Liu, S., Du, J., Li, D., Yang, P., Kou, Y., Li, C., et al. (2020). Oxidative stress induced pyroptosis leads to osteogenic dysfunction of MG63 cells. *J Mol Histol* 51(3)**,** 221-232. doi: 10.1007/s10735-020-09874-9.

Lo, C.-M., Keese, C.R., and Giaever, I. (1999). Cell–Substrate Contact: Another Factor May Influence Transepithelial Electrical Resistance of Cell Layers Cultured on Permeable Filters. *Experimental Cell Research* 250(2)**,** 576-580. doi: https://doi.org/10.1006/excr.1999.4538.

Lopez-Castejon, G., and Brough, D. (2011). Understanding the mechanism of IL-1β secretion. *Cytokine and Growth Factor Reviews* 22(4)**,** 189-195. doi: 10.1016/j.cytogfr.2011.10.001.

Lopez-Souza, N., Dolganov, G., Dubin, R., Sachs, L.A., Sassina, L., Sporer, H., et al. (2004). Resistance of differentiated human airway epithelium to infection by rhinovirus. *American Journal of Physiology-Lung Cellular and Molecular Physiology* 286(2)**,** L373-L381. doi: 10.1152/ajplung.00300.2003.

Luengen, A.E., Kniebs, C., Buhl, E.M., Cornelissen, C.G., Schmitz-Rode, T., Jockenhoevel, S., et al. (2020). Choosing the Right Differentiation Medium to Develop Mucociliary Phenotype of Primary Nasal Epithelial Cells In Vitro. *Scientific Reports* 10(1)**,** 6963. doi: 10.1038/s41598-020-63922-8.

Ma, C., Li, S., Hu, Y., Ma, Y., Wu, Y., Wu, C., et al. (2021). AIM2 controls microglial inflammation to prevent experimental autoimmune encephalomyelitis. *Journal of Experimental Medicine* 218(5). doi: 10.1084/jem.20201796.

Mailliard, R.B., Alber, S.M., Shen, H., Watkins, S.C., Kirkwood, J.M., Herberman, R.B., et al. (2005). IL-18-induced CD83+CCR7+ NK helper cells. *Journal of Experimental Medicine* 202(7)**,** 941-953. doi: 10.1084/jem.20050128.

Mallia, P., Footitt, J., Sotero, R., Jepson, A., Contoli, M., Trujillo-Torralbo, M.-B., et al. (2012). Rhinovirus Infection Induces Degradation of Antimicrobial Peptides and Secondary Bacterial Infection in Chronic Obstructive Pulmonary Disease. *American Journal of Respiratory and Critical Care Medicine* 186(11)**,** 1117-1124. doi: 10.1164/rccm.201205-0806OC.

Martinon, F., Burns, K., and Tschopp, J. (2002). The Inflammasome: A molecular platform triggering activation of inflammatory caspases and processing of proIL-β. *Molecular Cell* 10(2)**,** 417-426. doi: 10.1016/S1097-2765(02)00599-3.

Maurisse, R., De Semir, D., Emamekhoo, H., Bedayat, B., Abdolmohammadi, A., Parsi, H., et al. (2010). Comparative transfection of DNA into primary and transformed mammalian cells from different lineages. *BMC biotechnology* 10**,** 9-9. doi: 10.1186/1472-6750-10-9.

Mayer, A.K., Muehmer, M., Mages, J., Gueinzius, K., Hess, C., Heeg, K., et al. (2007). Differential Recognition of TLR-Dependent Microbial Ligands in Human Bronchial Epithelial Cells. *The Journal of Immunology* 178(5)**,** 3134-3142. doi: 10.4049/jimmunol.178.5.3134.

McHugh, B.J., Wang, R., Li, H.-N., Beaumont, P.E., Kells, R., Stevens, H., et al. (2019). Cathelicidin is a "fire alarm", generating protective NLRP3-dependent airway epithelial cell inflammatory responses during infection with Pseudomonas aeruginosa. *PLoS pathogens* 15(4)**,** e1007694-e1007694. doi: 10.1371/journal.ppat.1007694.

Meijer, M., Rijkers, G.T., and Van Overveld, F.J. (2013). Neutrophils and emerging targets for treatment in chronic obstructive pulmonary disease. *Expert Review of Clinical Immunology* 9(11), 1055-1068. doi: 10.1586/1744666X.2013.851347.

Miles, A.A., Misra, S.S., and Irwin, J.O. (1938). The estimation of the bactericidal power of the blood. *J Hyg (Lond)* 38(6), 732-749. doi: 10.1017/s002217240001158x.

Mishra, S., Raj, A.S., Kumar, A., Rajeevan, A., Kumari, P., and Kumar, H. (2022). Innate immune sensing of influenza A viral RNA through IFI16 promotes pyroptotic cell death. *iScience* 25(1), 103714. doi: https://doi.org/10.1016/j.isci.2021.103714.

Mitchell, P.S., Sandstrom, A., and Vance, R.E. (2019). The NLRP1 inflammasome: new mechanistic insights and unresolved mysteries. *Current opinion in immunology* 60, 37-45. doi: 10.1016/j.coi.2019.04.015.

Moecking, J., Laohamonthonkul, P., Chalker, K., White, M.J., Harapas, C.R., Yu, C.-H., et al. (2020). NLRP1 variant M1184V decreases inflammasome activation in the context of DPP9 inhibition and asthma severity. *Journal of Allergy and Clinical Immunology*. doi: https://doi.org/10.1016/j.jaci.2020.12.636.

Montoro, D.T., Haber, A.L., Biton, M., Vinarsky, V., Lin, B., Birket, S.E., et al. (2018). A revised airway epithelial hierarchy includes CFTR-expressing ionocytes. *Nature* 560(7718), 319-324. doi: 10.1038/s41586-018-0393-7.

Mortaz, E., Henricks, P.A.J., Kraneveld, A.D., Givi, M.E., Garssen, J., and Folkerts, G. (2011). Cigarette smoke induces the release of CXCL-8 from human bronchial epithelial cells via TLRs and induction of the inflammasome. *Biochimica et Biophysica Acta (BBA) - Molecular Basis of Disease* 1812(9), 1104-1110. doi: https://doi.org/10.1016/j.bbadis.2011.06.002.

Mosley, B., Urdal, D.L., Prickett, K.S., Larsen, A., Cosman, D., Conlon, P.J., et al. (1987). The interleukin-1 receptor binds the human interleukin-1 alpha precursor but not the interleukin-1 beta precursor. *Journal of Biological Chemistry* 262(7), 2941-2944. doi: https://doi.org/10.1016/S0021-9258(18)61450-4.

Muller, T., Vieira, R.P., Grimm, M., Durk, T., Cicko, S., Zeiser, R., et al. (2011). A potential role for P2X7R in allergic airway inflammation in mice and humans. *Am J Respir Cell Mol Biol* 44(4), 456-464. doi: 10.1165/rcmb.2010-0129OC.

Nakajima, M., Kawanami, O., Jin, E., Ghazizadeh, M., Honda, M., Asano, G., et al. (1998). Immunohistochemical and ultrastructural studies of basal cells, Clara cells and bronchiolar cuboidal cells in normal human airways. *Pathol Int* 48(12), 944-953.

Nakamoto, K., Watanabe, M., Sada, M., Inui, T., Nakamura, M., Honda, K., et al. (2019). Pseudomonas aeruginosa-derived flagellin stimulates IL-6 and IL-8 production in human bronchial epithelial cells: A potential mechanism for progression and exacerbation of COPD. *Exp Lung Res* 45(8), 255-266. doi: 10.1080/01902148.2019.1665147.

Nakanishi, K., Yoshimoto, T., Tsutsui, H., and Okamura, H. (2001). Interleukin-18 is a unique cytokine that stimulates both Th1 and Th2 responses depending on its cytokine milieu. *Cytokine and Growth Factor Reviews* 12(1), 53-72. doi: 10.1016/S1359-6101(00)00015-0.

Netea, M.G., Van De Veerdonk, F.L., Van Der Meer, J.W.M., Dinarello, C.A., and Joosten, L.A.B. (2015). "Inflammasome-independent regulation of IL-1-family cytokines".).

Nunes, A.T., and Annunziata, C.M. (2017). Proteasome inhibitors: structure and function. *Semin Oncol* 44(6), 377-380. doi: 10.1053/j.seminoncol.2018.01.004.

O'Connor Jr, W., Harton, J.A., Zhu, X., Linhoff, M.W., and Ting, J.P.Y. (2003). Cutting Edge: CIAS1/Cryopyrin/PYPAF1/NALP3/CATERPILLER 1.1 Is an Inducible Inflammatory Mediator with NF-κB Suppressive Properties. *Journal of Immunology* 171(12), 6329-6333.

O'Neill, L.A.J. (2008). The interleukin-1 receptor/Toll-like receptor superfamily: 10 years of progress. *Immunological Reviews* 226(1), 10-18. doi: https://doi.org/10.1111/j.1600-065X.2008.00701.x.

Ohkuni, T., Kojima, T., Ogasawara, N., Masaki, T., Fuchimoto, J., Kamekura, R., et al. (2011). Poly(I:C) reduces expression of JAM-A and induces secretion of IL-8 and TNF-alpha via distinct NF-kappaB pathways in human nasal epithelial cells. *Toxicol Appl Pharmacol* 250(1), 29-38. doi: 10.1016/j.taap.2010.09.023.

Ohno, T., Oboki, K., Kajiwara, N., Morii, E., Aozasa, K., Flavell, R.A., et al. (2009). Caspase-1, caspase-8, and calpain are dispensable for IL-33 release by macrophages. *Journal of Immunology* 183(12), 7890-7897. doi: 10.4049/jimmunol.0802449.

Okondo, M.C., Johnson, D.C., Sridharan, R., Go, E.B., Chui, A.J., Wang, M.S., et al. (2017). DPP8 and DPP9 inhibition induces pro-caspase-1-dependent monocyte and macrophage pyroptosis. *Nature chemical biology* 13(1), 46-53. doi: 10.1038/nchembio.2229.

Okondo, M.C., Rao, S.D., Taabazuing, C.Y., Chui, A.J., Poplawski, S.E., Johnson, D.C., et al. (2018). Inhibition of Dpp8/9 Activates the Nlrp1b Inflammasome. *Cell chemical biology* 25(3), 262-267.e265. doi: 10.1016/j.chembiol.2017.12.013.

Oliver, B.G.G., Lim, S., Wark, P., Laza-Stanca, V., King, N., Black, J.L., et al. (2008). Rhinovirus exposure impairs immune responses to bacterial products in human alveolar macrophages. *Thorax* 63(6), 519. doi: 10.1136/thx.2007.081752.

Oosenbrug, T., van de Graaff, M.J., Ressing, M.E., and van Kasteren, S.I. (2017). Chemical Tools for Studying TLR Signaling Dynamics. *Cell Chem Biol* 24(7), 801-812. doi: 10.1016/j.chembiol.2017.05.022.

Osman, K.L., Jefferies, J.M.C., Woelk, C.H., Devos, N., Pascal, T.G., Mortier, M.-C., et al. (2018). Patients with Chronic Obstructive Pulmonary Disease harbour a variation of Haemophilus species. *Scientific Reports* 8(1), 14734. doi: 10.1038/s41598-018-32973-3.

Ozretić, P., da Silva Filho, M.I., Catalano, C., Sokolović, I., Vukić-Dugac, A., Šutić, M., et al. (2019). Association of NLRP1 Coding Polymorphism with Lung Function and Serum IL-1β Concentration in Patients Diagnosed with Chronic Obstructive Pulmonary Disease (COPD). *Genes* 10(10), 783. doi: 10.3390/genes10100783.

Park, S.H., Ham, S., Lee, A., Möller, A., and Kim, T.S. (2019). NLRP3 negatively regulates Treg differentiation through Kpna2-mediated nuclear translocation. *J Biol Chem* 294(47), 17951-17961. doi: 10.1074/jbc.RA119.010545.

Parker, D., and Prince, A. (2011). Innate immunity in the respiratory epithelium. *Am J Respir Cell Mol Biol* 45(2)**,** 189-201. doi: 10.1165/rcmb.2011-0011RT.

Pascoe S., K.F., Bonner J., Lloyd P., Lowe P., Beier J., Woessner R. (2006). "A monoclonal antibody to IL-1beta attenuates the late asthmatic response to antigen challenge in patients with mild asthma", in: *ERS Annual Congress.* (Munich, Germany: Eur Respir J).

Pauwels, N.S., Bracke, K.R., Dupont, L.L., Van Pottelberge, G.R., Provoost, S., Vanden Berghe, T., et al. (2011). Role of IL-1alpha and the Nlrp3/caspase-1/IL-1beta axis in cigarette smoke-induced pulmonary inflammation and COPD. *Eur Respir J* 38(5)**,** 1019-1028. doi: 10.1183/09031936.00158110.

Peeters, P.M., Perkins, T.N., Wouters, E.F.M., Mossman, B.T., and Reynaert, N.L. (2013). Silica induces NLRP3 inflammasome activation in human lung epithelial cells. *Particle and Fibre Toxicology* 10(1)**,** 3. doi: 10.1186/1743-8977-10-3.

Periasamy, S., Le, H.T., Duffy, E.B., Chin, H., and Harton, J.A. (2016). Inflammasome-Independent NLRP3 Restriction of a Protective Early Neutrophil Response to Pulmonary Tularemia. *PLOS Pathogens* 12(12)**,** e1006059. doi: 10.1371/journal.ppat.1006059.

Perotin, J.-M., Polette, M., Deslée, G., and Dormoy, V. (2021). CiliOPD: a ciliopathy-associated COPD endotype. *Respiratory Research* 22(1)**,** 74. doi: 10.1186/s12931-021-01665-4.

Pezzulo, A.A., Starner, T.D., Scheetz, T.E., Traver, G.L., Tilley, A.E., Harvey, B.G., et al. (2011). The air-liquid interface and use of primary cell cultures are important to recapitulate the transcriptional profile of in vivo airway epithelia. *Am J Physiol Lung Cell Mol Physiol* 300(1)**,** L25-31. doi: 10.1152/ajplung.00256.2010.

Pichlmair, A., Schulz, O., Tan, C.P., Näslund, T.I., Liljeström, P., Weber, F., et al. (2006). RIG-I-Mediated Antiviral Responses to Single-Stranded RNA Bearing 5'-Phosphates. *Science* 314(5801)**,** 997-1001. doi: doi:10.1126/science.1132998.

Piper, S.C., Ferguson, J., Kay, L., Parker, L.C., Sabroe, I., Sleeman, M.A., et al. (2013). The role of interleukin-1 and interleukin-18 in pro-inflammatory and anti-viral responses to rhinovirus in primary bronchial epithelial cells. *PLoS One* 8(5)**,** e63365. doi: 10.1371/journal.pone.0063365.

Plasschaert, L.W., Žilionis, R., Choo-Wing, R., Savova, V., Knehr, J., Roma, G., et al. (2018). A single-cell atlas of the airway epithelium reveals the CFTR-rich pulmonary ionocyte. *Nature* 560(7718)**,** 377-381. doi: 10.1038/s41586-018-0394-6.

Platz, J., Beisswenger, C., Dalpke, A., Koczulla, R., Pinkenburg, O., Vogelmeier, C., et al. (2004). Microbial DNA induces a host defense reaction of human respiratory epithelial cells. *J Immunol* 173(2)**,** 1219-1223. doi: 10.4049/jimmunol.173.2.1219.

Poeck, H., Bscheider, M., Gross, O., Finger, K., Roth, S., Rebsamen, M., et al. (2010). Recognition of RNA virus by RIG-I results in activation of CARD9 and inflammasome signaling for interleukin 1B production. *Nature Immunology* 11(1)**,** 63-69. doi: 10.1038/ni.1824.

Pothlichet, J., Meunier, I., Davis, B.K., Ting, J.P.Y., Skamene, E., von Messling, V., et al. (2013). Type I IFN Triggers RIG-I/TLR3/NLRP3-dependent Inflammasome Activation in Influenza A Virus Infected Cells. *PLoS Pathogens* 9(4). doi: 10.1371/journal.ppat.1003256.

Powell, D.W. (1981). Barrier function of epithelia. *American Journal of Physiology-Gastrointestinal and Liver Physiology* 241(4)**,** G275-G288. doi: 10.1152/ajpgi.1981.241.4.G275.

Qiu, C., Li, Y., Li, M., Li, M., Liu, X., McSharry, C., et al. (2013). Anti-interleukin-33 inhibits cigarette smoke-induced lung inflammation in mice. *Immunology* 138(1)**,** 76-82. doi: 10.1111/imm.12020.

Qu, Y., Franchi, L., Nunez, G., and Dubyak, G.R. (2007). Nonclassical IL-1β secretion stimulated by P2X7 receptors is dependent on inflammasome activation and correlated with exosome release in murine macrophages. *Journal of Immunology* 179(3)**,** 1913-1925.

Ramirez, R.D., Sheridan, S., Girard, L., Sato, M., Kim, Y., Pollack, J., et al. (2004). Immortalization of human bronchial epithelial cells in the absence of viral oncoproteins. *Cancer Res* 64(24)**,** 9027-9034. doi: 10.1158/0008-5472.Can-04-3703.

Rapiteanu, R., Karagyozova, T., Zimmermann, N., Singh, K., Wayne, G., Martufi, M., et al. (2020). Highly efficient genome editing in primary human bronchial epithelial cells differentiated at air-liquid interface. *European Respiratory Journal***,** 1900950. doi: 10.1183/13993003.00950-2019.

Rathinam, V.A.K., and Fitzgerald, K.A. (2016). Inflammasome Complexes: Emerging Mechanisms and Effector Functions. *Cell* 165(4)**,** 792-800. doi: 10.1016/j.cell.2016.03.046.

Rayner, R.E., Makena, P., Prasad, G.L., and Cormet-Boyaka, E. (2019). Optimization of Normal Human Bronchial Epithelial (NHBE) Cell 3D Cultures for in vitro Lung Model Studies. *Scientific Reports* 9(1)**,** 500. doi: 10.1038/s41598-018-36735-z.

Reddel, R.R., Ke, Y., Gerwin, B.I., McMenamin, M.G., Lechner, J.F., Su, R.T., et al. (1988). Transformation of human bronchial epithelial cells by infection with SV40 or adenovirus-12 SV40 hybrid virus, or transfection via strontium phosphate coprecipitation with a plasmid containing SV40 early region genes. *Cancer Res* 48(7)**,** 1904-1909.

Regan, T., Nally, K., Carmody, R., Houston, A., Shanahan, F., MacSharry, J., et al. (2013). Identification of TLR10 as a Key Mediator of the Inflammatory Response to Listeria monocytogenes in Intestinal Epithelial Cells and Macrophages. *The Journal of Immunology* 191(12)**,** 6084-6092. doi: 10.4049/jimmunol.1203245.

Rehwinkel, J., and Gack, M.U. (2020). RIG-I-like receptors: their regulation and roles in RNA sensing. *Nature Reviews Immunology* 20(9)**,** 537-551. doi: 10.1038/s41577-020-0288-3.

Robinson, K.S., Teo, D.E.T., Tan, K.S., Toh, G.A., Ong, H.H., Lim, C.K., et al. (2020). Enteroviral 3C protease activates the human NLRP1 inflammasome in airway epithelia. eaay2002. doi: 10.1126/science.aay2002 %J Science.

Rock, Jason R., Gao, X., Xue, Y., Randell, Scott H., Kong, Y.-Y., and Hogan, Brigid L.M. (2011). Notch-Dependent Differentiation of Adult Airway Basal Stem Cells. *Cell Stem Cell* 8(6)**,** 639-648. doi: https://doi.org/10.1016/j.stem.2011.04.003.

Rock, J.R., Onaitis, M.W., Rawlins, E.L., Lu, Y., Clark, C.P., Xue, Y., et al. (2009). Basal cells as stem cells of the mouse trachea and human airway epithelium. *Proc Natl Acad Sci U S A* 106(31)**,** 12771-12775. doi: 10.1073/pnas.0906850106.

Rock, J.R., Randell, S.H., and Hogan, B.L.M. (2010). Airway basal stem cells: a perspective on their roles in epithelial homeostasis and remodeling. *Disease Models & Mechanisms* 3(9-10)**,** 545. doi: 10.1242/dmm.006031.

Rosell, A., Monso, E., Soler, N., Torres, F., Angrill, J., Riise, G., et al. (2005). Microbiologic determinants of exacerbation in chronic obstructive pulmonary disease. *Arch Intern Med* 165(8)**,** 891-897. doi: 10.1001/archinte.165.8.891.

Rossios, C., Pavlidis, S., Hoda, U., Kuo, C.H., Wiegman, C., Russell, K., et al. (2018). Sputum transcriptomics reveal upregulation of IL-1 receptor family members in patients with severe asthma. *J Allergy Clin Immunol* 141(2)**,** 560-570. doi: 10.1016/j.jaci.2017.02.045.

Rotta detto Loria, J., Rohmann, K., Droemann, D., Kujath, P., Rupp, J., Goldmann, T., et al. (2013). Nontypeable Haemophilus Influenzae Infection Upregulates the NLRP3 Inflammasome and Leads to Caspase-1-Dependent Secretion of Interleukin-1β — A Possible Pathway of Exacerbations in COPD. *PLOS ONE* 8(6)**,** e66818. doi: 10.1371/journal.pone.0066818.

Ruiz García, S., Deprez, M., Lebrigand, K., Cavard, A., Paquet, A., Arguel, M.-J., et al. (2019). Novel dynamics of human mucociliary differentiation revealed by single-cell RNA sequencing of nasal epithelial cultures. *Development (Cambridge, England)* 146(20)**,** dev177428. doi: 10.1242/dev.177428.

Ryu, J.H., Yoo, J.Y., Kim, M.J., Hwang, S.G., Ahn, K.C., Ryu, J.C., et al. (2013). Distinct TLR-mediated pathways regulate house dust mite-induced allergic disease in the upper and lower airways. *J Allergy Clin Immunol* 131(2)**,** 549-561. doi: 10.1016/j.jaci.2012.07.050.

Sandstrom, A., Mitchell, P.S., Goers, L., Mu, E.W., Lesser, C.F., and Vance, R.E. (2019). Functional degradation: A mechanism of NLRP1 inflammasome activation by diverse pathogen enzymes. *Science* 364(6435). doi: 10.1126/science.aau1330.

Saresella, M., La Rosa, F., Piancone, F., Zoppis, M., Marventano, I., Calabrese, E., et al. (2016). The NLRP3 and NLRP1 inflammasomes are activated in Alzheimer's disease. *Molecular Neurodegeneration* 11(1)**,** 23. doi: 10.1186/s13024-016-0088-1.

Schleimer, R.P., Kato, A., Kern, R., Kuperman, D., and Avila, P.C. (2007). Epithelium: at the interface of innate and adaptive immune responses. *The Journal of allergy and clinical immunology* 120(6)**,** 1279-1284. doi: 10.1016/j.jaci.2007.08.046.

Schneider, D., Ganesan, S., Comstock, A.T., Meldrum, C.A., Mahidhara, R., Goldsmith, A.M., et al. (2010). Increased cytokine response of rhinovirus-infected airway epithelial cells in chronic obstructive pulmonary disease. *Am J Respir Crit Care Med* 182(3)**,** 332-340. doi: 10.1164/rccm.200911-1673OC.

Schwaid, A.G., and Spencer, K.B. (2021). Strategies for Targeting the NLRP3 Inflammasome in the Clinical and Preclinical Space. *Journal of Medicinal Chemistry* 64(1)**,** 101-122. doi: 10.1021/acs.jmedchem.0c01307.

Seemungal, T., Harper-Owen, R., Bhowmik, A., Moric, I., Sanderson, G., Message, S., et al. (2001). Respiratory viruses, symptoms, and inflammatory markers in acute exacerbations and stable chronic obstructive pulmonary disease. *Am J Respir Crit Care Med* 164(9)**,** 1618-1623. doi: 10.1164/ajrccm.164.9.2105011.

Sellin, M.E., Müller, A.A., and Hardt, W.D. (2018). Consequences of Epithelial Inflammasome Activation by Bacterial Pathogens. *J Mol Biol* 430(2)**,** 193-206. doi: 10.1016/j.jmb.2017.03.031.

Serebrisky, D., and Wiznia, A. (2019). Pediatric Asthma: A Global Epidemic. *Annals of global health* 85(1), 6. doi: 10.5334/aogh.2416.
Sethi, S., Evans, N., Grant, B.J.B., and Murphy, T.F. (2002). New Strains of Bacteria and Exacerbations of Chronic Obstructive Pulmonary Disease. *New England Journal of Medicine* 347(7), 465-471. doi: 10.1056/NEJMoa012561.
Sethi, S., and Murphy, T.F. (2001). Bacterial infection in chronic obstructive pulmonary disease in 2000: a state-of-the-art review. *Clin Microbiol Rev* 14(2), 336-363. doi: 10.1128/cmr.14.2.336-363.2001.
Sha, Q., Truong-Tran, A.Q., Plitt, J.R., Beck, L.A., and Schleimer, R.P. (2004). Activation of Airway Epithelial Cells by Toll-Like Receptor Agonists. *American Journal of Respiratory Cell and Molecular Biology* 31(3), 358-364. doi: 10.1165/rcmb.2003-0388OC.
Sha, W., Mitoma, H., Hanabuchi, S., Bao, M., Weng, L., Sugimoto, N., et al. (2014). Human NLRP3 inflammasome senses multiple types of bacterial RNAs. *Proceedings of the National Academy of Sciences of the United States of America* 111(45), 16059-16064. doi: 10.1073/pnas.1412487111.
Shi, J., Zhao, Y., Wang, K., Shi, X., Wang, Y., Huang, H., et al. (2015). Cleavage of GSDMD by inflammatory caspases determines pyroptotic cell death. *Nature* 526(7575), 660-665. doi: 10.1038/nature15514.
Shlomovitz, I., Erlich, Z., Speir, M., Zargarian, S., Baram, N., Engler, M., et al. (2019). Necroptosis directly induces the release of full-length biologically active IL-33 in vitro and in an inflammatory disease model. *Febs j* 286(3), 507-522. doi: 10.1111/febs.14738.
Sims, J.E., March, C.J., Cosman, D., Widmer, M.B., Macdonald, H.R., McMahan, C.J., et al. (1988). cDNA expression cloning of the IL-1 receptor, a member of the immunoglobulin superfamily. *Science* 241(4865), 585-589.
Singh, D., Fox, S.M., Tal-Singer, R., Plumb, J., Bates, S., Broad, P., et al. (2011). Induced sputum genes associated with spirometric and radiological disease severity in COPD ex-smokers. *Thorax* 66(6), 489-495. doi: 10.1136/thx.2010.153767.
Singh, P.K., and Hollingsworth, M.A. (2006). Cell surface-associated mucins in signal transduction. *Trends in Cell Biology* 16(9), 467-476. doi: https://doi.org/10.1016/j.tcb.2006.07.006.
Slater, L., Bartlett, N.W., Haas, J.J., Zhu, J., Message, S.D., Walton, R.P., et al. (2010). Co-ordinated Role of TLR3, RIG-I and MDA5 in the Innate Response to Rhinovirus in Bronchial Epithelium. *PLOS Pathogens* 6(11), e1001178. doi: 10.1371/journal.ppat.1001178.
Slevogt, H., Seybold, J., Tiwari, K.N., Hocke, A.C., Jonatat, C., Dietel, S., et al. (2007). Moraxella catarrhalis is internalized in respiratory epithelial cells by a trigger-like mechanism and initiates a TLR2- and partly NOD1-dependent inflammatory immune response. *Cellular Microbiology* 9(3), 694-707. doi: https://doi.org/10.1111/j.1462-5822.2006.00821.x.
Slevogt, H., Tiwari, K.N., Schmeck, B., Hocke, A., Opitz, B., Suttorp, N., et al. (2005). Adhesion of Moraxella catarrhalis to human bronchial epithelium characterized by a novel fluorescence-based assay. *Medical Microbiology and Immunology* 195(2), 73. doi: 10.1007/s00430-005-0003-9.
Snell, N., Strachan, D., Hubbard, R., Gibson, J., Gruffydd-Jones, K., and Jarrold, I. (2016). Epidemiology of chronic obstructive pulmonary disease (COPD) in the UK: Findings from the british lung foundation's 'respiratory health of the nation' project. *Thorax* 71, A20. doi: 10.1136/thoraxjnl-2016-209333.38.

Stewart, C., Torr, E., Jamili, N., Bosquillon, C., and Sayers, I. (2012). Evaluation of Differentiated Human Bronchial Epithelial Cell Culture Systems for Asthma Research. *Journal of allergy* 2012**,** 943982. doi: 10.1155/2012/943982.

Stubbs, J.L., Vladar, E.K., Axelrod, J.D., and Kintner, C. (2012). Multicilin promotes centriole assembly and ciliogenesis during multiciliate cell differentiation. *Nature Cell Biology* 14(2)**,** 140-147. doi: 10.1038/ncb2406.

Su, Y.-C., Jalalvand, F., Thegerström, J., and Riesbeck, K. (2018). The Interplay Between Immune Response and Bacterial Infection in COPD: Focus Upon Non-typeable Haemophilus influenzae. *Frontiers in Immunology* 9(2530). doi: 10.3389/fimmu.2018.02530.

Su, Y.-C., Singh, B., and Riesbeck, K. (2012). Moraxella catarrhalis: from interactions with the host immune system to vaccine development. *Future Microbiology* 7(9)**,** 1073-1100. doi: 10.2217/fmb.12.80.

Sun, W.K., Lu, X., Li, X., Sun, Q.Y., Su, X., Song, Y., et al. (2012). Dectin-1 is inducible and plays a crucial role in Aspergillus-induced innate immune responses in human bronchial epithelial cells. *Eur J Clin Microbiol Infect Dis* 31(10)**,** 2755-2764. doi: 10.1007/s10096-012-1624-8.

Symons, J.A., Young, P.R., and Duff, G.W. (1995). Soluble type II interleukin 1 (IL-1) receptor binds and blocks processing of IL-1 beta precursor and loses affinity for IL-1 receptor antagonist. *Proc Natl Acad Sci U S A* 92(5)**,** 1714-1718. doi: 10.1073/pnas.92.5.1714.

Taabazuing, C.Y., Griswold, A.R., and Bachovchin, D.A. (2020). The NLRP1 and CARD8 inflammasomes. *Immunological Reviews* 297(1)**,** 13-25. doi: https://doi.org/10.1111/imr.12884.

Tago, K., Noda, T., Hayakawa, M., Iwahana, H., Yanagisawa, K., Yashiro, T., et al. (2001). Tissue distribution and subcellular localization of a variant form of the human ST2 gene product, ST2V. *Biochemical and Biophysical Research Communications* 285(5)**,** 1377-1383. doi: 10.1006/bbrc.2001.5306.

Tanabe, N., Hoshino, Y., Marumo, S., Kiyokawa, H., Sato, S., Kinose, D., et al. (2013). Thioredoxin-1 Protects against Neutrophilic Inflammation and Emphysema Progression in a Mouse Model of Chronic Obstructive Pulmonary Disease Exacerbation. *PLOS ONE* 8(11)**,** e79016. doi: 10.1371/journal.pone.0079016.

Tang, A., Sharma, A., Jen, R., Hirschfeld, A.F., Chilvers, M.A., Lavoie, P.M., et al. (2012). Inflammasome-Mediated IL-1β Production in Humans with Cystic Fibrosis. *PLOS ONE* 7(5)**,** e37689. doi: 10.1371/journal.pone.0037689.

Tata, P.R., Mou, H., Pardo-Saganta, A., Zhao, R., Prabhu, M., Law, B.M., et al. (2013). Dedifferentiation of committed epithelial cells into stem cells in vivo. *Nature* 503(7475)**,** 218-223. doi: 10.1038/nature12777.

Taylor, S.C., Nadeau, K., Abbasi, M., Lachance, C., Nguyen, M., and Fenrich, J. (2019). The Ultimate qPCR Experiment: Producing Publication Quality, Reproducible Data the First Time. *Trends in Biotechnology* 37(7)**,** 761-774. doi: 10.1016/j.tibtech.2018.12.002.

The Human Protein Atlas (2021a). *DPP8* [Online]. HPA. Available: https://www.proteinatlas.org/ENSG00000074603-DPP8/cell+line [Accessed 5 November 2021].

The Human Protein Atlas (2021b). *DPP9* [Online]. HPA. Available: https://www.proteinatlas.org/ENSG00000142002-DPP9/cell+line [Accessed 5 November 2021].

The Human Protein Atlas (2021c). *NLRP1* [Online]. HPA. Available: https://www.proteinatlas.org/ENSG00000091592-NLRP1/cell+line [Accessed 5 November 2021].

Tokita, E., Tanabe, T., Asano, K., Suzaki, H., and Rubin, B.K. (2014). Club cell 10-kDa protein attenuates airway mucus hypersecretion and inflammation. *Eur Respir J* 44(4)**,** 1002-1010. doi: 10.1183/09031936.00080913.

Tong, J., Zhou, X.-d., Perelman, Juliy M., and Kolosov, Victor P. (2014). Effect of epithelium ATP release on cyclic pressure-induced airway mucus secretion. *Bioscience Reports* 34(1). doi: 10.1042/bsr20130109.

Tran, H.B., Hamon, R., Jersmann, H., Ween, M.P., Asare, P., Haberberger, R., et al. (2021). AIM2 nuclear exit and inflammasome activation in chronic obstructive pulmonary disease and response to cigarette smoke. *Journal of Inflammation* 18(1)**,** 19. doi: 10.1186/s12950-021-00286-4.

Triantafilou, K., Kar, S., Vakakis, E., Kotecha, S., and Triantafilou, M. (2013). Human respiratory syncytial virus viroporin SH: a viral recognition pathway used by the host to signal inflammasome activation. 68(1)**,** 66-75. doi: 10.1136/thoraxjnl-2012-202182 %J Thorax.

Tsu, B.V., Beierschmitt, C., Ryan, A.P., Agarwal, R., Mitchell, P.S., and Daugherty, M.D. (2021). Diverse viral proteases activate the NLRP1 inflammasome. *eLife* 10**,** e60609. doi: 10.7554/eLife.60609.

Tye, H., Yu, C.-H., Simms, L.A., de Zoete, M.R., Kim, M.L., Zakrzewski, M., et al. (2018). NLRP1 restricts butyrate producing commensals to exacerbate inflammatory bowel disease. *Nature communications* 9(1)**,** 3728-3728. doi: 10.1038/s41467-018-06125-0.

Vaughan, M.B., Ramirez, R.D., Wright, W.E., Minna, J.D., and Shay, J.W. (2006). A three-dimensional model of differentiation of immortalized human bronchial epithelial cells. *Differentiation* 74(4)**,** 141-148. doi: https://doi.org/10.1111/j.1432-0436.2006.00069.x.

Vieira Braga, F.A., Kar, G., Berg, M., Carpaij, O.A., Polanski, K., Simon, L.M., et al. (2019). A cellular census of human lungs identifies novel cell states in health and in asthma. *Nature Medicine* 25(7)**,** 1153-1163. doi: 10.1038/s41591-019-0468-5.

Wang, H., Lv, C.e., Wang, S., Ying, H., Weng, Y., and Yu, W. (2018a). NLRP3 Inflammasome Involves in the Acute Exacerbation of Patients with Chronic Obstructive Pulmonary Disease. *Inflammation* 41(4)**,** 1321-1333. doi: 10.1007/s10753-018-0780-0.

Wang, J., Sahoo, M., Lantier, L., Warawa, J., Cordero, H., Deobald, K., et al. (2018b). Caspase-11-dependent pyroptosis of lung epithelial cells protects from melioidosis while caspase-1 mediates macrophage pyroptosis and production of IL-18. *PLoS pathogens* 14(5)**,** e1007105-e1007105. doi: 10.1371/journal.ppat.1007105.

Wang, J.H., Kwon, H.J., and Jang, Y.J. (2009). Rhinovirus enhances various bacterial adhesions to nasal epithelial cells simultaneously. *The Laryngoscope* 119(7)**,** 1406-1411. doi: https://doi.org/10.1002/lary.20498.

Warner, S.M., Wiehler, S., Michi, A.N., and Proud, D. (2019). Rhinovirus replication and innate immunity in highly differentiated human airway epithelial cells. *Respiratory Research* 20(1)**,** 150. doi: 10.1186/s12931-019-1120-0.

Watson, Julie K., Rulands, S., Wilkinson, Adam C., Wuidart, A., Ousset, M., Van Keymeulen, A., et al. (2015). Clonal Dynamics Reveal Two Distinct

Populations of Basal Cells in Slow-Turnover Airway Epithelium. *Cell Reports* 12(1), 90-101. doi: 10.1016/j.celrep.2015.06.011.
West, J.B. (2012). *Respiratory physiology: the essentials.* Lippincott Williams & Wilkins.
White, A.J., Gompertz, S., Bayley, D.L., Hill, S.L., O'Brien, C., Unsal, I., et al. (2003). Resolution of bronchial inflammation is related to bacterial eradication following treatment of exacerbations of chronic bronchitis. *Thorax* 58(8), 680-685. doi: 10.1136/thorax.58.8.680.
Whitsett, J.A., and Alenghat, T. (2014). Respiratory epithelial cells orchestrate pulmonary innate immunity. *Nature immunology* 16(1), 27-35. doi: 10.1038/ni.3045.
Wilson, C.H., Indarto, D., Doucet, A., Pogson, L.D., Pitman, M.R., McNicholas, K., et al. (2013). Identifying Natural Substrates for Dipeptidyl Peptidases 8 and 9 Using Terminal Amine Isotopic Labeling of Substrates (TAILS) Reveals in Vivo Roles in Cellular Homeostasis and Energy Metabolism*♦. *Journal of Biological Chemistry* 288(20), 13936-13949. doi: https://doi.org/10.1074/jbc.M112.445841.
Wilson, J.E., Petrucelli, A.S., Chen, L., Koblansky, A.A., Truax, A.D., Oyama, Y., et al. (2015). Inflammasome-independent role of AIM2 in suppressing colon tumorigenesis via DNA-PK and Akt. *Nat Med* 21(8), 906-913. doi: 10.1038/nm.3908.
Winton, H.L., Wan, H., Cannell, M.B., Gruenert, D.C., Thompson, P.J., Garrod, D.R., et al. (1998). Cell lines of pulmonary and non-pulmonary origin as tools to study the effects of house dust mite proteinases on the regulation of epithelial permeability. *Clin Exp Allergy* 28(10), 1273-1285. doi: 10.1046/j.1365-2222.1998.00354.x.
Wlodarska, M., Thaiss, Christoph A., Nowarski, R., Henao-Mejia, J., Zhang, J.-P., Brown, Eric M., et al. (2014). NLRP6 Inflammasome Orchestrates the Colonic Host-Microbial Interface by Regulating Goblet Cell Mucus Secretion. *Cell* 156(5), 1045-1059. doi: https://doi.org/10.1016/j.cell.2014.01.026.
World Health Organization (2020). *The top 10 causes of death* [Online]. WHO. Available: https://www.who.int/news-room/fact-sheets/detail/the-top-10-causes-of-death [Accessed 5 November 2021].
Wu, C.A., Peluso, J.J., Zhu, L., Lingenheld, E.G., Walker, S.T., and Puddington, L. (2010). Bronchial epithelial cells produce IL-5: implications for local immune responses in the airways. *Cell Immunol* 264(1), 32-41. doi: 10.1016/j.cellimm.2010.04.008.
Wu, H., Yang, S., Wu, X., Zhao, J., Zhao, J., Ning, Q., et al. (2014). Interleukin-33/ST2 signaling promotes production of interleukin-6 and interleukin-8 in systemic inflammation in cigarette smoke-induced chronic obstructive pulmonary disease mice. *Biochemical and Biophysical Research Communications* 450(1), 110-116. doi: 10.1016/j.bbrc.2014.05.073.
Xia, J., Zhao, J., Shang, J., Li, M., Zeng, Z., Zhao, J., et al. (2015). Increased IL-33 expression in chronic obstructive pulmonary disease. *American Journal of Physiology - Lung Cellular and Molecular Physiology* 308(7), L619-L627. doi: 10.1152/ajplung.00305.2014.
Yang, J., Zhao, Y., Shi, J., and Shao, F. (2013). Human NAIP and mouse NAIP1 recognize bacterial type III secretion needle protein for inflammasome activation. *Proceedings of the National Academy of Sciences* 110(35), 14408. doi: 10.1073/pnas.1306376110.

Yoon, J.H., Gray, T., Guzman, K., Koo, J.S., and Nettesheim, P. (1997). Regulation of the secretory phenotype of human airway epithelium by retinoic acid, triiodothyronine, and extracellular matrix. *American Journal of Respiratory Cell and Molecular Biology* 16(6), 724-731. doi: 10.1165/ajrcmb.16.6.9191474.

Yoon, J.H., Koo, J.S., Norford, D., Guzman, K., Gray, T., and Nettesheim, P. (1999). Lysozyme expression during metaplastic squamous differentiation of retinoic acid-deficient human tracheobronchial epithelial cells. *Am J Respir Cell Mol Biol* 20(4), 573-581. doi: 10.1165/ajrcmb.20.4.3127.

You, Y., Huang, T., Richer, E.J., Schmidt, J.-E.H., Zabner, J., Borok, Z., et al. (2004). Role of f-box factor foxj1 in differentiation of ciliated airway epithelial cells. *American Journal of Physiology-Lung Cellular and Molecular Physiology* 286(4), L650-L657. doi: 10.1152/ajplung.00170.2003.

Zaidman, N.A., Panoskaltsis-Mortari, A., and O'Grady, S.M. (2016). Differentiation of human bronchial epithelial cells: role of hydrocortisone in development of ion transport pathways involved in mucociliary clearance. *American journal of physiology. Cell physiology* 311(2), C225-C236. doi: 10.1152/ajpcell.00073.2016.

Zeng, Q., Yang, Q., Jia, J., and Bi, H. (2020). A Moraxella Virulence Factor Catalyzes an Essential Esterase Reaction of Biotin Biosynthesis. *Frontiers in Microbiology* 11(148). doi: 10.3389/fmicb.2020.00148.

Zhang, H., Luo, J., Alcorn, J.F., Chen, K., Fan, S., Pilewski, J., et al. (2017). AIM2 Inflammasome Is Critical for Influenza-Induced Lung Injury and Mortality. *Journal of immunology (Baltimore, Md. : 1950)* 198(11), 4383-4393. doi: 10.4049/jimmunol.1600714.

Zhang, H., Maqsudi, S., Rainczuk, A., Duffield, N., Lawrence, J., Keane, F.M., et al. (2015). Identification of novel dipeptidyl peptidase 9 substrates by two-dimensional differential in-gel electrophoresis. *Febs j* 282(19), 3737-3757. doi: 10.1111/febs.13371.

Zhao, C., Gu, Y., Zeng, X., and Wang, J. (2018). NLRP3 inflammasome regulates Th17 differentiation in rheumatoid arthritis. *Clinical Immunology* 197, 154-160. doi: https://doi.org/10.1016/j.clim.2018.09.007.

Zhao, J., Shang, J., Zhao, J., Wu, X., Xu, Y., and Xie, J. (2015). Interleukin-33 promotes inflammatory cytokine production in chronic airway inflammation. *Biochemistry and Cell Biology* 93(4), 359-366. doi: 10.1139/bcb-2014-0163.

Zhao, K., Huang, T., Lin, J., Yan, C., Du, L., Song, T., et al. (2020). Genetic and Functional Diversity of Pseudomonas aeruginosa in Patients With Chronic Obstructive Pulmonary Disease. *Frontiers in Microbiology* 11. doi: 10.3389/fmicb.2020.598478.

Zhong, F.L., Mamaï, O., Sborgi, L., Boussofara, L., Hopkins, R., Robinson, K., et al. (2016). Germline NLRP1 Mutations Cause Skin Inflammatory and Cancer Susceptibility Syndromes via Inflammasome Activation. *Cell* 167(1), 187-202.e117. doi: https://doi.org/10.1016/j.cell.2016.09.001.

Zhong, F.L., Robinson, K., Teo, D.E.T., Tan, K.-Y., Lim, C., Harapas, C.R., et al. (2018). Human DPP9 represses NLRP1 inflammasome and protects against autoinflammatory diseases via both peptidase activity and FIIND domain binding. *Journal of Biological Chemistry* 293(49), 18864-18878. doi: https://doi.org/10.1074/jbc.RA118.004350.

Zhou, J., Wang, C., Wu, J., Fukunaga, A., Cheng, Z., Wang, J., et al. (2020). Anti-Allergic and Anti-Inflammatory Effects and Molecular Mechanisms of

Thioredoxin on Respiratory System Diseases. *Antioxid Redox Signal* 32(11)**,** 785-801. doi: 10.1089/ars.2019.7807.

Zong, J., Zhang, H., Li, F.F., Liang, K., Liu, J.L., Xu, L.H., et al. (2018). NLRP1 promotes TGF-β1-induced myofibroblast differentiation in neonatal rat cardiac fibroblasts. *J Mol Histol* 49(5)**,** 509-518. doi: 10.1007/s10735-018-9789-9.

Zou, Y., Chen, X., Liu, J., bo Zhou, D., Kuang, X., Xiao, J., et al. (2017). Serum IL-1β and IL-17 levels in patients with COPD: Associations with clinical parameters. *International Journal of COPD* 12**,** 1247-1254. doi: 10.2147/COPD.S131877.